

# A new carcharodontosaurid (Dinosauria, Theropoda) from the Upper Cretaceous of Argentina

Rodolfo A. CORIA

CONICET, Museo Carmen Funes, Av. Córdoba 55,  
8318 Plaza Huincul, Neuquén (Argentina)  
coriarod@copelnet.com.ar

Philip J. CURRIE

University of Alberta, Department of Biological Sciences,  
Edmonton, Alberta T6G 2E9 (Canada)  
philip.currie@ualberta.ca

Coria R. A. & Currie P. J. 2006. — A new carcharodontosaurid (Dinosauria, Theropoda) from the Upper Cretaceous of Argentina. *Geodiversitas* 28 (1): 71-118.

## ABSTRACT

A new carcharodontosaurid theropod from the Huincul Formation (Aptian-Cenomanian, Upper Cretaceous) of Neuquén Province, Argentina, is described. Approximately the same size as *Giganotosaurus carolinii* Coria & Salgado, 1995, *Mapusaurus roseae* n. gen., n. sp. is characterized by many features including a deep, short and narrow skull with relatively large triangular antorbital fossae, relatively small maxillary fenestra, and narrow, unfused rugose nasals. *Mapusaurus roseae* n. gen., n. sp. has cervical neural spines and distally tapering epiphyses, tall dorsal neural spines, central pleurocoels as far back as the first sacral vertebra, accessory caudal neural spines, stout humerus with poorly defined distal condyles, fused metacarpals, ilium with brevis fossa extending deeply into ischial peduncle, and femur with low fourth trochanter. Phylogenetic analysis indicates that *Mapusaurus* n. gen. shares with *Carcharodontosaurus* Stromer, 1931 and *Giganotosaurus* Coria & Salgado, 1995 several derived features that include narrow blade-like teeth with wrinkled enamel, heavily sculptured facial bones, supraorbital shelf formed by a postorbital/palpebral complex, and a dorsomedially directed femoral head. Remains of *Mapusaurus* n. gen. were recovered from a bonebed where 100% of the identifiable dinosaur bones can be assigned to this new genus. Based on the metatarsals recovered, a minimum of seven individuals was buried at the site. It is conceivable that this bonebed represents a long term or coincidental accumulation of carcasses. The presence of a single carnivorous taxon with individuals of different ontogenetic stages provides evidence of variation within a single population, and may also indicate some behavioural traits for *Mapusaurus roseae* n. gen., n. sp.

## KEY WORDS

Dinosauria,  
Theropoda,  
Carcharodontosauridae,  
Upper Cretaceous,  
Argentina,  
new genus,  
new species.

## RÉSUMÉ

*Un nouveau carcharodontosauridé (Dinosauria, Theropoda) du Crétacé supérieur d'Argentine.*

Un nouveau théropode carcharodontosauride de la Formation Huincul, datée du Crétacé supérieur, de la Province de Neuquén, Argentine, est décrit. D'une taille proche de celle de *Giganotosaurus carolinii* Coria & Salgado, 1995, *Mapusaurus roseae* n. gen., n. sp. est défini par des caractères qui incluent : un crâne haut, court et étroit, avec une fosse antorbitaire assez large, une fenêtre maxillaire petite et étroite et des os nasaux non fusionnés et d'aspect rugueux. Au niveau cervical, les vertèbres de *Mapusaurus roseae* n. gen., n. sp. porte des épines neurales, et, distalement, des épipophyses effilées, de grandes épines neurales dorsales, et des pleurocèles centraux jusqu'à la première vertèbre sacrée et accessoirement des épines neurales dans la région caudale. L'humérus est robuste avec des condyles distaux peu développés, les métacarpes sont fusionnés, l'ilion dont la brevis fossa s'étend loin vers le pédoncule ischiatrique. Le fémur porte un quatrième trochanter en position basse. Les résultats de l'analyse phylogénétique indiquent que *Mapusaurus roseae* n. gen., n. sp. partage avec *Carcharodontosaurus* Stromer, 1931 et *Giganotosaurus* Coria & Salgado, 1995 plusieurs caractères dérivés dont : des dents en forme de lame étroite à émail plissé, des os de la face profondément sculptés, une voûte supraorbitaire constituée par le complexe postorbitaire-palpébrale et une tête fémorale dirigée dorsomédalement. Des restes de *Mapusaurus* n. gen. ont été trouvés dans un « bonebed » où 100 % des os de dinosaures identifiables sont rapportés à ce genre. Si l'on prend en considération les métatarses, on peut dénombrer que sept individus au minimum furent fossilisés sur le site. La formation de ce « bonebed » résulterait d'une accumulation d'os sur la durée ou d'une accumulation plus rapide de carcasses. La présence de ce seul taxon de carnivore représente par des individus d'âges différents apporte des données tant sur la variation au sein d'une seule et même population que sur des traits du comportement de *Mapusaurus roseae* n. gen., n. sp.

## MOTS CLÉS

Dinosauria,  
Theropoda,  
Carcharodontosauridae,  
Crétacé supérieur,  
Argentine,  
nouveau genre,  
nouvelle espèce.

## INTRODUCTION

Recent discoveries of theropod dinosaurs in the Cretaceous of Patagonia have unveiled an unexpected diversity of this group of vertebrates. These findings include *Carnotaurus sastrei* Bonaparte, 1985; *Abelisaurus comahuensis* Bonaparte & Novas, 1985; *Xenotarsosaurus bonapartei* Martínez, Giménez, Rodríguez & Bochatey, 1986; *Giganotosaurus carolinii* Coria & Salgado, 1995; *Uenlagia comahuensis* Novas & Puerta, 1997; *Megaraptor namunhuaikei* Novas, 1998; *Ilokelesia aguadagrändensis* Coria & Salgado, 1998; *Quilmesaurus curriei* Coria, 2001; *Aucasaurus garridoi* Coria, Chiappe & Dingus, 2002, and several new taxa

still under study. Most of these forms have been recovered from the Neuquén Basin of northern Patagonia.

In 1997, members of the Argentinean-Canadian Dinosaur Project were collecting fossils at the Cañadón del Gato site (Fig. 1) in rocks of the Huincul Formation of the Río Limay Group (Ramos 1981; Garrido 2000), which are thought to be Albian to Cenomanian in age (Legarreta & Gulisano 1989; Lanza *et al.* 2004). Excavation commenced on what was initially thought to be a single skeleton of a giant theropod (Coria & Currie 1997). Preparation later revealed that skeletal parts represented more than a single individual, ranging in size from about five to 11 m.

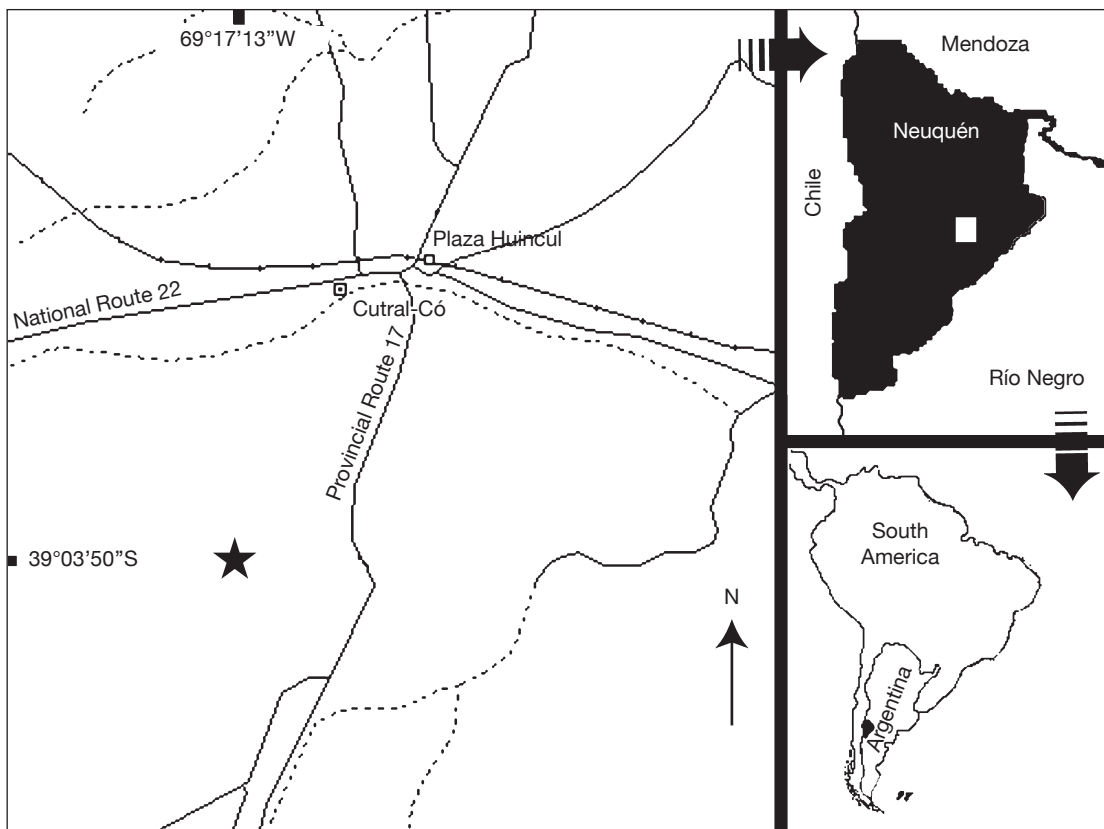


FIG. 1. — Location map of the site "Cañadón del Gato" (★) where the remains of *Mapusaurus roseae* n. gen., n. sp. were found.

After five consecutive field seasons between 1997 and 2001, a minimum of seven to nine individuals have been recognized, all assigned to a single theropod species. The monospecific nature of the assemblage makes the Cañadón del Gato site interesting, especially considering the rarity of fossilized bones in the Huincul Formation (Eberth *et al.* 2000). The monospecific nature and some taphonomic characteristics of the burial have implications on our understanding of the social behavior of large theropods (Currie 2000).

The specimens collected from the Cañadón del Gato site share derived characters with members of the Carcharodontosauridae. These include heavy sculpturing of the external surface of the maxilla; heavily ornamented, thick, unfused nasals; a strongly upturned femoral head; and a distally positioned

lesser trochanter. Carcharodontosaurids, one of the most poorly understood large Cretaceous theropod families, have been recovered from Africa (Depéret & Savornin 1927; Stromer 1931; Rauhut 1995; Russell 1996; Sereno *et al.* 1994) and South America (Coria & Salgado 1995; Vickers-Rich *et al.* 1999). The report of a possible carcharodontosaurid from Japan (Chure *et al.* 1999) is based on a single tooth, and its identification can only be considered tentative. Although *Acrocanthosaurus* Stovall & Langston, 1950, from the United States, has been referred to the Carcharodontosauridae (Sereno *et al.* 1996; Harris 1998), the assignment has been questioned by others (Currie & Carpenter 2000; Coria & Currie 2002).

*Giganotosaurus* (Coria & Salgado 1995) was the first South American carcharodontosaurid

identified (Sereno *et al.* 1996). Since then, carcharodontosaurid remains have been reported from widespread South American localities (Novas *et al.* 1999; Vickers-Rich *et al.* 1999; Calvo & Coria 2000; Rich *et al.* 2000). In this contribution, we describe a new carcharodontosaurid, *Mapusaurus roseae* n. gen., n. sp., which can be distinguished from *Giganotosaurus carolinii* on the basis of anatomical differences and stratigraphic provenance. Nevertheless, *Mapusaurus* n. gen. is an animal of comparable size to *Giganotosaurus* (Coria & Salgado 1995), arguably the largest known theropod, suggesting a previously unrecognized diversity of large-sized theropods in the Late Cretaceous of South America. Furthermore, *Mapusaurus* n. gen. is associated in the Huincul Formation with giant sauropods, including *Argentinosaurus huinculensis* Bonaparte & Coria, 1993.

In recent years, the analysis of theropod systematics (Harris 1998; Sereno 1999; Holtz 2000; Currie & Carpenter 2000) has become complicated because of the wealth of information from newly described basal forms (Currie & Zhao 1993; Zhao & Currie 1993; Sereno *et al.* 1994; Coria & Salgado 1995, 2000; Hutt *et al.* 1996; Coria 2001; Coria *et al.* 2002; Arcucci & Coria 2003). Although there is broad agreement on the relationships of many of the major theropod lineages, the positions of specific branches are in a state of flux, including the composition and relationships of Carcharodontosauridae. Consider, for example, that carcharodontosaurids have been allied with tyrannosaurids (Lapparent 1960), megalosaurids (Romer 1966), allosauroids (Rauhut 1995; Sereno *et al.* 1996; Harris 1998; Currie & Carpenter 2000), and abelisaurids (Novas 1997). Although the family has been known for more than 70 years (Stromer 1931), detailed descriptions of carcharodontosaurid anatomy are only starting to be published (Larsson 2001; Coria & Currie 2002). In this contribution, we present a description of the characters that support the new taxon *Mapusaurus roseae* n. gen., n. sp., and conduct a preliminary phylogenetic analysis.

## ABBREVIATIONS

BHI	Black Hills Institute of Geological Research, Hill City, South Dakota;
-----	--

BMNH	The Natural History Museum, London;
FPDM	Fukui Prefectural Dinosaur Museum, Katsuyama, Japan;
MACN	Museo Argentino de Ciencias Naturales, Buenos Aires;
MCF-PVPH	Museo Carmen Funes, Paleontología de Vertebrados, Plaza Huincul, Neuquén;
MPCA	Museo Provincial "Carlos Ameghino", Cipolletti, Río Negro;
MUCPv-CH	Museo de la Universidad Nacional del Comahue, El Chocón collection, Neuquén;
NCSM	North Carolina State Museum of Natural Sciences, Raleigh;
SGM	Ministère de l'Énergie et des Mines, Rabat;
USNM	United States National Museum of Natural History, Smithsonian Institution, Washington, D.C.;
UUVP	University of Utah, Vertebrate Paleontology, Salt Lake City.

## SYSTEMATICS

DINOSAURIA Owen, 1842  
THEROPODA Marsh, 1881  
Family CARCHARODONTOSAURIIDAE  
Stromer, 1931

### GIGANOTOSAURINAE n. subfam.

TYPE GENUS. — *Giganotosaurus* Coria & Salgado, 1995.

DIAGNOSIS. — Carcharodontosaurids linked by the derived femur with a weak fourth trochanter, and a shallow, broad extensor groove on the distal end.

### *Mapusaurus* n. gen.

TYPE SPECIES. — *Mapusaurus roseae* n. sp.

ETYMOLOGY. — “*Mapu*” is a Mapuche (local indigenous people) term for Earth. Therefore “*Mapusaurus*” should be translated as “Earth reptile”.

HORIZON AND LOCALITY. — Huincul Formation, Río Limay Group (Cenomanian), of the Neuquén Group. Cañadón del Gato in the Cortaderas area 20 km southwest of Plaza Huincul, Neuquén Province, Argentina (Fig. 1).

**DIAGNOSIS.** — *Mapusaurus* n. gen. is a carcharodontosaurid theropod whose skull differs from *Giganotosaurus* in having thick, rugose unfused nasals that are narrower anterior to nasal/maxilla/lacrimal junction; larger extension of antorbital fossa onto maxilla; smaller maxillary fenestra; wider bar (interfenestral strut) between antorbital and maxillary fenestrae; lower, flatter lacrimal horn; transversely wider prefrontal in relation to lacrimal width; ventrolaterally curving lateral margin of palpebral; shallower interdental plates; higher position of Meckelian canal; more posteriorly sloping anteroventral margin of dentary. *Mapusaurus roseae* n. gen., n. sp. is unique in that upper quadratojugal process of jugal splits into two prongs; small anterior mylohyoid foramen positioned above dentary contact with splenial; second and third metacarpals fused; humerus with broad distal end and little separation between condyles; brevis fossa of ilium extends deeply into excavation dorsal to ischial peduncle. It also differs from *Giganotosaurus* in having conical, slightly curving cervical epiphyses that taper distally; axial posterior zygapophyses joined on midline; smaller and less elaborate prespinal lamina on midline of cervicals; remarkably sharp dorsal margin of cervical neural spines; taller, wider neural spines; curved ischiatic shaft; more slender fibula.

### *Mapusaurus roseae* n. sp.

**HOLOTYPE.** — MCF-PVPH-108.1, right nasal.

**PARATYPES.** — MCF-PVPH-108.5, left lacrimal/pre-frontal; MCF-PVPH-108.45, right humerus; MCF-PVPH-108.83, axis; MCF-PVPH-108.90, cervical neural arch; MCF-PVPH-108.115, right maxilla; MCF-PVPH-108.125, left dentary; MCF-PVPH-108.128, left ilium; MCF-PVPH-108.165, left ischium; MCF-PVPH-108.167, jugal; MCF-PVPH-108.177, right post-orbital-palpebral; MCF-PVPH-108.179, right splenial; MCF-PVPH-108.202, right fibula.

**ETYMOLOGY.** — The term “*roseae*” refers to the rose-colored rocks that surround the site where *Mapusaurus* n. gen. was found, and to Rose Letwin (Seattle) who sponsored the expeditions in 1999, 2000 and 2001.

**DIAGNOSIS.** — The same as genus by monotypy.

### DESCRIPTION

*Mapusaurus roseae* n. gen., n. sp. is known from most skeletal parts, although the bones represent at least seven individuals (discussed in subsequent text).

Overall, the skull of *Mapusaurus* n. gen. appears to be deeper and narrower than that of *Giganotosaurus*, because the maxilla is not elongate, and the nasal is

relatively narrower (Figs 2; 3). The antorbital fossa of *Mapusaurus roseae* n. gen., n. sp. is as large as in *Giganotosaurus* (MUCPv-CH-1) and *Carcharodontosaurus* Stromer, 1931 (SGM-Din 1). It is almost triangular, with a height close to its anteroposterior length. The fossa extends anteriorly onto the lateral surface of the maxilla for a short distance. There is a maxillary fenestra that is barely visible in lateral view. Posterodorsally the fossa is continuous with a pair of pneumatopores in the lacrimal, and postero-ventrally it invades the jugal. The orbit is subdivided into upper and lower regions by processes of the lacrimal and possibly by the postorbital as well, although this character, present in *Giganotosaurus* (MUCPv-CH-1), remains unclear for *Mapusaurus* n. gen. As in all other theropods, the eye was housed in the upper part of the orbital opening. A nearly vertical postorbital bar separates the orbit and lateral temporal fenestra. Based on the sizes and shapes of the jugal and quadrate, the lower temporal fenestra seems to have been as large an opening as in the other carcharodontosaurids.

The maxilla (Fig. 2) is known from three specimens from the left side (MCF-PVPH-108.11, -108.142, -108.169) and two from the right (MCF-PVPH-108.115, -108.138). The largest well preserved maxilla (MCF-PVPH-108.169) is 620 mm long, but lacks most of the jugal process (Fig. 2A, B). The maxillary tooth row is 560 mm long, which is 90 mm shorter than the preserved portion of the tooth row in the holotype of *Giganotosaurus*. MCF-PVPH-108.115 (Fig. 2C, D) is a right maxilla of a slightly smaller individual (tooth row length is 520 mm). It is virtually complete, and displays a number of differences from *Giganotosaurus*. For example, it is relatively tall compared with its length, whereas the maxilla of *Giganotosaurus* is more elongate. *Mapusaurus* n. gen. and the other carcharodontosaurids lack the elongate anterior (rostral) rami of the maxillae that are present in *Afrovenator* Sereno, Wilson, Larsson, Dutheil & Sues, 1994, “*Megalosaurus*” *hesperis* Waldman, 1974 (BMNH R332), and *Monolophosaurus* Zhao & Currie, 1993.

As in *Allosaurus* Marsh, 1877, *Sinraptor* Currie & Zhao, 1993, *Yangchuanosaurus* Dong, Chang, Li & Zhou, 1978 and most other large theropods (Currie

& Zhao 1993), the lateral surface of MCF-PVPH-108.115 is rugose only along its anterior edge and immediately above the tooth row (Fig. 2C), and is not as rugose laterally as those of abelisaurids (Bonaparte & Novas 1985; Bonaparte *et al.* 1990; Lamanna *et al.* 2002). However, MCF-PVPH-108.169 and MCF-PVPH-108.11 (Fig. 2A, B, E-G) represent larger animals than MCF-PVPH-108.115, and the external surfaces of their maxillae are more rugose. In *Giganotosaurus*, the lateral surface of the bone posterior to the narial opening is relatively smooth, whereas the lateral surface of the maxilla of *Mapusaurus* n. gen. is sculptured for most of its length.

The main body of the maxilla tapers posteriorly beneath the antorbital fossa as in *Carcharodontosaurus* (Sereno *et al.* 1996), which contrasts strongly with *Giganotosaurus* where the dorsal and ventral margins of the region below the antorbital fenestra are almost parallel for most of their length (MUCPv-CH-1). The antorbital fossa extends 75 mm beyond the anterior margin of the antorbital fenestra in MCF-PVPH-108.169 (Fig. 2A), and 70 mm in MCF-PVPH-108.115 (Fig. 2C). The smooth surface for the fossa tapers posteroventrally behind the anterior margin of the antorbital fenestra, but a ridge separates it from the lateral surface of the maxilla. As in other carcharodontosaurids, the area between the margins of the antorbital fossa and antorbital fenestra is not as extensive as in *Ceratosaurus* Gilmore, 1920, *Indosuchus* Huene & Matley, 1933 (Chatterjee 1978), *Torvosaurus* Galton & Jensen, 1979 (Britt 1991) and most coelurosaurs.

The posterior end of the lacrimal (posterior dorsal) process of the maxilla of *Mapusaurus* n. gen. (Fig. 2C) bifurcates, as in most theropods, for the insertion of the anteroventral process of the lacrimal. The posterior half of the lacrimal process, along with the nasal and lacrimal, form the dorsomedial limit of the antorbital fossa. In tyrannosauroids, in contrast, the upper limit of the antorbital fossa is formed by the lacrimal process of the maxilla (Currie pers. obs.).

Unlike *Acrocanthosaurus*, *Allosaurus* and most advanced carnosaurs (Currie & Carpenter 2000), there is only a single accessory opening in the maxilla anterior to the antorbital fenestra. This opening

is the maxillary fenestra. The fenestra is relatively small, and the opening itself is not visible in lateral aspect. However, a round depression 34 mm high leads into this fenestra in MCF-PVPH-108.115 (Fig. 2C) and can be seen posteromedial to the anterior rim of the antorbital fossa. In *Giganotosaurus*, this opening is larger (78 mm), triangular, exposed laterally, and positioned relatively lower. The single fenestra anterior to the antorbital fenestra of *Mapusaurus* n. gen. compares well with *Abelisaurus*, *Afrovenator*, *Carnotaurus*, *Ceratosaurus*, *Carcharodontosaurus*, *Giganotosaurus*, *Indosuchus*, *Majungatholus* Sues & Taquet, 1979 (Sampson *et al.* 1998), *Monolophosaurus* and *Torvosaurus*. The fenestra passes anteromedially into a medially faceted, large depression on the internal surface of the maxilla that may be the promaxillary recess, but is more likely the maxillary antrum. It is separated from a more posterior depression by a dorsally tapering bar of bone (probably the postantral strut) that rises vertically from the palatal shelf (Fig. 2B, D). This bar of bone is pierced ventrally by an opening (the posterior fenestra of the maxillary antrum) that connects the two medial depressions (MCF-PVPH-108.115, -108.169). If this bar of bone is in fact the postantral strut and the more anterior depression is the maxillary antrum, then the single opening in the anterior rim of the antorbital fossa is best interpreted as a maxillary fenestra. The floor of the maxillary antrum is pierced by a large pneumatopore (diameter of 4 cm) that leads into a huge sinus lateral to the anteromedial process (MCF-PVPH-108.11, Fig. 2E), which may be the promaxillary recess.

The pronounced anteromedial process (Fig. 2B, D, F, G) extends from the anterior end of the wide palatal shelf to protrude anteriorly beyond the level of the lateral surface (Fig. 2C) of the maxilla as in most theropods. MCF-PVPH-108.115 also shows the premaxillary suture, which tapers posterodorsally and seems to reach the nasal suture. This suggests that the maxilla was excluded from the margin of the external naris by the contact between the premaxilla and nasal as in the majority of theropods.

On the medial surface, the interdental plates are fused to each other and to the margin of the maxilla as in abelisaurids (Lamanna *et al.* 2002), *Allosaurus*

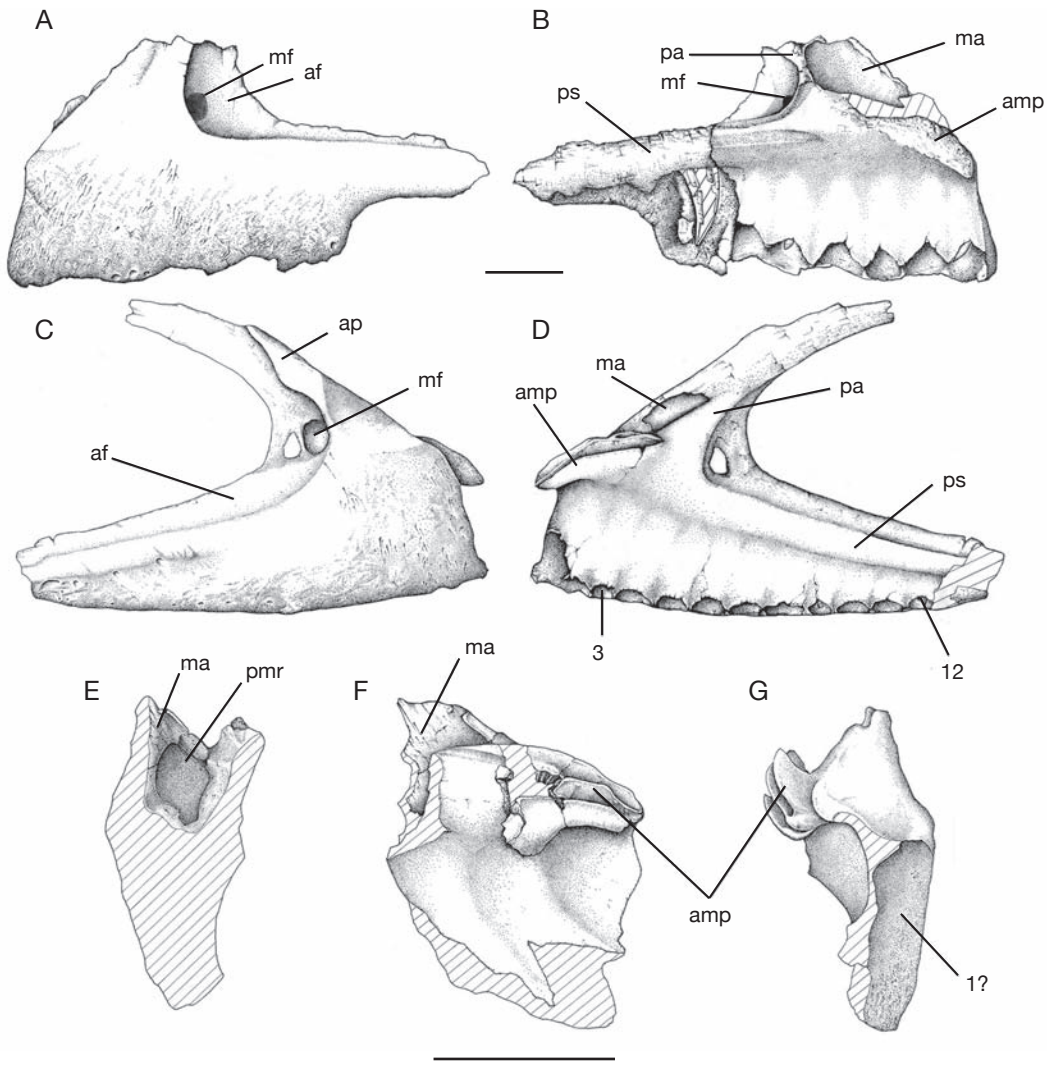


FIG. 2. — *Mapusaurus roseae* n. gen., n. sp.: A, B, left maxilla (MCF-PVPH-108.169); A, lateral view; B, medial view; C, D, right maxilla (MCF-PVPH-108.115); C, lateral view; D, medial view; E-G, left maxillary fragment (MCF-PVPH-108.11); E, posterior view; F, medial view; G, anterior view. Abbreviations: 1, 3, 12, first, third and 12th alveoli; af, antorbital fossa; amp, anteromedial process; ap, ascending process; ma, maxillary antrum; mf, maxillary fenestra; pa, postantral strut; pmr, promaxillary recess; ps, palatal shelf. Scale bars: 10 cm.

(Madsen 1976a), *Giganotosaurus* (MUCPv-CH-1), *Torvosaurus* (Britt 1991), and dromaeosaurids (Currie 1995), but in contrast with *Marshosaurus* Madsen, 1976 (Madsen 1976b), “*Megalosaurus*” *hesperis* (BMNH R332), *Monolophosaurus* (Zhao & Currie 1993), *Piatnitzkysaurus* Bonaparte, 1986, *Sinraptor* (Currie & Zhao 1993), and tyrannosau-

rids (Witmer 1997). The interdental plates do not extend as far ventrally as the lateral margin of the maxilla (Fig. 2B, D).

There are 12 maxillary alveoli in *Mapusaurus* n. gen. (MCF-PVPH-108.125, -108.169), compared with 14 in *Carcharodontosaurus* (Sereno et al. 1996). The exact number of maxillary teeth in

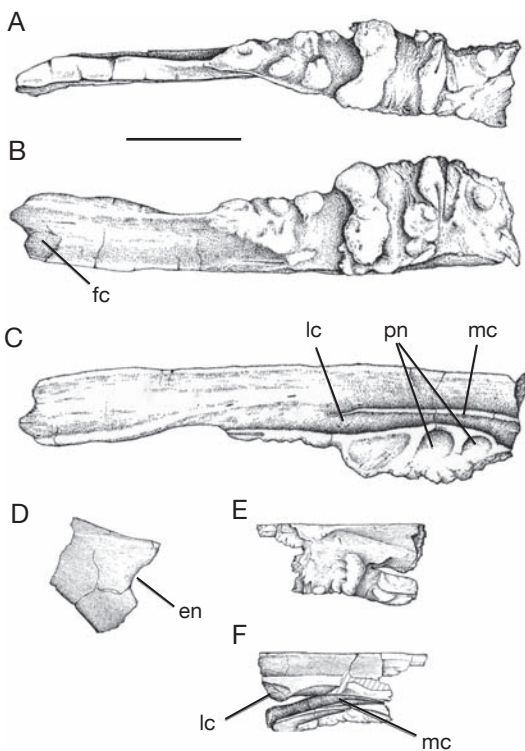


FIG. 3. — *Mapusaurus roseae* n. gen., n. sp.: A–C, right nasal (MCF-PVPH-108.1); A, lateral view; B, dorsal view; C, ventral view; D, right nasal fragment (MCF-PVPH-108.12) in lateral view; E, F, left nasal fragment (MCF-PVPH-108.17); E, dorsal view; F, ventral view. Abbreviations: en, external naris; fc, frontal contact; lc, lacrimal contact; mc, maxillary contact; pn, pneumatopores. Scale bar: 10 cm.

*Giganotosaurus* is unknown, but it was at least 12 (MUCPv-CH-1).

The long, massive nasals (MCF-PVPH-108.1, -108.12, -108.17; Fig. 3) are not co-ossified and are relatively smooth and shallowly concave behind the narial region as in carcharodontosaurids and allosauroids. The nasals show the remarkable condition of having well developed dorsolateral rugosities above the antorbital fossa (Fig. 3A–C). As in *Giganotosaurus* (MUCPv-CH-1) and *Carcharodontosaurus* (SGM-Din 1), the rugosities expand transversely anterior to the nasal-lacrimal-maxilla junction until they cover the entire dorsal surface of the anterior part of the bone (Fig. 3A, B). Rugosities on the dorsolateral margin of the

nasal are common in many other theropods, including *Allosaurus*, *Acrocanthosaurus* and *Sinraptor* (Madsen 1976a; Currie & Zhao 1993; Currie & Carpenter 2000), but they are never as prominent as in *Mapusaurus* n. gen., *Carcharodontosaurus* and *Giganotosaurus*. Abelisaurid nasals (Bonaparte & Novas 1985; Bonaparte *et al.* 1990; Sampson *et al.* 1998), in contrast, have dorsal surfaces that are convex in cross-section, and are almost entirely rugose. This is also characteristic for tyrannosauroids (Russell 1970).

The posterodorsal margin of the external naris is partially preserved in MCF-PVPH-108.12 (Fig. 3D), behind which is a shallow depression that was called a narial fossa in *Carcharodontosaurus* (Sereno *et al.* 1996). There was a long subnarial process that probably extended forward to contact the premaxilla as in most theropods.

In MCF-PVPH-108.17, there is a finger-like process extending posterolaterally from the main body of this left nasal fragment (Fig. 3E, F). It is grooved on the ventral surface, presumably for contact with the anterior tip of the lacrimal as in *Sinraptor* (Currie & Zhao 1993). There is also a long, curving trough, best seen in MCF-PVPH-108.1, for articulation with the dorsal edge of the maxilla. Lateral to the area where the trough is closest to the midline, the nasal forms a lateral shelf that roofs the antorbital fossa. As in *Allosaurus* (Gilmore 1920), *Giganotosaurus* (MUCPv-CH-1) and *Sinraptor* (Currie & Zhao 1993), this shelf is pierced by two pneumatopores (25 mm in diameter) that probably pneumatized the nasal as in *Giganotosaurus* and *Sinraptor*. Nasal pneumatopores are highly variable in number and size (Currie & Zhao 1993), and therefore should be treated with caution in phylogenetic analysis.

The lacrimal (MCF-PVPH-108.5, -108.100, -108.101, -108.183) of *Mapusaurus* n. gen. (Fig. 4) has a flattened preorbital process that expands anteroposteriorly towards the bottom as in most other theropods. In lateral view, the posterior edge of the preorbital process has a rounded projection that marks the lower limit of the eye socket (Fig. 4A, E). This small convexity is also present in *Abelisaurus* (Bonaparte & Novas 1985), *Majungatholus* (Sampson *et al.* 1998), *Monolophosaurus*,

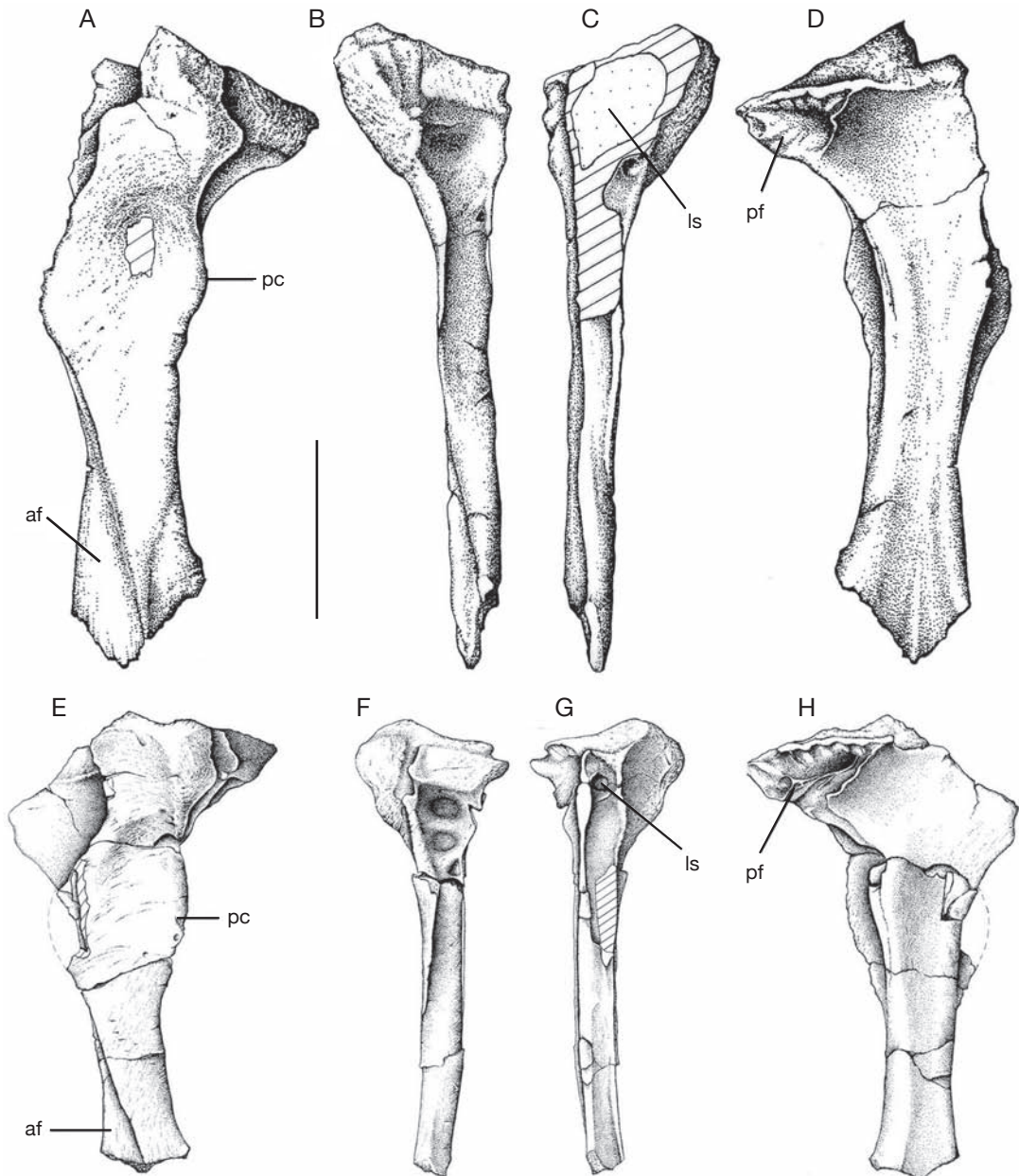


FIG. 4. — *Mapusaurus roseae* n. gen., n. sp.: A–D, left lacrimal-prefrontal complex (MCF-PVPH-108.183); A, left lacrimal in lateral view; B, posterior view; C, anterior view; D, medial view; E–H, left lacrimal (MCF-PVPH-108.5); E, lateral view; F, posterior view; G, anterior view; H, medial view. Abbreviations: af, antorbital fossa; ls, lacrimal recess; pc, preorbital convexity; pf, prefrontal. Scale bar: 10 cm.

*Sinraptor* and *Yangchuanosaurus* (Currie & Zhao 1993). The lateral surface of the upper part of this process is shallowly concave, whereas it is convex

in *Giganotosaurus*. There are well defined margins on the lateral surface for the posterodorsal and posteroventral limits of the antorbital fossa. One or

more pneumatopores expand into a large sinus (the lacrimal pneumatic recess of Witmer 1997) from the posterodorsal corner of the antorbital fossa, as in *Giganotosaurus* and most other theropods. The lacrimal duct passes through the uppermost region of the preorbital bar in MCF-PVPH-108.5 and -108.183 (Fig. 4). Unlike *Allosaurus*, *Ceratosaurus*, *Sinraptor* and albertosaurine tyrannosaurids (Currie 2003b), there is no conical lacrimal horn. The posterodorsal surface of MCF-PVPH-108.5 is in the same plane as the dorsal surface of the prefrontal, and is only slightly elevated and ridge-like on the dorsolateral margin in comparison with *Giganotosaurus* and *Carcharodontosaurus*. In both MCF-PVPH-108.5 and -108.183, despite their size difference, the angle between the dorsal and medial surfaces is 106° in anterior view. Therefore, this feature might not be controlled by ontogeny. In the largest lacrimal of *Mapusaurus* n. gen. (MCF-PVPH-108.183), which is 350 mm high, the dorsal surface is rugose, whereas that of *Giganotosaurus* (MUCPv-CH-1) has deep grooves in the long, ridge-like horn. The posterolateral edge in posterior aspect forms a sutural surface, presumably for contact with the palpebral.

The prefrontal is fused to the lacrimal (MCF-PVPH-108.5, -108.183), as in *Giganotosaurus* and many other theropods (Fig. 4D, H). It is a relatively large, triangular bone in dorsal view that is slightly wider than the adjacent part of the lacrimal in MCF-PVPH-108.5. The dorsal surface is smooth and almost flat. The prefrontal forms a posteromedial sub-horizontal ridge anterodorsal to the orbit. The posterolaterally facing surface of this ridge is smooth in MCF-PVPH-108.5, whereas in MCF-PVPH-108.183 the surface is rugose, likely for the contact with the palpebral-postorbital complex as in *Giganotosaurus* and probably *Carcharodontosaurus* (Coria & Currie 2002). This difference is correlated with a difference in size of the two specimens and is probably ontogenetic. A tall, rod-like, ventrally tapering process extends almost half way down the medial side of the orbital margin of the lacrimal (MCF-PVPH-108.5, -108.183). On the medial surface of the prefrontal, there is a triangular, interdigitating suture for the frontal (Fig. 4).

In *Mapusaurus* n. gen. (MCF-PVPH-108.4, -108.153, -108.177; Fig. 5), there is a supraorbital shelf formed either by the postorbital, or by an additional bone that is fused to the front of the postorbital as in *Giganotosaurus* (Coria & Currie 2002). On the right side of the skull of the *Giganotosaurus* holotype (MUCPv-CH-1), the supraorbital shelf is a separate bone that is best identified as the palpebral. In *Mapusaurus* n. gen., the shelf is similar in shape to that of *Giganotosaurus*, suggesting that it is formed by a co-ossified postorbital and palpebral. Palpebrals also seem to be present in *Abelisaurus* (MPCA 11098) and *Carcharodontosaurus* (SGM-Din 1).

Like *Giganotosaurus*, the palpebral of *Mapusaurus* n. gen. roofed over the orbit and contacted both the prefrontal and lacrimal anteriorly. The dorsal surface is not as rugose as that of the *Giganotosaurus* palpebral (MUCPv-CH-1). The angle between the postorbital bar and the palpebral is acute in lateral view in *Mapusaurus* n. gen. and obtuse in *Giganotosaurus*. Furthermore, the lateral margin of the palpebral extends relatively farther from the postorbital in the former genus, and curves more ventrally so that the dorsal surface can be seen in lateral aspect. Laterally, it bridged the orbital notch (an emargination of the orbital rim between the frontal, prefrontal and postorbital in most large theropods), separating the medial part of the notch from the orbital rim. In MCF-PVPH-108.4 and -108.177, the palpebral is fused posteriorly to the postorbital. The co-ossification of the bones is complete, and only a pair of foramina (Fig. 5D) marks the position of contact between the palpebral and postorbital. In MCF-PVPH-108.177, the medial edge of the palpebral is 11 mm thick (high) over the orbit, but thickens anterolaterally to 44 mm at the contact with the lacrimal. In lateral view, the palpebral is 26 mm over the orbit, but thickens posteriorly to 37 mm above the back of the orbit, where it forms a somewhat rugose boss. In *Acrocanthosaurus*, the prefrontal and postorbital form the supraorbital shelf, and the lacrimal may participate in the dorsal part of the orbital margin (Currie & Carpenter 2000). In *Tyrannosaurus rex*, the major contact is between the postorbital and lacrimal. However, one specimen, BHI 3033, has

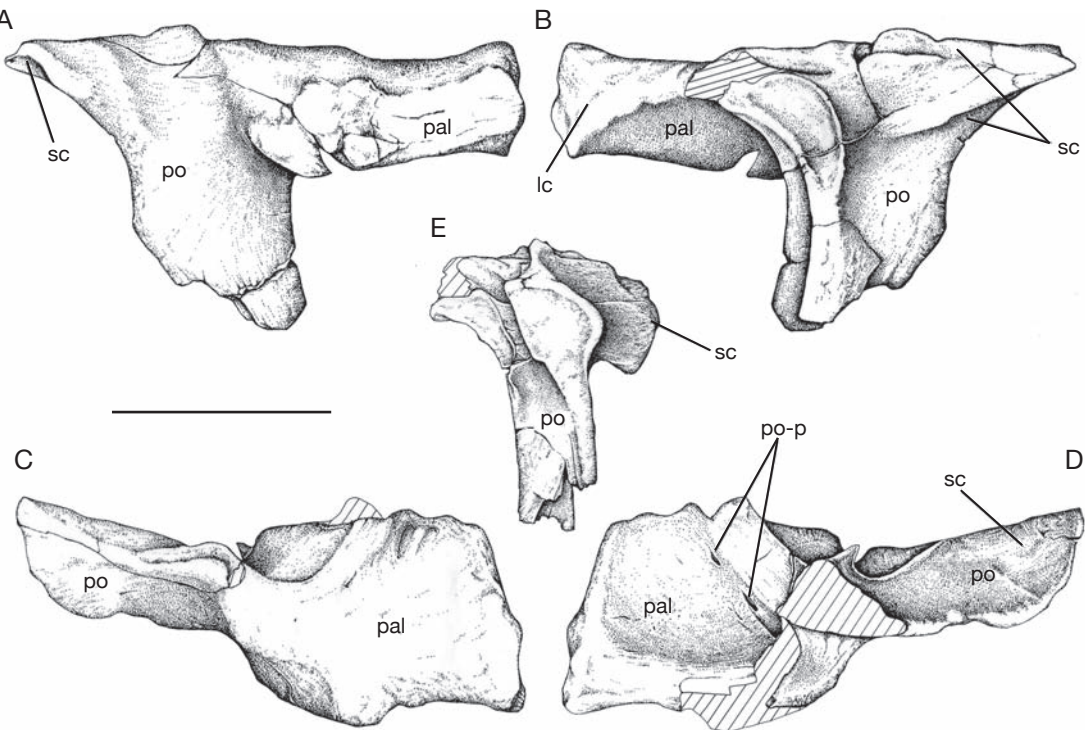


FIG. 5.—*Mapusaurus roseae* n. gen., n. sp., right postorbital-palpebral complex (MCF-PVPH-108.177): A, lateral view; B, medial view; C, dorsal view; D, ventral view; E, posterior view. Abbreviations: lc, lacrimal contact; pal, palpebral; po, postorbital; po-p, suture postorbital-palpebral; sc, supraorbital crest. Scale bar: 10 cm.

an additional, small bone that sits on the outside of the postorbital boss and appears to have been a palpebral.

Medially, the postorbital of *Mapusaurus* n. gen. (MCF-PVPH-108.4, -108.177) has a relatively small contact surface with the frontal-parietal (Fig. 5B). Posteroventral to this there is a long, concave, crescentic sutural surface for the laterosphenoid. A powerful ridge on the dorsal surface extends posterolaterally to form the anterior limit of the supratemporal fossa. As in *Giganotosaurus* (Coria & Currie 2002), this ridge slightly overhangs the fossa. Behind the ridge, the dorsal surface of the postorbital is deeply invaded anteromedial to the intertemporal bar for the origin of temporal musculature. On the medial surface of the intertemporal bar there is a deep groove near the dorsal margin for the upper fork of the anterior ramus of the squamosal (Fig. 5B). Ventrally, the jugal ramus of the

postorbital is anteroposteriorly broad and forms a convex projection into the anterodorsal corner of the lateral temporal fenestra.

Two left jugals (MCF-PVPH-108.167, -108.168) were recovered from the Cañadon del Gato bonebed (Fig. 6). The anterolateral surface of the jugal is depressed where it contributes to the antorbital fossa (Fig. 6A). A single, 36 mm high slit-like pneumatic opening (jugal pneumatic recess) invades the jugal from the posteroventral edge of this depression in MCF-PVPH-108.168. *Allosaurus* (USNM 4734, UUVP 1403, UUVP 3894, UUVP 3981), *Molophosaurus* (Zhao & Currie 1993), sinraptorids (Currie & Zhao 1993) and tyrannosaurids also have pneumatized jugals. However, only the last two taxa have openings that are as large as *Mapusaurus* n. gen. The ventral margin of the front of the jugal (MCF-PVPH-108.168; Fig. 6A, D) is emarginated for its contact with the maxilla. This

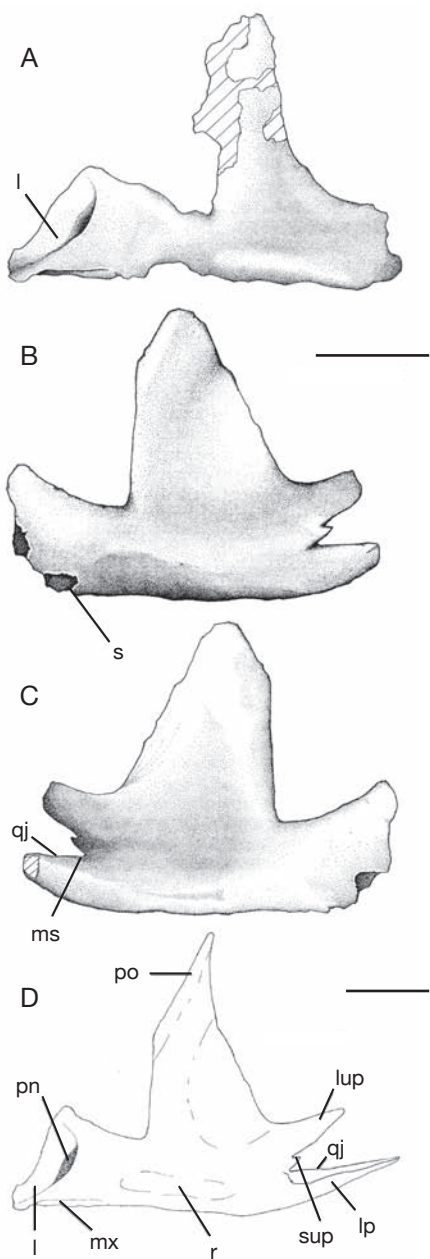


FIG. 6. — *Mapusaurus roseae* n. gen., n. sp.: A, left jugal (MCF-PVPH-108.167) in lateral view; B, C, left jugal (MCF-PVPH-108.168); B, lateral view; C, medial view; D, reconstruction of jugal in lateral view. Abbreviations: I, overlapping external surface of maxilla; lp, lower prong; lup, large upper prong; ms, medioventral shelf; mx, maxillary suture; pn, pneumatopore (jugal pneumatic recess); po, postorbital suture; qj, quadratojugal suture; r, ridge; s, socket for back of maxilla; sup, small upper prong. Scale bars: 10 cm.

contact, which overlaps the maxilla dorsally and somewhat medially, ends posteriorly in a socket below the orbit (Fig. 6B). Close to the anterior end of the jugal, there is a lappet on the ventrolateral margin that overlaps the external surface of the maxilla (Fig. 6B, D). There is a conspicuous ridge on the lateral surface of the jugal posteroventral to the orbit (Fig. 6A, B, D). This is in the position of a low, cone-like process or rugosity in many large theropods, and presumably marked the attachment of cheek musculature. The postorbital process of the jugal is triangular in lateral view, and distinctly broad-based (Fig. 6). As in *Sinraptor* and *Allosaurus*, the sloping, laterally overlapping contact for the postorbital bone does not reach the lower margin of the orbit, whereas in *Edmarka* these are at the same level (Bakker *et al.* 1992). In most theropods, the quadratojugal process of the jugal splits posteriorly into two prongs. In *Mapusaurus* n. gen. (MCF-PVPH-108.167), the upper of the two prongs autapomorphically subdivides into two, so there is in fact a total of three prongs on the quadratojugal process of the jugal (Fig. 6B, D). The short lower process of the upper prong presumably fits in a groove on the anterolateral surface of the quadratojugal. The dorsal edge of the lower prong was laterally overlapped by the anteroventral margin of the quadratojugal. This suture extends anteriorly beyond the bifurcation of the prongs. Curiously, the jugal of *Sinraptor dongi* also has three quadratojugal prongs (Currie & Zhao 1993), although it is the lower of the normal two prongs that subdivides into two, and it fits on a groove on the internal surface of the quadratojugal. The upper and lower quadratojugal processes of MCF-PVPH-108.168 are incomplete distally so it is not possible to determine which one was longer. The lower prong is lateromedially thicker, however, suggesting that it may have been longer than the dorsal process. The medial surface of the jugal (Fig. 6C) is concave at the base of the postorbital process, and the concavity extends posteriorly to form a deep trough between the prongs of the quadratojugal process. The ventral prong forms a broad medioventral shelf (Fig. 6C) as in *Sinraptor*.

The quadrate (MCF-PVPH-108.6, -108.102, -108.170) of *Mapusaurus* n. gen. (Fig. 7) is tall

with a broadly expanded mandibular articulation as in *Giganotosaurus* and abelisaurids. The preserved quadrates are between 310 and 350 mm tall, all of which are significantly less than the 410 mm tall quadrate of *Giganotosaurus*. In contrast with abelisaurids and *Ceratosaurus* (Bakker 2000), a quadratic foramen is present between the quadrate and quadratojugal, although it was relatively small compared with those of dromaeosaurids, tyrannosaurids and many other theropods (Fig. 7A, C, D). The quadratic foramen of allosauroids is different in that it is virtually surrounded by the quadrate in *Acrocanthosaurus* (Currie & Carpenter 2000), *Allosaurus* (Madsen 1976a) and *Sinraptor* (Currie & Zhao 1993). Unlike *Carnotaurus* and tyrannosaurids, there is no fusion between quadrate and quadratojugal. Instead, it shows a comparable condition to *Giganotosaurus*, *Sinraptor* and other primitive theropods. The ventral suture for the quadratojugal is almost round (MCF-PVPH-108.6) and has a rugose, slightly concave surface. The pterygoid flange of MCF-PVPH-108.170 (Fig. 7B) is as long (179 mm) anteroposteriorly as it is tall. The quadrate cotyle is considerably smaller than that of *Giganotosaurus*. Although the largest quadrate of *Mapusaurus* n. gen. is only 77% that of the holotype of *Giganotosaurus*, the diameter of the quadrate cotyle is only 64%. The quadrate of *Mapusaurus* n. gen. (MCF-PVPH-108.102) is pneumatic like those of tyrannosaurids. The pneumatopore is on the medial surface of the quadrate between the pterygoid flange and the main vertical shaft of bone. It is 20% of the total height of the bone in MCF-PVPH-108.170 (Fig. 7C). A ridge extends anteriorly (and somewhat dorsally) above the depression housing the pneumatopores and extends onto the medial surface of the pterygoid flange. This ridge defines the ventral margin of a second pneumatic depression that is also well defined in tyrannosaurids (Currie 2003b).

Four partial dentaries (MCF-PVPH-108.2, -108.3, -108.39, -108.125) have been collected from the Cañadón del Gato bonebed (Fig. 8). The minimum height of the dentigerous part of the dentary is 112 mm in MCF-PVPH-108.2 (Fig. 8A, B), whereas MCF-PVPH-108.3 (Fig. 8E, F) is half the height (56 mm) and represents a juvenile with a

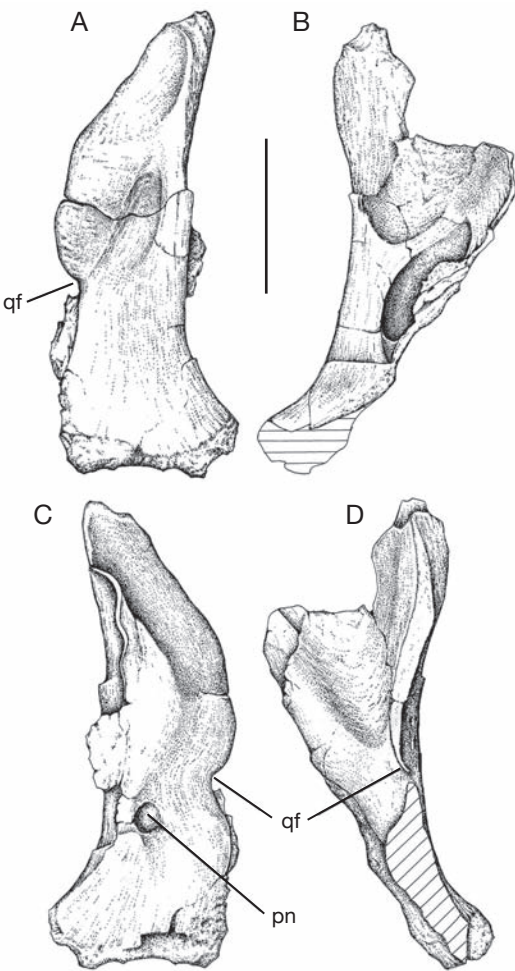


FIG. 7. — *Mapusaurus roseae* n. gen., n. sp., left quadrate (MCF-PVPH-108.102): A, posterior view; B, medial view; C, anterior view; D, lateral view. Abbreviations: pn, pneumatopore; qf, quadratic foramen. Scale bar: 10 cm.

body length of about 5 to 5.5 m (Table 1). MCF-PVPH-108.125 (Fig. 8C, D) is an almost complete dentary, 440 mm long with a minimum height of 72 mm. By comparison, the dentary of the *Giganotosaurus* holotype is 135 mm deep, and that of MUCPv-CH-95 (Calvo & Coria 2000) is 138 mm. *Mapusaurus* n. gen. is like *Giganotosaurus* in that the dentary expands anteriorly to a greater degree than most other theropods. A flange at the ventral end of the symphysis emphasizes this expansion.

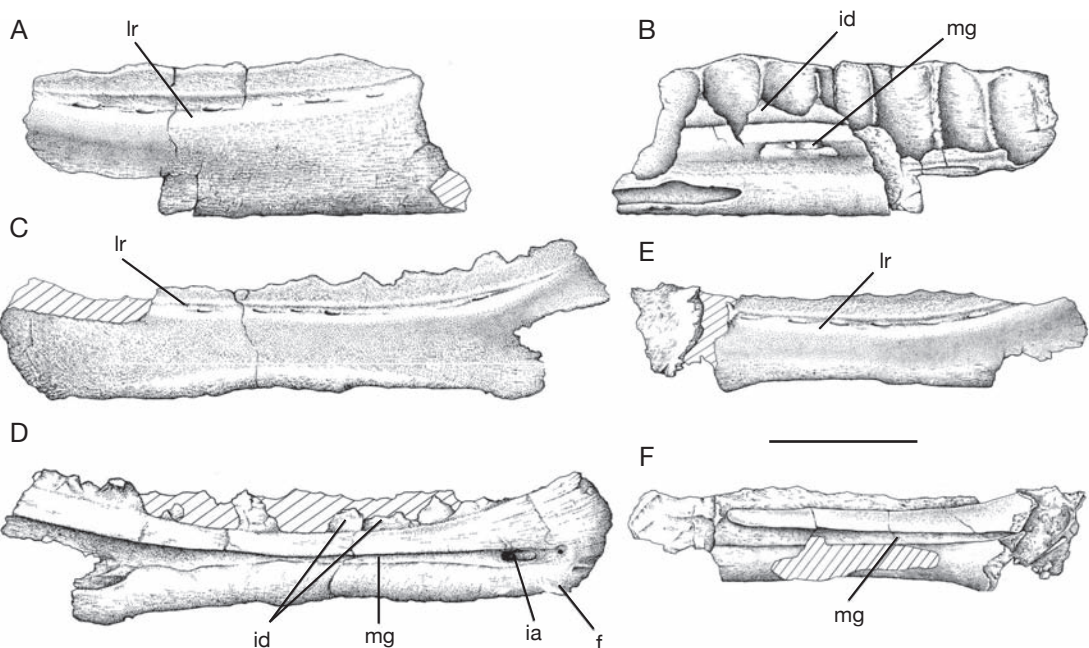


FIG. 8. — *Mapusaurus roseae* n. gen., n. sp.: **A, B**, right dentary (MCF-PVPH-108.2); **A**, lateral view; **B**, medial view; **C, D**, left dentary (MCF-PVPH-108.125); **C**, lateral view; **D**, medial view; **E, F**, left dentary (MCF-PVPH-108.3); **E**, lateral view; **F**, medial view. Abbreviations: **f**, flange at ventral end of symphysis; **ia**, inferior alveolar nerve foramen; **id**, interdental plate; **lr**, lateral ridge; **mg**, Meckelian groove. Scale bar: 10 cm.

The fact that it is present in a small specimen (MCF-PVPH-108.125) shows that the feature is not controlled by ontogeny, as it appears to be in tyrannosaurids where it is present in only the largest specimens of *Tyrannosaurus rex*. It is not known whether this flange is present in *Carcharodontosaurus*, and it is not present in *Acrocanthosaurus* (Currie & Carpenter 2000). In MCF-PVPH-108.3, the dorsoventral expansion at the front of the dentary is 18% higher than it is at the level of the eighth alveolus. In MCF-PVPH-108.125 (Fig. 8C, D), the upper margin at the front of the dentary is broken externally, but medially the front of the jaw is about 24% deeper than minimum dentary height. In comparison, dentary height increases anteriorly in *Giganotosaurus* by 33%. *Acrocanthosaurus* (Currie & Carpenter 2000) and other large theropods also have dentaries that increase in height between mid-length and the front, but the increase rarely amounts to much more than 10%.

The lateral surface of the large dentary of *Mapusaurus* n. gen. is not as rough as that of *Giganotosaurus*, but is more textured than that of the juvenile. There is a prominent lateral longitudinal ridge that extends from the level of the third tooth to the posterior end of the dentigerous part of the dentary. There is a row of foramina above the ridge as in most theropods. Unlike *Sinraptor*, *Allosaurus* and most other theropods, however, the foramina do not become more dispersed posteriorly. Each foramen is positioned between a pair of tooth sockets, just as they are in *Giganotosaurus*. There are significant differences between these two animals on the medial surface of the dentary, however. The interdental plates are fused in both genera, but are only about half the height in *Mapusaurus* n. gen. The Meckelian groove is shallow in both, but is positioned higher in *Mapusaurus* n. gen. (52% of the height from the bottom in the juvenile, 38% in the adult) than *Giganotosaurus* (31%). Both of

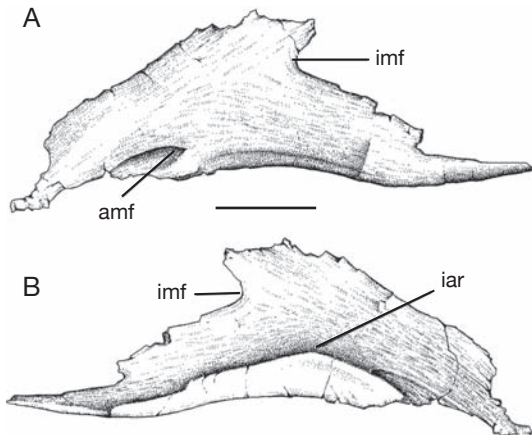


FIG. 9. — *Mapusaurus roseae* n. gen., n. sp., left splenial (MCF-PVPH-108.179): A, medial view; B, lateral view. Abbreviations: amf, anterior mylohyoid foramen; iar, infra-angular ridge; imf, internal mandibular fenestra. Scale bar: 10 cm.

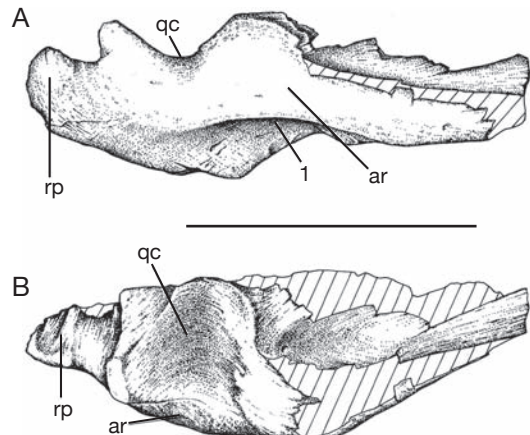


FIG. 10. — *Mapusaurus roseae* n. gen., n. sp., right surangular (MCF-PVPH-108.15): A, lateral view; B, dorsal view. Abbreviations: 1, fossa for (*M.*) *adductor mandibulae externus*; ar, adductor ridge; qc, quadrate cotyle; rp, retroarticular process. Scale bar: 10 cm.

these characters may be related to absolute size or ontogeny. The exit for the symphyseal ramus of the inferior alveolar nerve (Fig. 8D) opens at the front of the Meckelian canal in *Mapusaurus* n. gen., *Giganotosaurus* (MUCPv-CH-1), *Allosaurus* (Madsen 1976a), *Sinraptor* (Currie & Zhao 1993) and other theropods.

The third to 10th alveoli, identified by comparison with the dentary of *Giganotosaurus* (MUCPv-CH-1), are preserved in MCF-PVPH-108.2 (Fig. 8B), and their dimensions suggest they contained large teeth. The anteroposterior diameter of each alveolus is about 40 mm, which is the same size as in the holotype of *Giganotosaurus*. Although the front of the juvenile jaw is damaged, nine alveoli are present. This suggests that *Mapusaurus* n. gen. had about 15 dentary tooth positions compared with the complete dentaries known in the holotype specimen of *Giganotosaurus*.

One large right splenial (MCF-PVPH-108.179) was collected (Fig. 9). Although some of the thinner edges are incomplete, the specimen is 525 mm long. It is a relatively thin, curved plate of bone, concave laterally and almost flat medially. The ventral margin has a gentle, sigmoidal curvature in lateral view, whereas that of *Allosaurus* is almost

straight (Madsen 1976a). The posterior margin is emarginated to form the anterior border of the internal mandibular fenestra, which is positioned far forward (44% of the total length) from the back of the splenial. The ventral margin of the bone thickens posterolaterally to form a prominent ridge that contacts the medial surface of the dentary and cradles the anterior end of the angular (Fig. 9). The splenial does not wrap around the ventral margin of the dentary as in *Herrerasaurus* (Sereno & Novas 1993), *Ceratosaurus* (USNM 4735), and dromaeosaurids (Currie 1995). The anterior mylohyoid foramen (Meckelian canal) is completely surrounded by the splenial and is positioned above the dentary contact (Fig. 9A) like in *Sinraptor* (Currie & Zhao 1993). In contrast, the mylohyoid opening in *Allosaurus*, *Monolophosaurus* and tyrannosaurids is positioned relatively lower, passes through the ridge that contacts the dentary, and is often a ventrally open slot rather than a foramen. The anteroposterior diameter of the foramen is relatively small (21 mm), as in all theropods except tyrannosaurids.

A partial right surangular (MCF-PVPH-108.15) is known from a small individual of *Mapusaurus* n. gen. (Fig. 10). It is similar to the surangular of

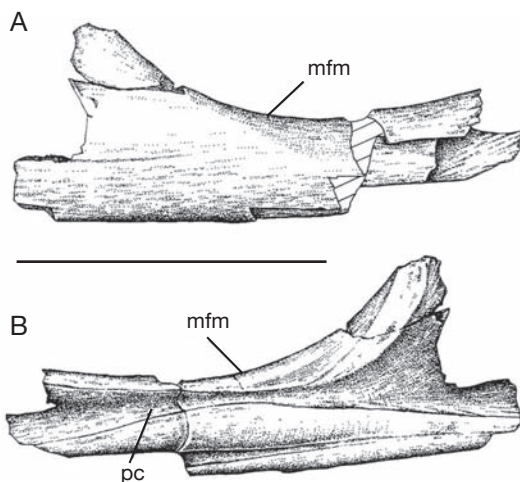


FIG. 11. — *Mapusaurus roseae* n. gen., n. sp., left prearticular (MCF-PVPH-108.139): A, medial view; B, lateral view. Abbreviations: mfm, mandibular fenestra margin; pc, prearticular contact. Scale bar: 10 cm.

*Giganotosaurus* (MUCPv-CH-1) in all respects. The surangular formed most of the lateral cotyle of the articulation with the quadrate, and extended posteriorly to participate in the lateral margin of the short retroarticular process (Fig. 10). Antero-laterally, the surangular formed a broad, shelf-like ridge, the dorsal surface of which was a wide, deeply concave fossa for insertion of the (*M.*) *adductor mandibulae externus* (Fig. 10A) as in *Giganotosaurus*, *Acrocanthosaurus* and *Tyrannosaurus*. Below the ridge, the surangular sloped ventromedially at a higher angle than almost all theropods other than *Giganotosaurus* (MUCPv-CH-1) and *Carnotaurus* (MACN-CH 894). In most theropods, the surangular tends to be almost vertical beneath the lateral “adductor ridge”, which is rarely so prominent (Fig. 10A). The result is that the ventromedial edge of the surangular is positioned directly under the middle of the jaw articulation. There is a shallow canal that extends anteromedially beneath the adductor ridge to enter the small posterior surangular foramen (Fig. 10A).

The angular is represented in the collection by a single fragment from the right side (MCF-PVPH-108.7). The bone is strengthened by a thick margin that formed part of the ventral edge of the mandible.

There is a shallow, posteromedial groove along this margin for the prearticular contact, which tapers posteriorly as the bone thins and is replaced by the prearticular on the ventral margin of the jaw.

The central part of a left prearticular (MCF-PVPH-108.139) was recovered from the *Mapusaurus* n. gen. bonebed (Fig. 11). On the lateral surface, the ventral ridge is grooved for its contact with the angular (Fig. 11B). This groove is oriented postero-dorsally, showing that the prearticular would have had limited exposure in lateral view posteriorly. The features preserved suggest that the bone is conservative and is not significantly different from the prearticulars of *Allosaurus* (Madsen 1976a) and *Sinraptor* (Currie & Zhao 1993).

### Teeth

Teeth with crowns and roots are scattered throughout the quarry. They are relatively flat, narrow blades (Table 2) that are similar to the teeth of other carcharodontosaurids (Sereno *et al.* 1996; Novas *et al.* 1999; Vickers-Rich *et al.* 1999). MCF-PVPH-108.8 (Fig. 12A) seems to be an anterior right dentary tooth. MCF-PVPH-108.9 (Fig. 12B) is close in size but has a taller but narrower crown. It seems to have been a mid-dentary tooth from the right side. Both anterior and posterior carina extended to the base of the enameled crown. Two other teeth, MCF-PVPH-108.10 (Fig. 12C) and MCF-PVPH-108.103, are shorter but come from the backs of the jaws of large individuals. The smallest tooth has 12 denticles per 5 mm, whereas the next smallest tooth has 10 denticles per 5 mm on anterior and posterior carina. There are eight to nine denticles per 5 mm in the larger teeth (Table 2), which compares well with *Giganotosaurus* and *Carcarodontosaurus*. These are much larger than the denticles in large *Acrocanthosaurus* teeth (Currie & Carpenter 2000) where there are 13 to 15 serrations per 5 mm.

The anterior carina of the anterior dentary tooth (MCF-PVPH-108.8) is lingual in position to the midline (on the vertical plane passing through the long axis of the cross section) of the tooth. In more posterior teeth (MCF-PVPH-108.9, -108.10), the anterior carina follows the midline. The posterior carina of the anterior dentary tooth twists labial to the midline. However, when the anterior dentary

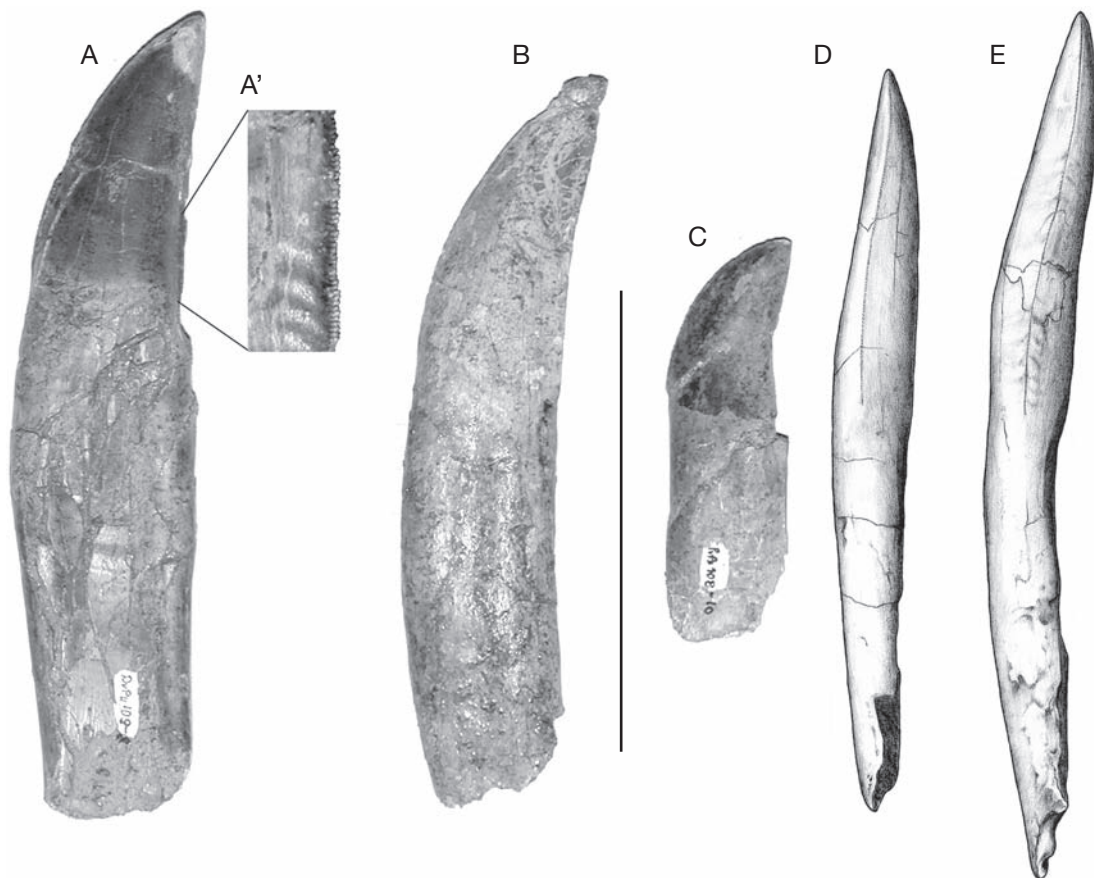


FIG. 12. — **A-D**, *Mapusaurus roseae* n. gen., n. sp.: **A**, tooth (MCF-PVPH-108.8) in labial view; **A'**, close up of posterior denticles and enamel crenulations of MCF-PVPH-108.8; **B**, tooth (MCF-PVPH-108.9) in labial view; **C**, tooth (MCF-PVPH-108.10) in labial view; **D**, tooth (MCF-PVPH-108.9) in posterior view; **E**, *Giganotosaurus carolinii*, tooth (MUCPv-CH-1) in posterior view. Scale bar: 10 cm.

tooth was in the jaw, the tooth was oriented so that the plane passing through the anterior and posterior carina was parallel to the sagittal skull plane. Farther back in the jaws, the carinae coincide with tooth midlines and both are parallel to the sagittal skull plane. When viewed anteriorly or posteriorly, a *Mapusaurus* n. gen. tooth has a flattened S-shaped curvature such as is also seen in *Giganotosaurus* (Fig. 12D, E). When the crown exits the alveolus, it is curving labially. But towards the tip, it curves lingually. The carinae describe the same crown curvature.

Individual serrations are wider (labiolingually) than they are dorsoventrally long, but the dispar-

ity is not nearly as great as it is in tyrannosaurids. Blood grooves, similar to those of tyrannosaurids (Currie *et al.* 1990), extend onto the surface of the tooth from between the bases of most denticles. Crenulations (wrinkles, undulations) in the enamel curve towards the posterior denticles on the labial surface of MCF-PVPH-108.8, but are not present in the other teeth. Similar arcuate crenulations are characteristic of *Carcharodontosaurus* (Sereno *et al.* 1996), *Giganotosaurus* (MUCPv-CH-1) and other theropods attributed to the Carcharodontosauridae (Chure *et al.* 1999). They are not present in the teeth of *Acrocanthosaurus* (NCSM 14345). However, wrinkles in the enamel are also present in isolated

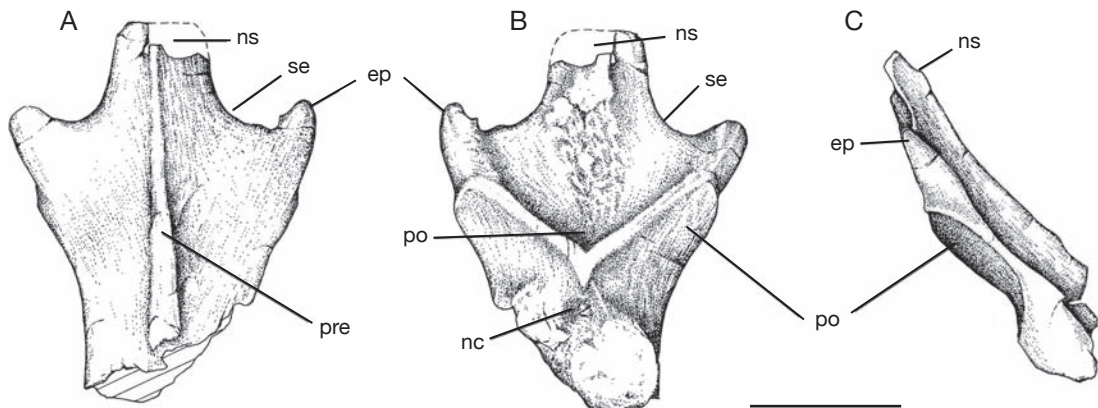


FIG. 13. — *Mapusaurus roseae* n. gen., n. sp., axis neural arch (MCF-PVPH-108.83): A, anterodorsal view; B, posteroventral view; C, lateral view. Abbreviations: ep, epipophysis; nc, roof of neural canal; ns, neural spine; po, postspinal basin; pre, prespinal lamina; se, spinopropophysial lamina. Scale bar: 10 cm.

theropod teeth from around the world, including those of tyrannosaurids (Currie *et al.* 1990), so their taxonomic significance is presently unclear.

#### Vertebrae

Measurements of MCF-PVPH-108.83, the neural arch of an axis, show it is about the same size as that of the *Giganotosaurus* holotype. The axial neural arch of *Mapusaurus* n. gen. (Fig. 13) is morphologically similar to that of *Giganotosaurus* (MUCPv-CH-1), and to a lesser extent *Sinraptor*. The neural arch inclines posterodorsally as in most carnosaurs. Anteriorly it does not extend beyond the anterior zygapophyses as it does in forms like *Carnotaurus* and *Ceratosaurus*. The epipophysis is more prominent than it is in *Allosaurus* (Madsen 1976a) and *Acrocanthosaurus* (Harris 1998), but is relatively shorter than that of *Sinraptor* (Fig. 13). The conical, slightly curving epipophysis tapers distally, unlike the broader, tab-like epipophysis of *Giganotosaurus*. The neural spine is incomplete distally, but seems to be somewhat longer and more gracile than that of *Giganotosaurus*. The neural spine of *Mapusaurus* n. gen. is connected to the epipophysis by a well developed spinopropophysial lamina with a shallowly emarginated posterior edge (Fig. 13A, B). *Acrocanthosaurus* and *Allosaurus* lack these laminae and have stronger separations between neural spines and epipophyses. The neural

spines of these latter animals are taller and more expanded distally than in *Giganotosaurus* and likely in *Mapusaurus* n. gen. The posterior zygapophyses join on the midline, forming a V-shaped shelf below a deep depression (postspinal basin) at the base of the neural spine (Fig. 13B). In contrast, the posterior zygapophyses of *Giganotosaurus* are separate and the depression is open ventrally to the margin of the neural canal. The prespinal lamina on the midline of MCF-PVPH-108.83 is shallower and less elaborate than in *Giganotosaurus*.

The neural arch of a large mid-cervical (MCF-PVPH-108.90) is poorly preserved. The complete neural spine is low (60 mm anterior to the epipophysis) and relatively long (120 mm posterior to the prespinal basin). The dorsal margin is remarkably sharp, a condition not reported in any other large theropod. Equivalent sized vertebrae from the holotype of *Giganotosaurus* have taller and much wider neural spines. The anterodorsal length of the spine is similar to the conditions in *Allosaurus* and *Sinraptor*, but the height is more reminiscent of the condition described for abelisaurids (Bonaparte 1991). The epiphyses of this vertebra are incomplete, but an isolated cervical epiphysis (MCF-PVPH-108.162) has the same claw-like shape as that of the axis.

MCF-PVPH-108.82 (Fig. 14) is probably one of the cervicodorsals (11th to 13th presacrals)

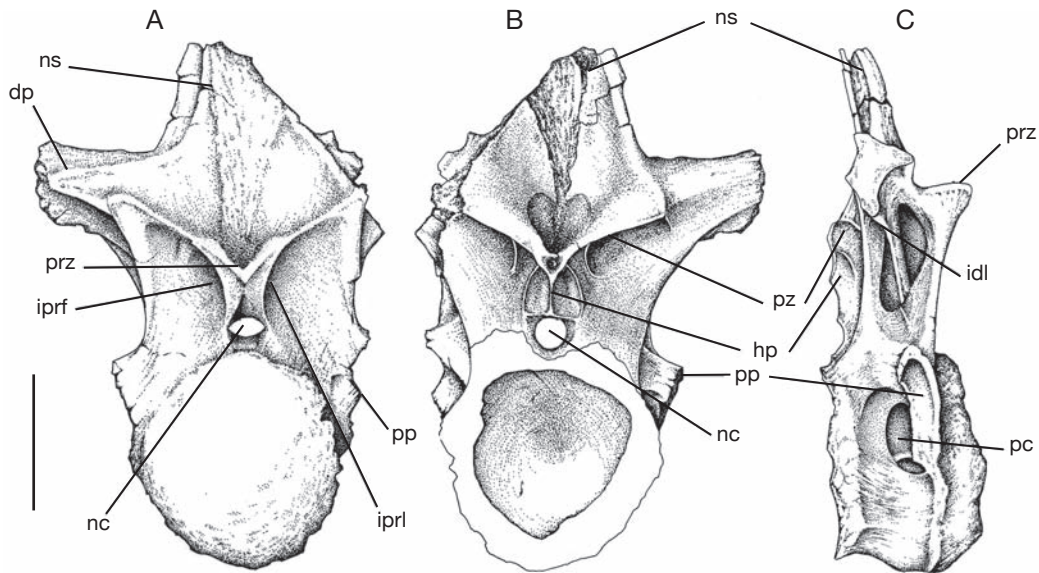


FIG. 14. — *Mapusaurus roseae* n. gen., n. sp., cervicodorsal vertebra (MCF-PVPH-108.82): A, anterior view; B, posterior view; C, right lateral view. Abbreviations: **dp**, diapophysis; **hp**, hypophene; **idl**, infradiapophysial laminae; **iprf**, infraprezygapophysial fossa; **iprl**, infraprezygapophysial laminae; **nc**, neural canal; **ns**, neural spine; **pc**, pleurocoel; **pp**, parapophysis; **prz**, prezygapophysis; **pz**, postzygapophysis. Scale bar: 10 cm.

vertebrae because the parapophysis spans the neurocentral suture and the centrum has a hypopophysis. As preserved, it is 390 mm in total height, and the neural arch is 227 mm measured from the bottom of the neural canal (Fig. 14A, B). The anterior zygapophyses meet on the midline and there is no hyantrum (Fig. 14A). A robust shelf joins the prezygapophysis to the diapophysis. Below their V-shaped contact is a pair of ridges (infraprezygapophysial laminae) that extend to the lateral margins of the neural canal. The anterior face of the neural arch is shallowly excavated lateral to each of these ridges. The width across the diapophyses would have been 310 mm. The opisthocoelic centrum is 87 mm long (excluding the ball-like anterior intercentral articulation), and on the posterior side is 174 across and 15 mm high (Fig. 14B). The neural arch is broad, and anteriorly is 150 mm across at the level of the neural canal, which has a diameter of 38 mm. The width across the anterior zygapophyses is 80 mm, and the inclined articular surface of the prezygapophysis is 100 mm. A relatively thick lamina connects the

prezygapophysis to the parapophysis (Fig. 14C). Two infradiapophysial laminae diverge ventrally, one converging with the posterodorsal corner of the centrum and the other with the parapophysis. A large infraprezygapophysial fossa penetrates deep into the interior of the neural arch (Fig. 14A). The infradiapophysial fossa also seems to extend into the core of the bone. It is 150 mm across the posterior zygapophyses, and each articular facet is 68 mm across and 32 mm anteroposteriorly. The medial margin of each facet turns ventromedially to form the hypophene (Fig. 14B). A medial ridge extends from the hypophene to the top of the neural canal, whereas a second, more lateral ridge ends at the dorsolateral corner of the neural canal. These two ridges are separated by a shallow concavity. A more lateral, relatively short ridge is the supplementary infrapostzygapophysial lamina, anterior to which is a pneumatic fossa. Each side of the centrum has two pneumatopores posteroventral to the dorsoventrally elongate parapophysis. There is a strong, sharp ventral keel (hypopophysis), almost 2 cm high, along the midline of the centrum.

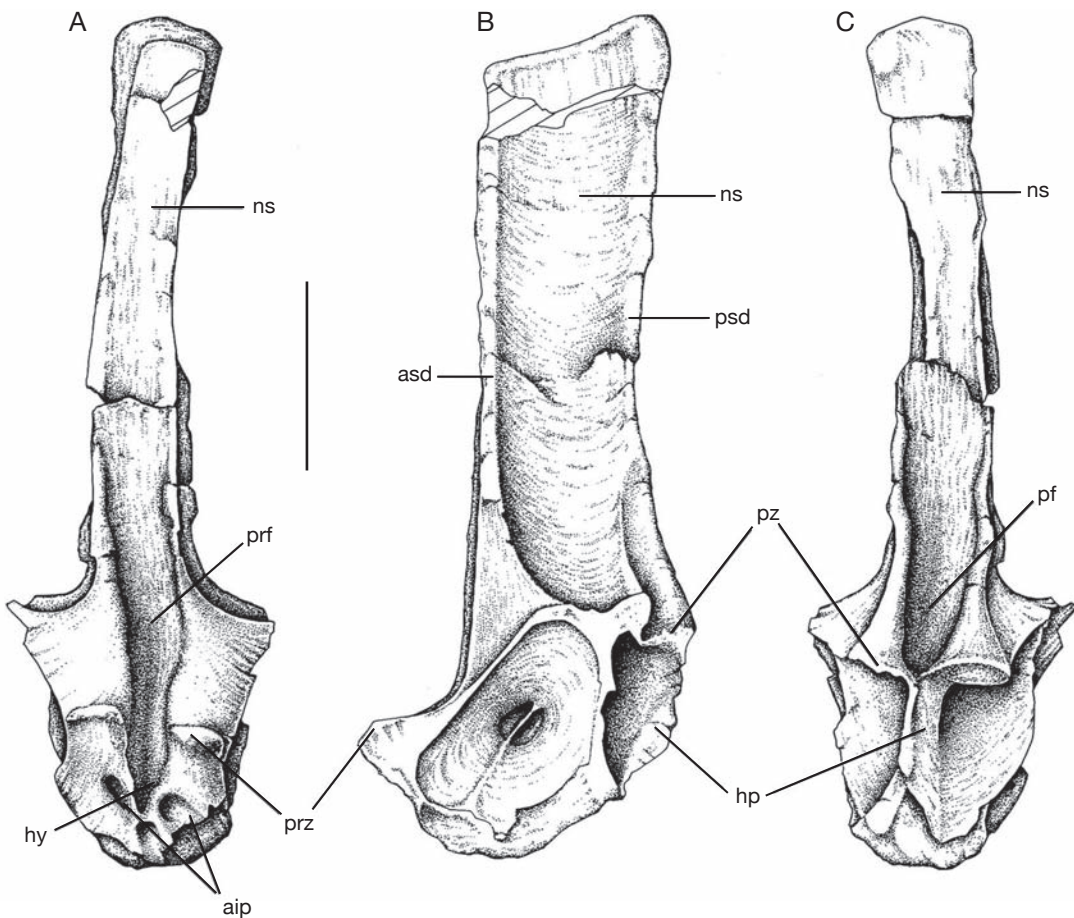


FIG. 15. — *Mapusaurus roseae* n. gen., n. sp., dorsal vertebra (MCF-PVPH-108.84): A, anterior view; B, lateral view; C, posterior view. Abbreviations: aip, anterior infraprezygapophysial fossae; asd, anterior spinodiapophysial lamina; hp, hypophene; hy, hypantrum; ns, neural spine; pf, postspinal fossa; prf, prespinal fossa; prz, prezygapophysis; psd, posterior spinodiapophysial lamina; pz, postzygapophysis. Scale bar: 10 cm.

The dorsal neural spines are relatively tall, and incline somewhat posteriorly. In MCF-PVPH-108.84 (Fig. 15), the entire arch of a mid-dorsal is preserved. There are anteriorly facing, deep circular fossae (infraprezygapophysial fossae) beneath the prezygapophyses (Fig. 15A). There are infrapost-, and infradiapophysial fossae separated by thin laminae that converge dorsally at the transverse process (Fig. 15B). Above the transverse processes, both sides of the neural spine are deeply excavated and are bordered by anterior and posterior spinodiapophysial laminae (Fig. 15B). There are also

excavations (prespinal and postspinal fossae) in the base of the neural spine between the prezygapophyses and the postzygapophyses (Fig. 15A, C). The neural spine is tall (410 mm in MCF-PVPH-108.84; 490 mm in -108.85) and rectangular in side view (the minimum anteroposterior length of the spine at midheight in MCF-PVPH-108.84 is 78 mm, but the spine expands distally to 95 mm; the same measurements are 92 and 108 in MCF-PVPH-108.85). The anterior, posterior and distal margins of the neural spine are transversely thick, whereas the central region of the blade is trans-

versely thin. In cross section, the neural spine has the shape of an I-beam (the thicker parts being the reinforced, rugose areas of attachment for the interspinous ligaments). The forward projecting prezygapophyses are relatively small, and are separated by a deep hypantrum. The articular surfaces are oriented dorsally and slightly laterally, and are almost horizontal. The distance between the lateral margins of the posterior zygapophyses is 100 mm in MCF-PVPH-108.84. There is a deep (46 mm), blade-like hypophene that projects posteriorly to at least the same level as the postzygapophyses.

Posterior dorsal centra of *Mapusaurus* n. gen. are amphiplatyan. MCF-PVPH-108.80 is 165 mm long, 205 mm wide (anterior end) and 215 mm tall (from the floor of the neural canal). There is a large (60 mm long by 45 mm tall), deep pleurocoel on each side of the centrum, each of which may be divided into two smaller pneumatopores as in *Giganotosaurus* (MUCPv-CH-1) and *Carcharodontosaurus* (Russell 1996).

Two unfused, sacral centra (MCF-PVPH-108.89, -108.209) were recovered from relatively young animals. Both are transversely narrow, a feature emphasized by crushing. MCF-PVPH-108.209 (Fig. 16) is the first sacral centrum, and has an anterior intervertebral articulation that is taller (150 mm) than broad (approximately 120 mm) (Fig. 16A). The posterior face does not expand much laterally or ventrally, is much narrower than the anterior articular surface, and has a roughened surface for contact with the second sacral. At midlength, the sacral is 43 mm wide, and the ventral surface is broadly convex in section. A small contact surface for the first sacral rib is found on the anterodorsal corner of the centrum, and a large (49 mm) contact surface for the second sacral rib is found on the posterodorsal corner of the centrum. The flat floor of the neural canal is 116 mm long, 20 mm wide anteriorly and 9 mm wide in the middle. The floor of the intervertebral (conjunction) foramen passes anterolaterally across the top of the second sacral rib contact as in *Allosaurus* (Madsen 1976a). There is a small round pleurocoel positioned near the anterodorsal corner of each side of the centrum (Fig. 16). MCF-PVPH-108.89 is another unfused sacral centrum, possibly the fifth that is 135 mm

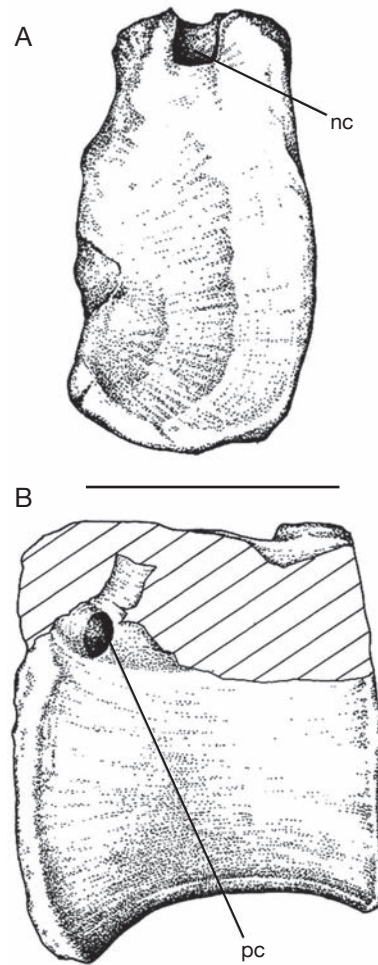


FIG. 16. — *Mapusaurus roseae* n. gen., n. sp., sacral centrum (MCF-PVPH-108.209): A, anterior view; B, lateral view. Abbreviations: nc, neural canal; pc, pleurocoel. Scale bar: 10 cm.

in anteroposterior length. The dorsolateral surface is depressed, contains two shallow pits, and has no pleurocoels.

Numerous caudal vertebrae were recovered (Fig. 17). The transverse processes of an anterior caudal vertebra (MCF-PVPH-108.81) extend laterally and somewhat posteriorly for 210 mm (Fig. 17A-D). The transverse process is 64 mm long at the base and expands distally to more than 92 mm (Fig. 17C). The neural spine is 185 mm tall and 94 mm anteroposteriorly at the base (Fig. 17A, B, D).

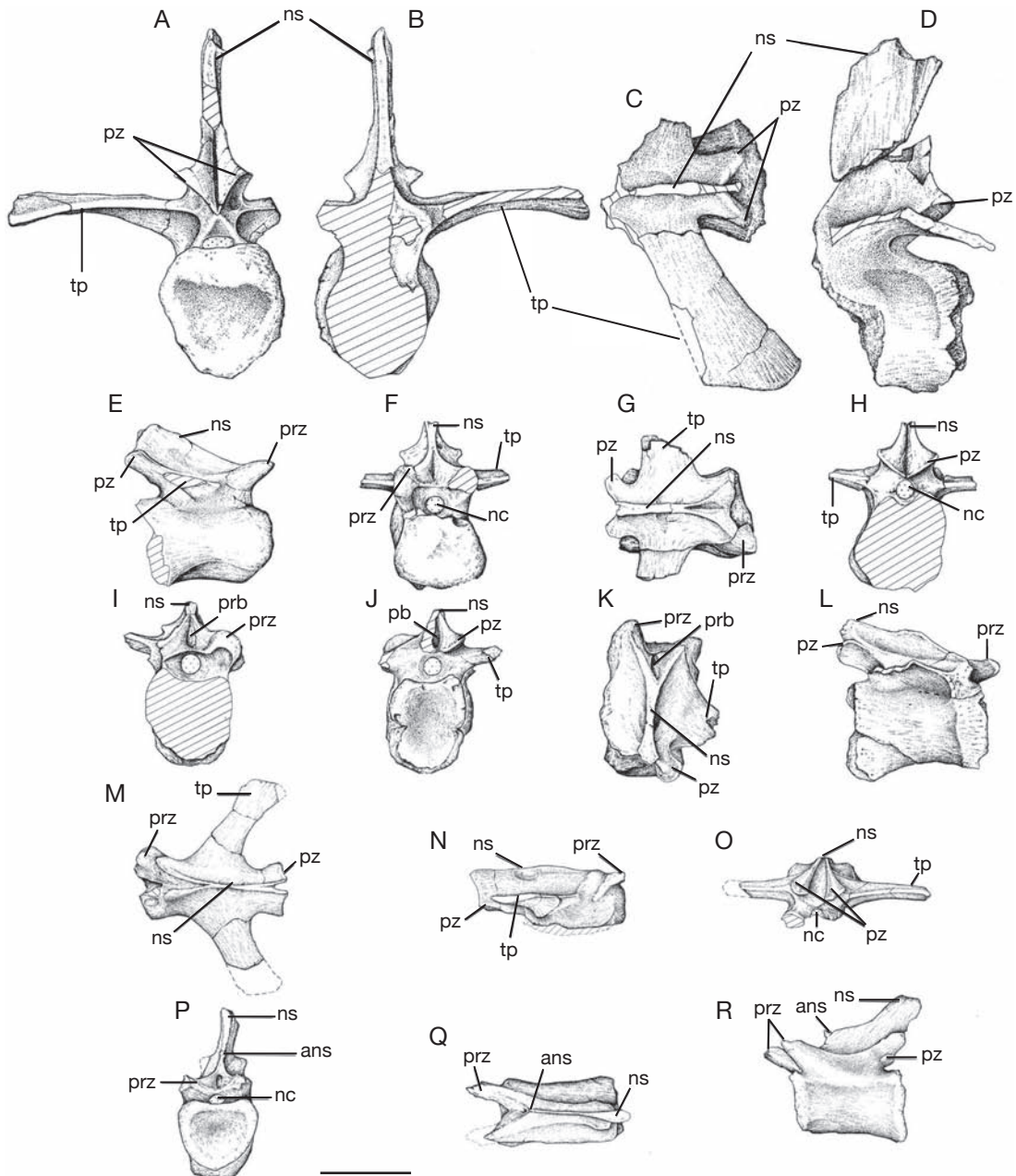


FIG. 17. — *Mapusaurus roseae* n. gen., n. sp.: A-D, anterior caudal vertebra (MCF-PVPH-108.81); A, posterior view; B, anterior view; C, dorsal view; D, left lateral view; E-H, mid-caudal vertebra (MCF-PVPH-108.76); E, right lateral view; F, anterior view; G, dorsal view; H, posterior view; I-L, mid-caudal vertebra (MCF-PVPH-108.78); I, anterior view; J, posterior view; K, dorsal view; L, right lateral view; M-O, mid-caudal vertebra (MCF-PVPH-108.75); M, dorsal view; N, right lateral view; O, posterior view; P-R, mid-caudal vertebra (MCF-PVPH-108.205); P, anterior view; Q, dorsal view; R, left lateral view. Abbreviations: **ans**, accessory neural spine; **nc**, neural canal; **ns**, neural spine; **pb**, postspinal basin; **prb**, prespinal basin; **prz**, prezygapophysis; **pz**, postzygapophysis; **tp**, transverse process. Scale bar: 10 cm.

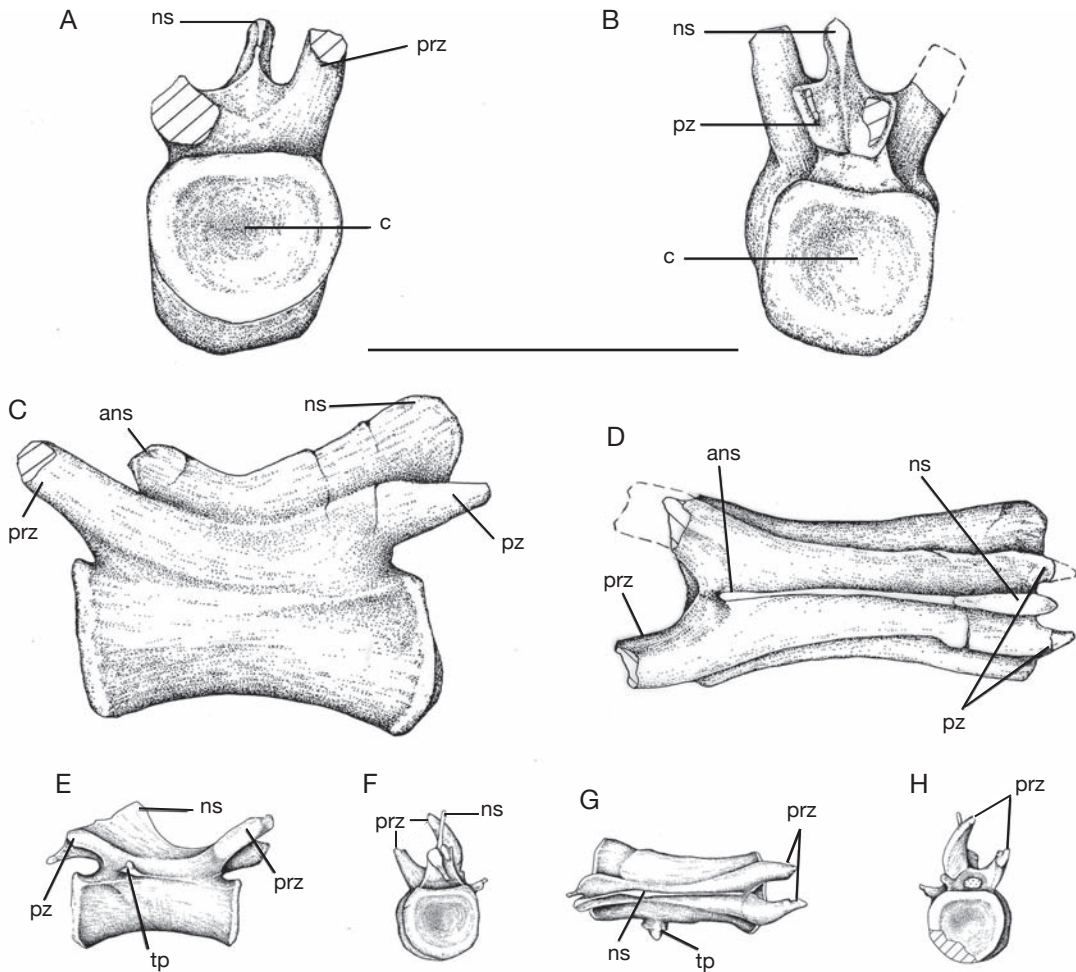


FIG. 18. — *Mapusaurus roseae* n. gen., n. sp.: A–D, distal caudal vertebra (MCF-PVPH-108.79); A, anterior view; B, posterior view; C, left lateral view; D, dorsal view; E–H, distal caudal vertebra (MCF-PVPH-108.247); E, right lateral view; F, posterior view; G, dorsal view; H, anterior view. Abbreviations: as in Figure 17 and c, centrum. Scale bar: 10 cm.

It is rectangular in side view and inclines slightly backward. The postzygapophysial articular facets are oriented lateroventrally, diverging at an angle of 75°. The centrum (about 140 mm long, 115 mm wide and 115 mm tall) has a shallow dorsolateral depression, but there is no evidence of pleurocoels. The neurocentral suture is fused.

The mid-caudals (MCF-PVPH-108.75, -108.76) have long and low neural arches. In MCF-PVPH-108.76 (Fig. 17E), the neurocentral suture is apparently not completely fused, even though it came

from an individual that was significantly larger than MCF-PVPH-108.75 (an unfused, isolated neural arch). The horizontal transverse processes project posterolaterally, and expand slightly distally in MCF-PVPH-108.75 (Fig. 17M). The neural spine is a long, low ridge that bifurcates anteriorly to connect with the prezygapophyses. The articular facets of the prezygapophyses face inward and do not extend anteriorly beyond the centrum (Fig. 17F). The postzygapophyses are anteroposteriorly short, and the articular facets face outward and down, diverging from each

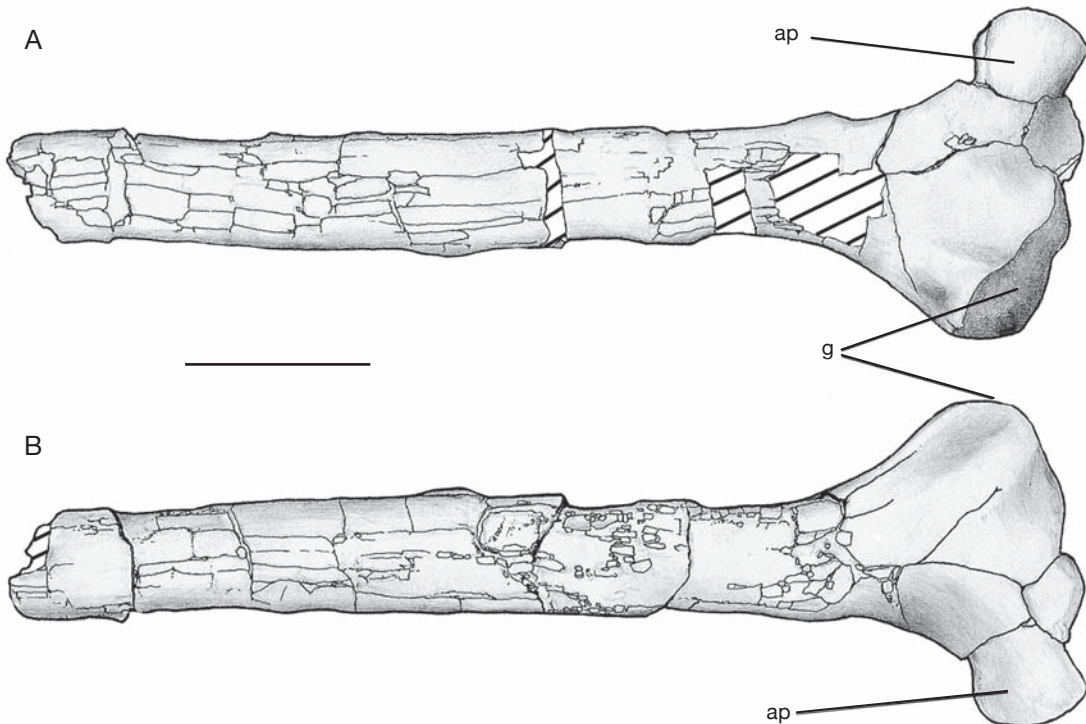


FIG. 19. — *Mapusaurus roseae* n. gen., n. sp., right scapula (MCF-PVPH-108.50); A, lateral view; B, medial view. Abbreviations: ap, acromial process; g, glenoid cavity. Scale bar: 10 cm.

other at an angle of 105° (Fig. 17H). The centrum of MCF-PVPH-108.76 is 165 mm long, 116 mm wide anteriorly, and 100 mm high posteriorly.

MCF-PVPH-108.205 (Fig. 17P-R) is a more distal caudal than MCF-PVPH-108.247, although it comes from a much larger individual. It is 120 mm long, and posteriorly is 65 mm wide and 75 mm high. The neural spine is relatively high posteriorly, but continues anteroposteriorly as a thin ridge. There is a low, accessory neural spine (Fig. 17R) on the anterior end of this ridge as in *Acrocanthosaurus* (Harris 1998; Currie & Carpenter 2000), *Sinosauopteryx* (Currie & Chen 2001) and other theropods. In the position where more anterior caudals have transverse processes, this vertebra has only a ridge. The articular surfaces of the centrum are almost triangular in outline.

The most distal caudal, MCF-PVPH-108.79 (Fig. 18), has a 97 mm long centrum with a poste-

rior intervertebral articulation that is 47 mm wide and 45 mm high. The outline of the centrum is almost rectangular in posterior view (Fig. 18B). The neural spine (Fig. 18A-C) is low (39 mm from the roof of the neural canal to the highest point). There is a distinct anterior accessory neural spine that extends 25 mm above the roof of the neural canal (Fig. 18C). The prezygapophyses project anterodorsally beyond the centrum. The articular surfaces face mostly medially. The postzygapophyses are posteriorly elongate, and converge distally. Their articular facets face laterally and slightly ventrally. MCF-PVPH-108.247 (Fig. 18E-H) is a small distal caudal whose centrum is 44 mm long, 22 mm wide and 20.5 mm high (39 mm high including the neural spine). There is a flat, blade-like neural spine, triangular in lateral aspect, and tallest in the posterior half of the vertebra (Fig. 18E). It continues anteriorly as a low ridge

between the bases of the prezygapophyses. The anterior zygapophyses are well separated from each other, but extend anterior to the intercentral articulation (Fig. 18E, H). The postzygapophyses are short and close to the midline. The vertebra has a small but conspicuous transverse process (Fig. 18E, G). Ventrally the centrum is convex in section at midlength, but has a shallow midline groove on either end close to the facets for the haemal arches.

MCF-PVPH-108.97 and -108.210 are the heads of chevrons, each showing a complete bar across the top of the haemal canal. The shafts were dorsoventrally elongate, and below the intervertebral articulations, each side of the haemal arch has a short anterior and short posterior extension.

#### Ribs

Hundreds of rib fragments and a few full ribs have been found in the quarry. They do not seem to differ significantly in any way from the ribs of *Allosaurus* (Madsen 1976a), *Monolophosaurus* (Zhao & Currie 1993), *Sinraptor* (Currie & Zhao 1993) and other large theropods. A large anterior dorsal rib (MCF-PVPH-108.106) has a broad depression on the posteromedial surface of the web between the capitulum and tuberculum. A pneumatopore enters the shaft of the rib from the distal end of the depression. Pneumatic dorsal ribs have been reported in *Sinraptor* (Currie & Zhao 1993). The ribs (and the vertebrae) suggest that *Mapusaurus* n. gen. had a chest that was deeper than wide.

Fragments of gastralia are also common in the quarry, but there is nothing to indicate any significant differences from the gastralia of other large theropods. A typical gastralia fragment, MCF-PVPH-108.230, has a maximum width of about 30 mm.

#### Pectoral girdle and limb

A partial right scapula (MCF-PVPH-108.50) of one of the smaller individuals was recovered (Fig. 19), along with sections of the shafts of other larger individuals (MCF-PVPH-108.69, -108.185, -108.187). It is a long, slender, gently curved element, and the preserved part is 60 cm long (Fig. 19). It is only 60 mm wide at its narrowest point when seen in lateral aspect. The glenoid faces as much laterally

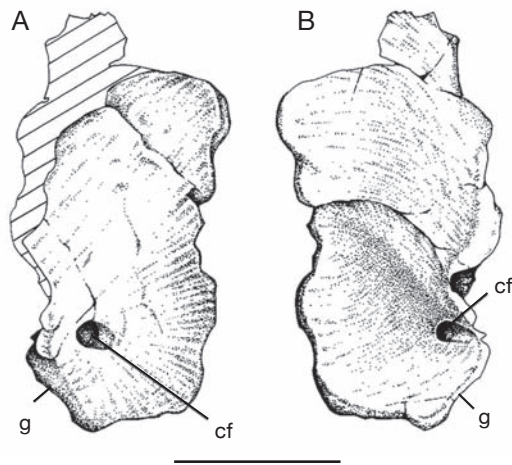


FIG. 20. — *Mapusaurus roseae* n. gen., n. sp., right coracoid (MCF-PVPH-108.71): A, lateral view; B, medial view. Abbreviations: cf, coracoid foramen; g, glenoid cavity. Scale bar: 10 cm.

as posteriorly, and the articular surface is 60 mm high and 55 mm wide. The acromial process is pronounced and is sharply offset from the anterodorsal margin of the scapular blade as in *Acrocanthosaurus* (Currie & Carpenter 2000), *Allosaurus* (Madsen 1976a), *Giganotosaurus* (MUCPv-CH-1), *Sinraptor* (Currie & Zhao 1993) and tyrannosaurids (Maleev 1974). The outer surface of the acromial process is concave (subacromial depression) next to the coracoid suture. The scapular blades of *Ceratosaurus* (Madsen 1976a), *Carnotaurus* (Bonaparte *et al.* 1990), *Edmarka* (Bakker *et al.* 1992), *Torvosaurus* (Bakker *et al.* 1992), and *Megalosaurus* Buckland, 1824 (Walker 1964) are more robust, and the anterior margin grades smoothly into the acromion process. Unlike *Carnotaurus* and *Aucasaurus*, the scapula and coracoid did not co-ossify in *Mapusaurus* n. gen.

A partial left coracoid (MCF-PVPH-108.71) includes part of the scapular suture, which is 82 mm wide (Fig. 20). The coracoid foramen is relatively small with a diameter of 15.5 mm. It passes posterodorsally through the bone to emerge on the mesial surface near the scapular suture at the point where it thins dramatically (Fig. 20B).

One bone (MCF-PVPH-108.116; Fig. 21) may be a furcula, although it is also possible it is a

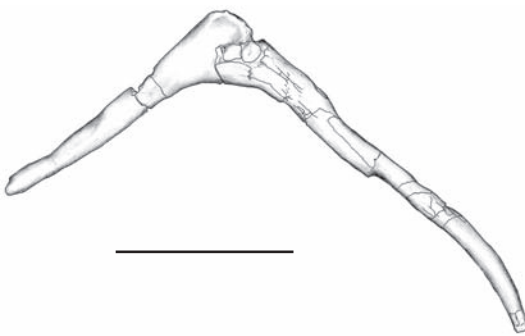


FIG. 21. — *Mapusaurus roseae* n. gen., n. sp., furcula (MCF-PVPH-108.116), ventral view. Scale bar: 10 cm.

pair of gastralia that have fused together (Harris 1998). However, the sigmoidal curvature of the shaft, the symmetry of the bone overall, and the lack of a joint or line of fusion medially favors the former interpretation. As in the furculae of other theropods (Chure & Madsen 1996; Makovicky & Currie 1998), each lateral shaft curves in two planes. In anterior aspect (with the midpoint of the “V”-oriented posteroventrally), the dorsal margin of each arm is convex mesially, but becomes shallowly concave distally (Fig. 21). In dorsal view, the anterior margin is concave proximally, but becomes convex distally. As preserved, the bone is 310 mm across, but if the left shaft were complete, the whole bone would have been about 360 mm across. The maximum dimension of the bone is on the midline, where it is 40 mm deep. Laterally it tapers to 12 mm.

Most of a right humerus (MCF-PVPH-108.45) of *Mapusaurus* n. gen. was found, lacking only the bone proximal to the deltopectoral crest (Fig. 22). In an allosaurid, this would amount to about a third of the length of the whole bone. Because the preserved length of the humerus of MCF-PVPH-108.45 is 210 mm, the bone must have been approximately 300 mm long. Although humerus length is highly variable in theropods, there is a strong correlation between humeral shaft width and the length of the femur ( $y = 0.82x - 0.81$ ,  $r^2 = .92$ , where  $y$  is the logarithm of femur length,  $x$  is the logarithm of humeral shaft width, and  $r^2$

is the correlation coefficient). The transverse shaft width of the humerus of MCF-PVPH-108.45 is 51 mm, and this suggests that the corresponding femur length for this individual was 1180 mm long. Two of the femora collected are about this length. All of this suggests that *Mapusaurus* n. gen. had a humerus that was only about a quarter the length of the femur. Tyrannosaurids, *Acrocanthosaurus*, *Carnotaurus* and *Aucasaurus* all have short arms with humeri that are less than a third the length of the femora. *Mapusaurus* n. gen., in consequence, had relatively short arms.

The humerus is relatively robust with a minimum transverse shaft width of 51 mm, and a distal expansion of 104 mm. The deltopectoral crest is a large plate-like process that projects approximately 33 mm from the shaft (Fig. 22A, B). The crest curves as it rises from the shaft and twists anteromedially until it is about 80° from the main axis of the proximal end (Fig. 22E). It rises at an angle of approximately 40° to the transverse axis of the distal end. The shaft is relatively short and robust, and is subcircular (44 by 51 mm) in cross-section with a midshaft circumference of 156 mm. The entepicondyle is relatively small but conspicuous (Fig. 22A). The distal end of the bone has a pair of condyles separated by a shallow depression (Fig. 22A, C, F), and the features are poorly defined compared with *Acrocanthosaurus* (Currie & Carpenter 2000) and *Allosaurus* (Gilmore 1920).

A left radius (MCF-PVPH-108.46) of *Mapusaurus* n. gen. is a relatively massive bone, slightly expanded in both proximal and distal ends (Fig. 23). The shaft is almost round in cross section with a minimum transverse diameter of 27.5 mm. Proximally, the transversely flattened humeral end twists posteriorly, likely for pathological reasons (Fig. 23D). The proximal articular surface has a smooth, slightly concave facet for the radial condyle of the humerus (Fig. 23E). The posterior side of the distal end (Fig. 23B) exhibits a lightly scarred contact for the ulna. In distal view (Fig. 23F), the articular surface for the carpus is convex with a triangular outline.

There is little available information on the *Mapusaurus* n. gen. manus. MCF-PVPH-108.48 (Fig. 24)

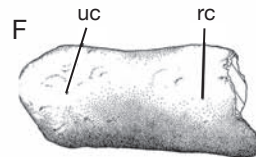
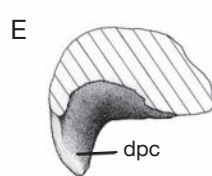
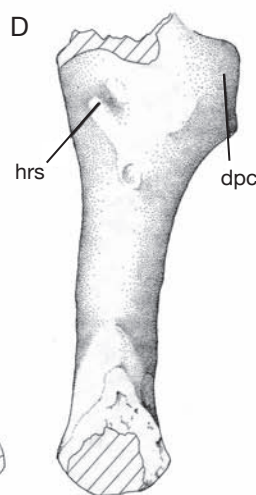
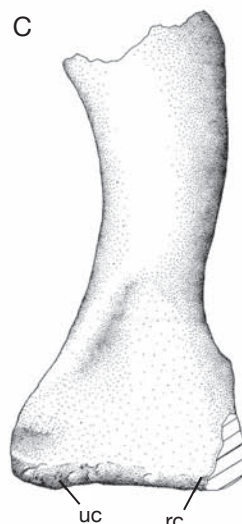
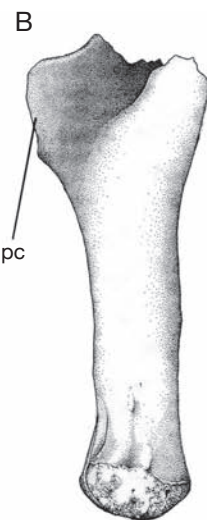
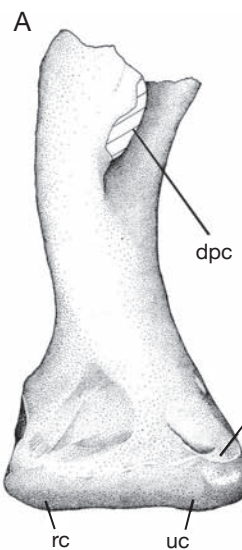


FIG. 22. — *Mapusaurus roseae* n. gen., n. sp., right humerus (MCF-PVPH-108.45): A, anterior view; B, medial view; C, posterior view; D, lateral view; E, proximal view; F, distal view. Abbreviations: dpc, deltopectoral crest; en, entepicondyle; hrs, humero-radialis origin scar; rc, radial condyle; uc, ulnar condyle. Scale bar: 10 cm.

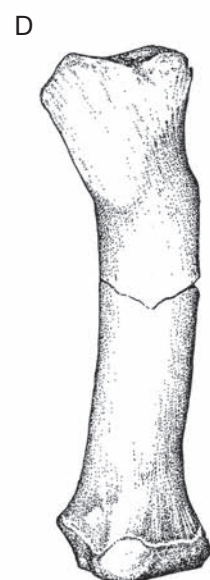
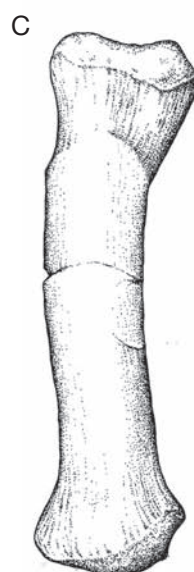
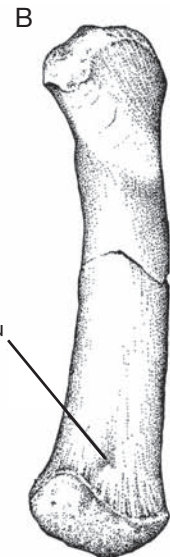
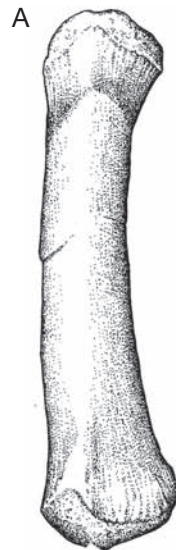


FIG. 23. — *Mapusaurus roseae* n. gen., n. sp., right radius (MCF-PVPH-108.46): A, anterior view; B, posterior view; C, lateral view; D, medial view; E, proximal view; F, distal view. Abbreviation: u, ulnar contact. Scale bar: 10 cm.

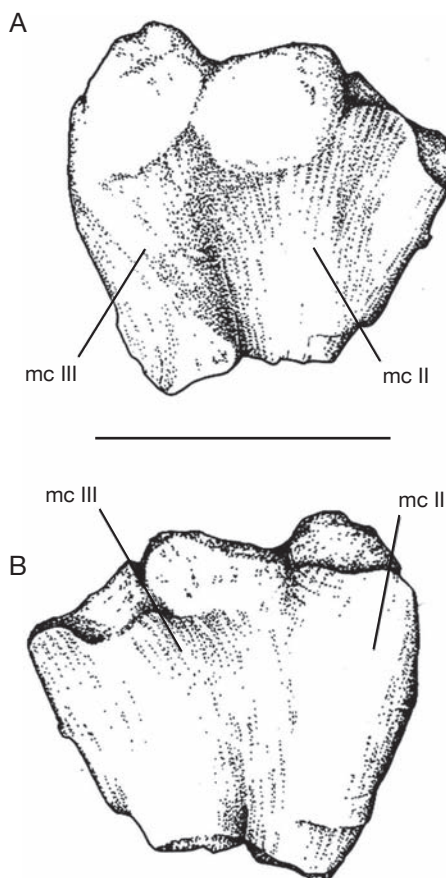


FIG. 24. — *Mapusaurus roseae* n. gen., n. sp., left? proximal metacarpals (MCF-PVPH-108.48): A, probable ventral view; B, probable dorsal view. Abbreviations: mc II, metacarpal II; mc III, metacarpal III. Scale bar: 10 cm.

consists of the proximal ends of metacarpals II and III, which seem to be partially fused proximally. Unfortunately, they are so weathered that it is difficult to determine whether they are from the right or left manus. Metacarpal II is the largest element (88 mm proximal width, 46 mm shaft diameter), and is comparable in size with that reported for *Acrocanthosaurus* (Currie & Carpenter 2000). In proximal view, the bone is transversely expanded and dorsoventrally compressed. The medial side shows a wide and strong contact for the first metacarpal, although there are no indications of fusion between these two bones.

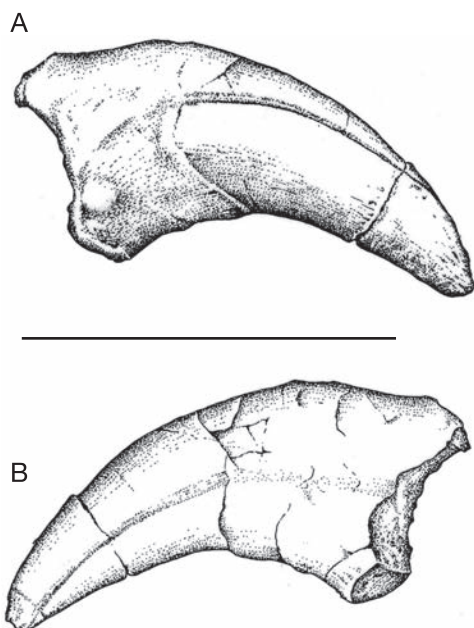


FIG. 25. — *Mapusaurus roseae* n. gen., n. sp., probable left manual ungual (MCF-PVPH-108.14): A, medial view; B, lateral view. Scale bar: 10 cm.

The preserved part of metacarpal III is 46 mm wide, but most of the details of the proximal articular surface are not preserved. The shaft has a transverse diameter of 35 mm, and is subcircular in cross-section.

Manual phalanx II-2 is represented by MCF-PVPH-108.109, which is 80 mm long (shortest length between lateral margins of the proximal and distal articulations). The proximal end has a tall, ginglymoid articulation with near perpendicular lateral and medial margins. There are strong attachment areas for ligaments on the medial and especially lateral surfaces near the proximal end. The collateral ligament pits are high in position, close to the extensor surface, and the lateral one is much larger than the medial. The double distal articulation is narrower dorsally (21 mm) than ventrally (37.5 mm), and is oriented more ventrally than distally. The transverse plane of the distal articulation is rotated some 10° medially when compared with the transverse plane of the proximal articulation. Effectively this turned the

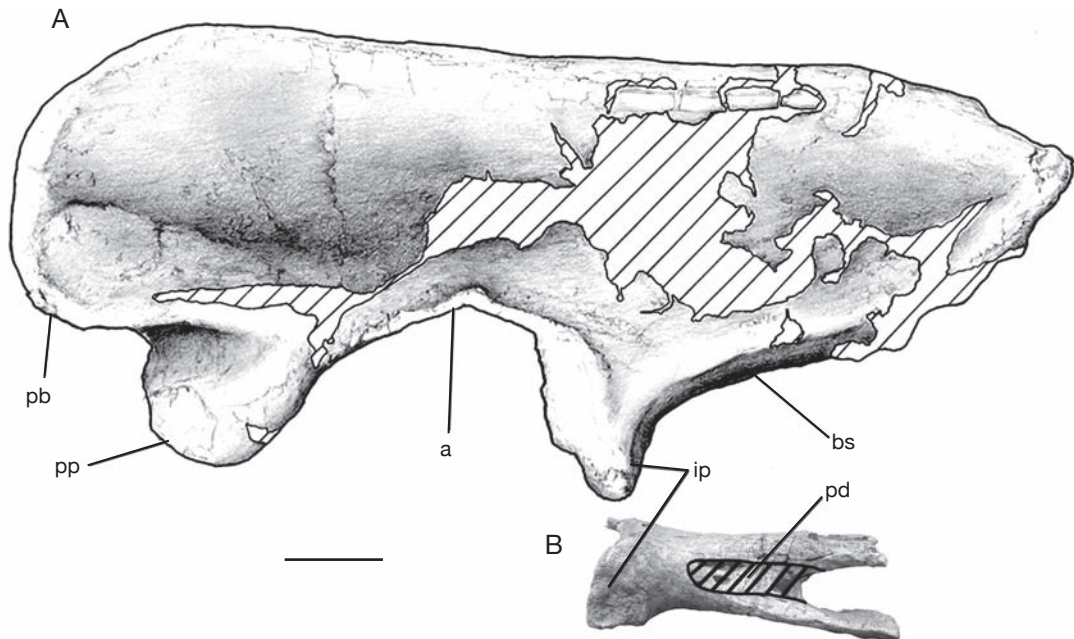


FIG. 26. — *Mapusaurus roseae* n. gen., n. sp.: A, left ilium (MCF-PVPH-108.128), lateral view; B, ventro-posterior fragment of right ilium (MCF-PVPH-108.181) in ventral view (the picture has been inverted to represent the left side; dashed area represents the internal projection of the pneumatic diverticulae). Abbreviations: a, acetabulum; bs, brevis shelf; ip, ischiatric peduncle; pb, preacetabular blade; pd, pneumatic diverticulae; pp, pubic peduncle. Scale bar: 10 cm.

tip of the ungual medially in apposition to the claw of the first digit.

The single manual ungual recovered (MCF-PVPH-108.14) might be phalanx I-2 (Fig. 25B), but is closer in shape to II-3 of *Allosaurus* (Madsen 1976a). It is 135 mm long when measured straight from the dorsal surface of the proximal articulation to the tip, or 155 mm when measured along the outside curve.

#### Pelvic girdle and limb

Most of the pelvis and hind limb are represented by well preserved bones.

Several ilia have been collected, the best preserved of which is MCF-PVPH-108.128, a 1050 mm long, left ilium (Fig. 26). MCF-PVPH-108.245 includes most of the acetabular and postacetabular regions of a left ilium from an animal of about the same size. MCF-PVPH-108.181 represents a larger animal, although the specimen only includes the region surrounding the ischial peduncle from the

right side. When viewed laterally, the dorsal margin is slightly concave above the acetabulum, and slightly convex towards either end. It has a height (top of acetabulum to dorsal edge) to length index of 30, which is comparable to *Ceratosaurus* and *Torvosaurus* (Britt 1991), but is less than that of *Giganotosaurus*, in which the H/L index is 36, and *Allosaurus* with 37. The preacetabular blade is about the same height (29 cm in MCF-PVPH-108.128, -108.245) as the postacetabular ala. However, the preacetabular blade is short, and in MCF-PVPH-108.128 it is 17 cm from the anterior margin of the base of the pubic peduncle, compared with a postacetabular length of 44 cm behind the ischial peduncle. The pre-/postacetabular ratio in *Mapusaurus* n. gen. (0.39) is almost the same as that in the holotype of *Giganotosaurus* (0.38). The pubic peduncle is incomplete in all specimens, but as preserved in MCF-PVPH-108.245 is 33% deeper than the ischial peduncle. In all probability, a complete pubic peduncle would

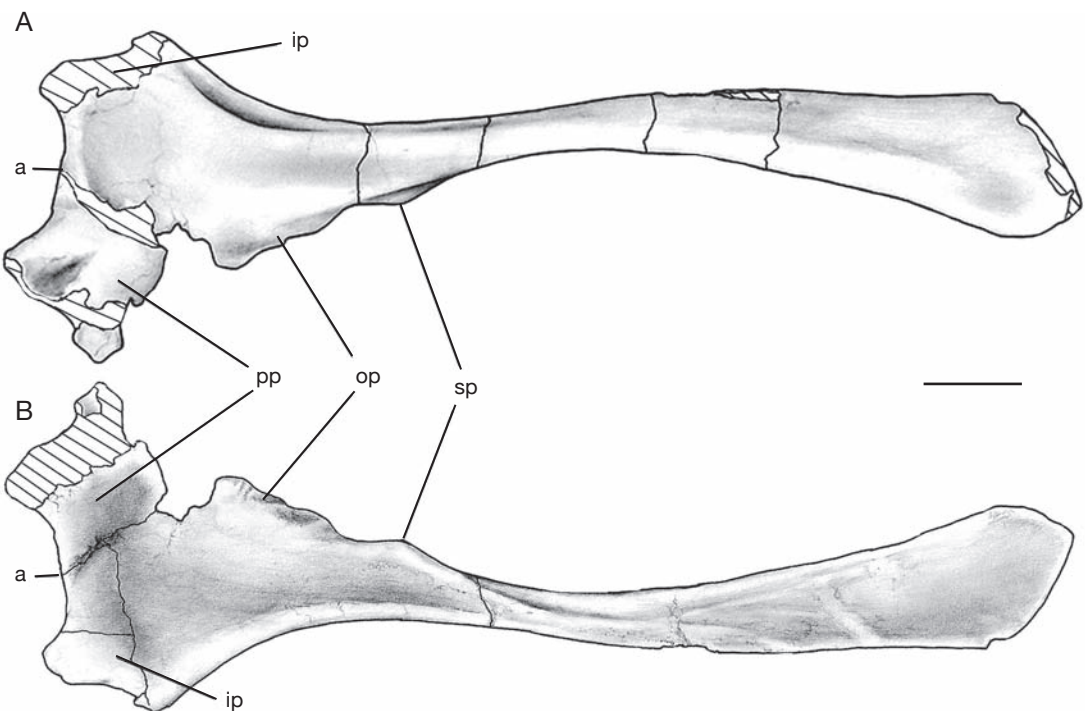


FIG. 27. — *Mapusaurus roseae* n. gen., n. sp., left ischium (MCF-PVPH-108.165): A, lateral view; B, medial view. Abbreviations: a, acetabulum; ip, iliac peduncle; op, obturator process; pp, pubic peduncle; sp, subsidiary process. Scale bar: 10 cm.

have been much longer because in *Giganotosaurus* it is double the depth. It is longer anteroposteriorly than it is wide. The ventral margin of this region expands medially to form a rudimentary cuppedicus fossa. The acetabulum is 240 mm long, and there is a pronounced supra-acetabular crest as in *Abelisaurus*, *Ceratosaurus*, *Sinraptor*, *Torvosaurus* and other large, relatively primitive theropods. The posteroventral margin of the ilium is incomplete in all specimens, but seems to have been squared off as in *Allosaurus*, *Giganotosaurus* and *Sinraptor*, rather than tapering as in *Megalosaurus* and *Torvosaurus* (Britt 1991). The brevis shelf is relatively narrow as in more advanced large theropods, rather than broad as in *Ceratosaurus* (Gilmore 1920) and abelisaurids (Bonaparte *et al.* 1990). However, it is apomorphic in that the shelf extends dorsoanteriorly into a broad (55 mm in MCF-PVPH-108.181, 40 mm in MCF-PVPH-108.245) excavation into the interior of the ilium.

In MCF-PVPH-108.181, this deep fossa penetrates 140 mm into the ilium, reaching a point above the middle of the ischial peduncle. Between this excavation and the base of the ischial peduncle, there are two shallow but distinct pits (diameters of 26 and 32 mm) in MCF-PVPH-108.245, and three (diameters of 20, 29 and 48 mm) in MCF-PVPH-108.181. These pits also fall within the margins of the brevis fossa (Fig. 26B). The deep excavation suggests the presence of powerful iliocaudalis musculature between the brevis fossa and the base of the tail, whereas the pits may have been associated with more lateral caudofemoralis brevis musculature.

The only substantial portions of *Mapusaurus* n. gen. pubes are MCF-PVPH-108.145, which is a 72 mm section of the shaft from the left side, and MCF-PVPH-108.148 and -108.149, which are respectively portions of the proximal ends of right and left pubes. The iliac suture is teardrop-shaped,

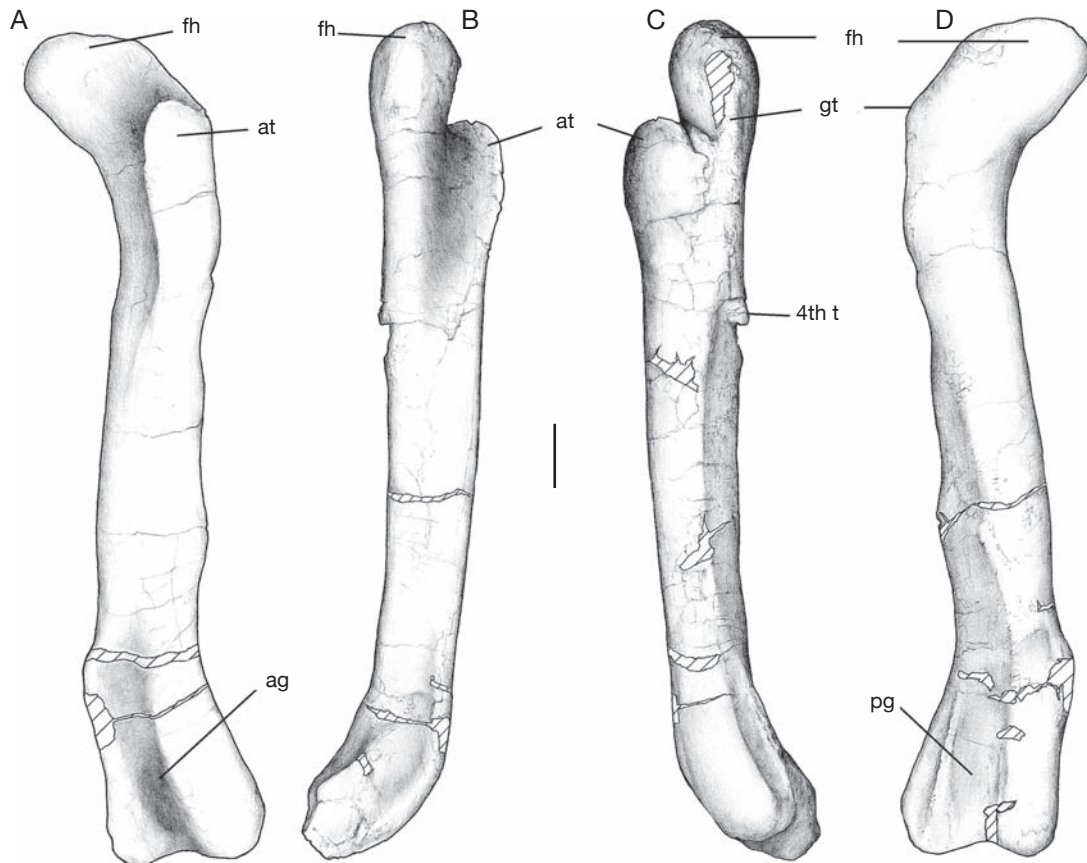


Fig. 28. — *Mapusaurus roseae* n. gen., n. sp., left femur (MCF-PVPH-108.203): A, anterior view; B, medial view; C, lateral view; D, posterior view. Abbreviations: 4th t, fourth trochanter; ag, anterior intercondylar groove; at, anterior (lesser) trochanter; fh, femoral head; gt, greater trochanter; pg, posterior intercondylar groove. Scale bar: 10 cm.

160 mm long and 55 mm wide in MCF-PVPH-108.148. Distolateral to the ischial peduncle there is a low ridge that defines a posteroventrally oriented oval depression that may have been the origin of the pelvic muscles (MCF-PVPH-108.149). The minimum shaft dimensions of MCF-PVPH-108.145 are 7.5 by 10 cm, which is 10% greater than those in the holotype of *Giganotosaurus*. This suggests that the specimen represents the largest individual of *Mapusaurus* n. gen. from the bonebed.

There is one complete (MCF-PVPH-108.165; Fig. 27) 1010 mm long (measured from the dorsal edge of the pubic peduncle to the distal end) left ischium, several proximal heads (MCF-PVPH-

108.95, -108.96), and numerous shaft fragments. The pubic and ischial peduncles are subequal in size, and are broadly separated by the acetabular margin. The head of a right ischium (MCF-PVPH-108.96) shows there was an almost circular concavity for contact with the ilium. MCF-PVPH-108.95 is the head of a left ischium, showing a well developed obturator process that is separated proximally from the pubic peduncle by a notch, and ends distally in another notch. A distinct obturator process (Fig. 27) is separated from the pubic peduncle by a notch, as in most advanced theropods including *Acrocanthosaurus*, *Allosaurus*, *Gasosaurus*, *Carcharodontosaurus* (Rauhut 1995) and *Giganotosaurus*.

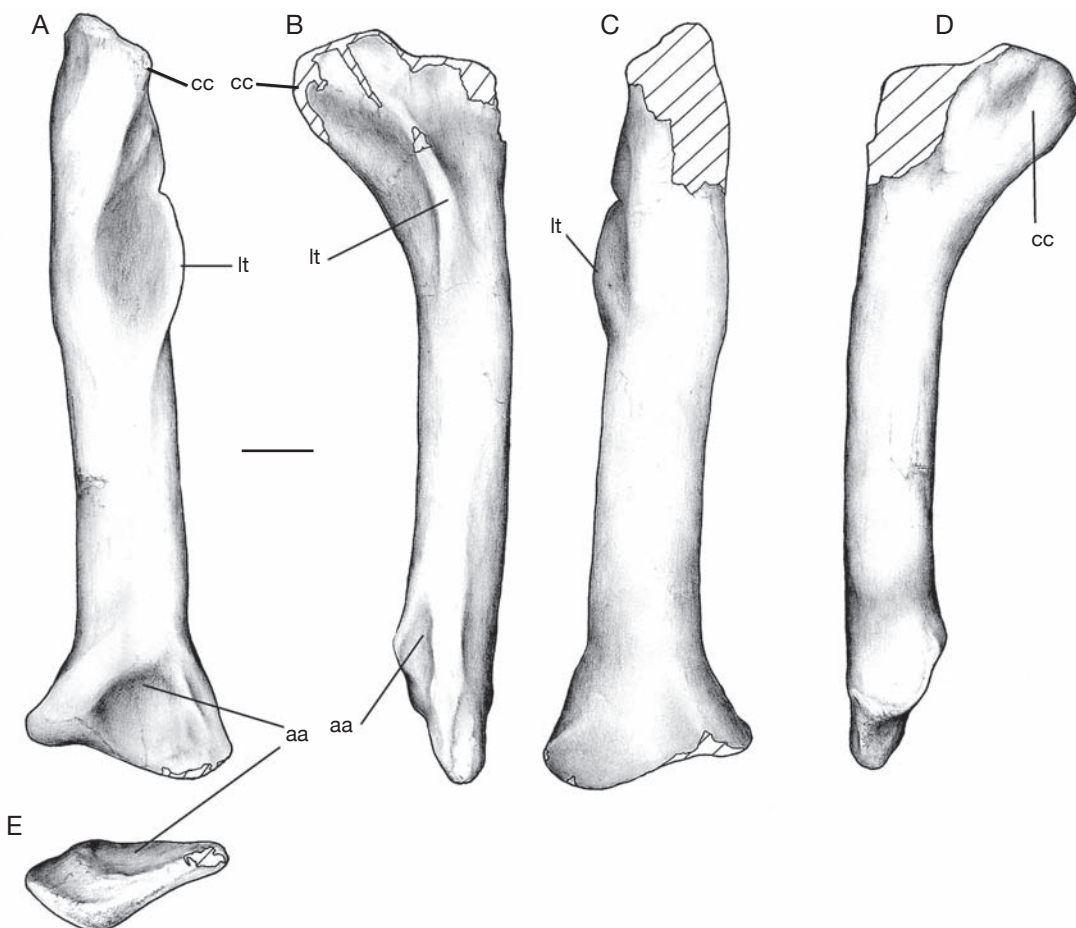


FIG. 29. — *Mapusaurus roseae* n. gen., n. sp., left tibia (MCF-PVPH-108.68): A, anterior view; B, lateral view; C, posterior view; D, medial view; E, distal view. Abbreviations: aa, area for ascending process of astragalus; cc, cnemial crest; lt, lateral tuberosity. Scale bar: 10 cm.

The plesiomorphic state for large theropods is a continuous ventral lamina (the “obturator flange” of Charig & Milner 1997) and is found in *Carnotaurus*, *Ceratosaurus*, *Dilophosaurus*, *Monolophosaurus*, *Piatnitzkysaurus* and *Torvosaurus*. A ridge continues distal to the obturator process, and expands into a smaller subsidiary process, presumably for part of the origin for adductor musculature (Romer 1966). The ridge continues distally along the medial surface of the shaft, eventually merging with the posterodorsal margin of the ischium. In the complete ischium, the minimum shaft diameter is

48 mm and the distal expansion is 129 mm. The dorsoposterior margin of the shaft is somewhat convex in lateral view, but because the distal end expands ventrally, it gives the shaft the appearance of a relatively strong ventral curvature. In contrast, the ischium of *Giganotosaurus* is straight in lateral aspect. The distal end of the shaft expands gradually and there is no distinct ischial boot. The expanded distal end has longitudinal ridges and grooves for contact with the other ischium, but this pair of bones did not fuse distally as they do in many large theropods, including *Sinraptor*.

Three complete femora assigned to adult individuals (MCF-PVPH-108.44, -108.203, -108.233) and 10 partial femora (MCF-PVPH-108.25, -108.54-108.57, -108.59, -108.61, -108.64, -108.65, -108.234) from medium- to large-sized individuals are known for *Mapusaurus* n. gen. (Fig. 28). The largest of these (MCF-PVPH-108.234) is 1300 mm long, with a shaft circumference of 455 cm. Using the formula developed by Anderson *et al.* (1985), a conservative weight estimate for this individual would have been 3000 kg. Like *Giganotosaurus* and other carcharodontosaurids, the head of the femur is angled upwards from the shaft, and rises high above the wing-like lesser trochanter. This is very different than in most large theropods where the head is perpendicular to the shaft and is at almost the same level as the lesser trochanter. In more primitive theropods (*Ceratosaurus*, *Dilophosaurus*, *Herrerasaurus*), the head is inclined at an angle of less than 90° to the shaft (Fig. 28). There is a deep groove on the back of the head near the flattened medial margin, similar to *Sinraptor* (Currie & Zhao 1993) and *Giganotosaurus* (MUCPv-CH-1). There is a shallow depression bound by a prominent ridge between the greater and lesser trochanters in MCF-PVPH-108.44. Unlike *Acrocanthosaurus*, *Allosaurus*, *Sinraptor* and other carnosaurs, the fourth trochanter is a conspicuous ridge next to the depression for the *M. caudifemoralis longus*. This ridge (Fig. 28C) is relatively low compared with that of *Carcharodontosaurus* (Stromer 1931), but is similar in development to that of *Giganotosaurus* (MUCPv-CH-1). The minimum transverse diameter of the relatively straight shaft of the largest femur is 150 mm. The distal end of the femur has a sharply defined distomedial ridge along the medial margin of the anterodorsal surface similar to *Giganotosaurus* (MUCPv-CH-1), *Sinraptor* (Currie & Zhao 1993) and most other carnosaurs. The ridge bounds the adductor fossa medially. The extensor groove is pronounced but relatively shallow, and is continuous with the intercondylar trough of the distal end, like in *Giganotosaurus* and unlike most theropods (Fig. 28D). There are well developed distal condyles, the lateral one associated with a distinct crista tibiofibularis. The floor of the flexor groove has rugose longitudinal ridges, but lacks

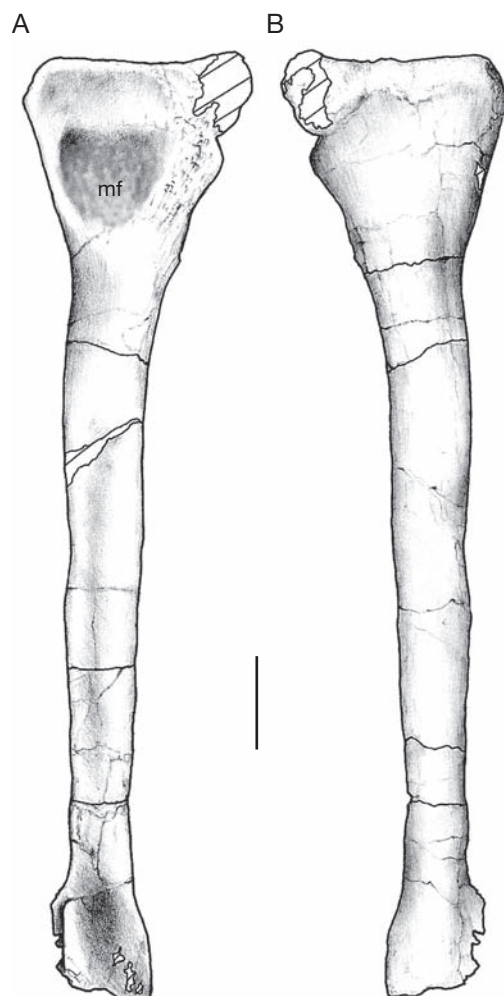


FIG. 30. — *Mapusaurus roseae* n. gen., n. sp., left fibula (MCF-PVPH-108.202): A, medial view; B, lateral view. Abbreviation: mf, medial fossa. Scale bar: 10 cm.

the ridge for cruciate ligaments that is found in allosauroids.

Three complete (MCF-PVPH-108.58, -108.67, -108.68) and six partial *Mapusaurus* n. gen. tibiae (MCF-PVPH-108.52, -108.53, -108.62, -108.63, -108.66, -108.73) have been collected from the Cañadón del Gato bonebed (Fig. 29). The smallest complete one is 887 mm long, and the largest is 1075 mm. They represent a minimum of five individuals (Table 3). In anterior view, the tibia

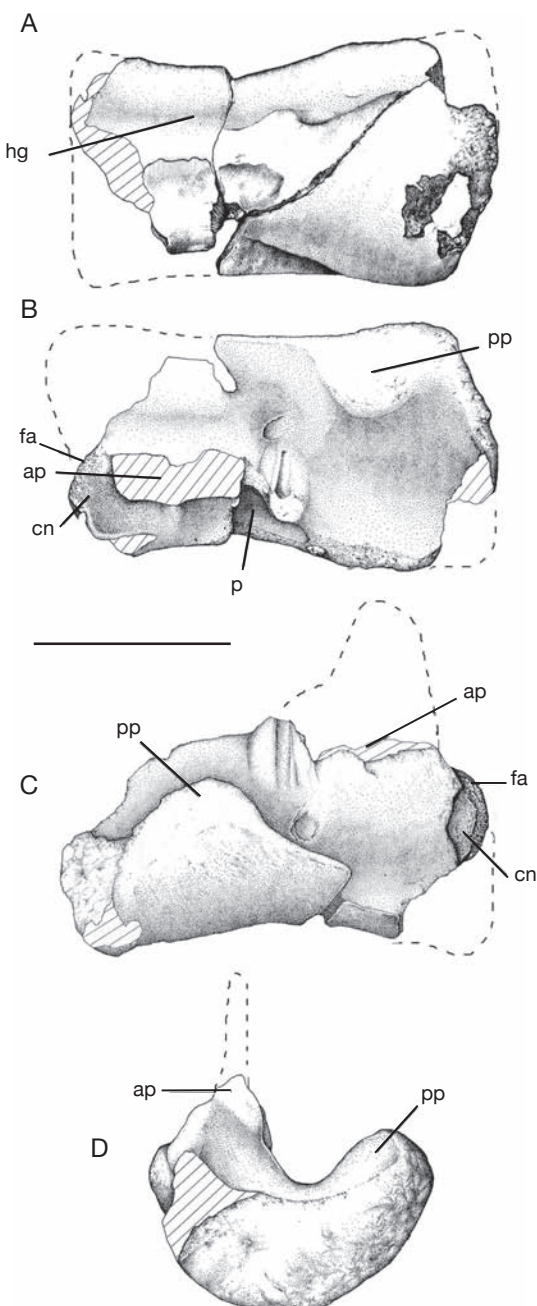


FIG. 31. — *Mapusaurus roseae* n. gen., n. sp., right astragalus (MCF-PVPH-108.70): **A**, ventral view; **B**, dorsal view; **C**, posterior view; **D**, medial view. Abbreviations: **ap**, base of ascending process; **cn**, calcaneal notch; **fa**, fibular articulation; **hg**, horizontal groove; **p**, pit in base of ascending process; **pp**, posterior process. Scale bar: 10 cm.

flares both medially and laterally at the distal end (Fig. 28A). The flat, anterior surface for the ascending process of the astragalus is delimited dorsomedially by a strong ridge. The tibia has a well developed, deep cnemial crest oriented anterodorsally from the shaft (Fig. 29B). The medial proximal head is higher than the lateral, but as in *Sinraptor* (Currie & Zhao 1993) there is little evidence of a posterior intercondylar groove such as there is in *Allosaurus* (Madsen 1976a). The fibular crest is positioned on the anterolateral corner of the proximal end (Fig. 29A, C). As in *Giganotosaurus* (MUCPv-CH-1), the lateral side of the tibia extends distally farther than the medial edge (Fig. 28A, C). The distal end is notched posteromedially for a process from the astragalus (Fig. 29E).

Four complete fibulae (MCF-PVPH-108.132, -108.202, -108.196, -108.189) and several partials (-108.51, -108.220) have been recovered and range in length from 640 to 860 mm. Although the largest one (MCF-PVPH-108.202) is 2.5 cm longer than the holotype fibula of *Giganotosaurus carolinii*, it is more gracile (Fig. 30). The proximal end is 220 cm wide, and has a shallowly hollow medial surface. The shaft width is 65 mm, and distal width is 98 mm, compared with 80 mm and 110 mm in the holotype of *Giganotosaurus carolinii*. The distal end twists so that it sits anterior to the expanded distal end of the tibia, and probably overlapped the edge of the astragalus. There is a rugose thickening on the anteromedial edge of the proximal end of the shaft for the interosseum tibiofibulare ligaments as in *Allosaurus* (Madsen 1976a), *Sinraptor* (Currie & Zhao 1993), and most other carnosaurs.

In most features, the right astragalus of *Mapusaurus* n. gen. (MCF-PVPH-108.70; Fig. 31) is directly comparable with carnosaurs like *Allosaurus* (Madsen 1976a) and especially *Sinraptor* (Currie & Zhao 1993). There is a horizontal groove (Fig. 31A) across the faces of the posteroventrally oriented condyles, and a shallow depression at the base of the ascending process. Laterally, the remnants of a notch can be seen for a process from the calcaneum. As in *Sinraptor*, there is a relatively high process on the posterior margin of the tibial articulation close to the medial surface (Fig. 31B, C). This plugged into a notch on the back of the distal end of the

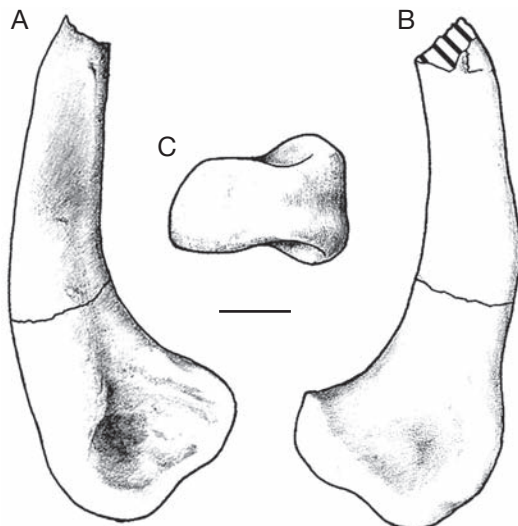


FIG. 32. — *Mapusaurus roseae* n. gen., n. sp., left Metatarsal I (MCF-PVPH-108.246): A, lateral view; B, medial view; C, distal view. Scale bar: 1 cm.

tibia. Because the tibia is shorter on the medial side than the lateral, it is not surprising that the proximodistal thickness of the medial condyle of the astragalus is thicker than the lateral (48 mm compared with 30 mm in MCF-PVPH-108.70). Lateral (and only slightly anterolaterally) to the base of the ascending process, there is a shallow socket for the distomedial end of the fibula. Although the ascending process is not preserved, its extent is well marked on the distal end of the tibia. Its upper margin was strongly inclined proximolaterally, fitting beneath the ridge on the distal end of the tibia. In MCF-PVPH-108.70, the ascending process would have risen at least 10 cm above the base of the astragalus. This suggests that the overall height of the astragalus in *Mapusaurus* n. gen. was approximately 20% of tibial length, which compares well with *Allosaurus*, other advanced carnosurs, and basal tetanurans.

The metatarsus of *Mapusaurus* n. gen. is similar to those of most carnosurs, including *Acrocanthosaurus*, *Allosaurus* and *Sinraptor*. Only one first metatarsal (Fig. 32) was recovered (MCF-PVPH-108.246). This one is from the right side, and probably represents a medium sized individual of *Mapusaurus* n. gen. The

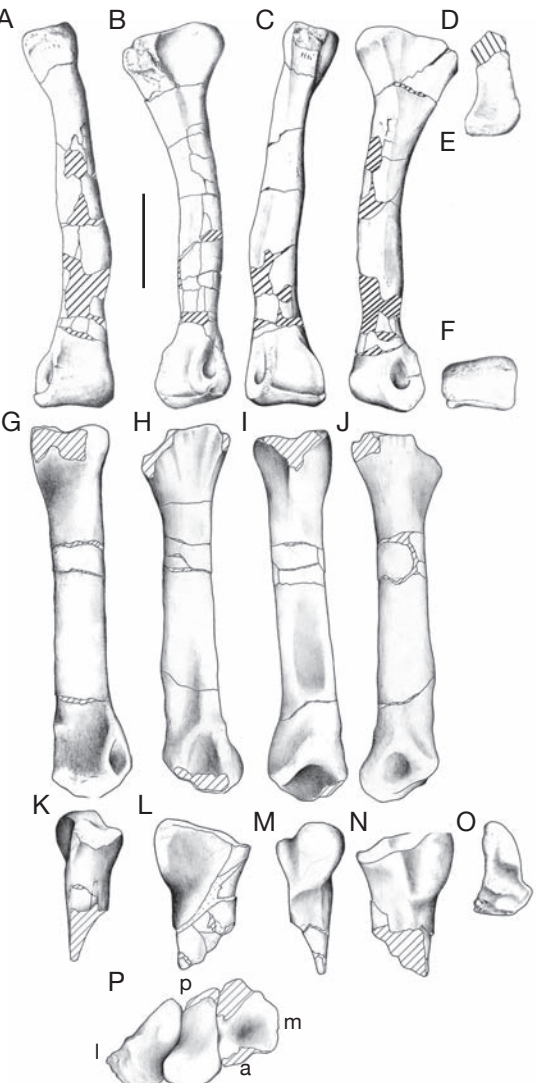


FIG. 33. — *Mapusaurus roseae* n. gen., n. sp.: A-F, right Metatarsal III (MCF-PVPH-108.32); A, anterior view; B, lateral view; C, posterior view; D, medial view; E, proximal view; F, distal view; G-J, right Metatarsal IV (MCF-PVPH-108.34); G, anterior view; H, lateral view; I, posterior view; J, medial view; K-O, proximal end of right metatarsal II (MCF-PVPH-108.35); K, anterior view; L, lateral view; M, posterior view; N, medial view; O, proximal view; P, metatarsals II to IV in proximal view. Abbreviations: a, anterior; p, posterior; I, lateral; m, medial sides. Scale bar: 10 cm.

distal third of the metatarsal is inflected anteriorly and laterally from the dorsally tapering shaft of the bone (Fig. 32A, B). The medial colateral ligament

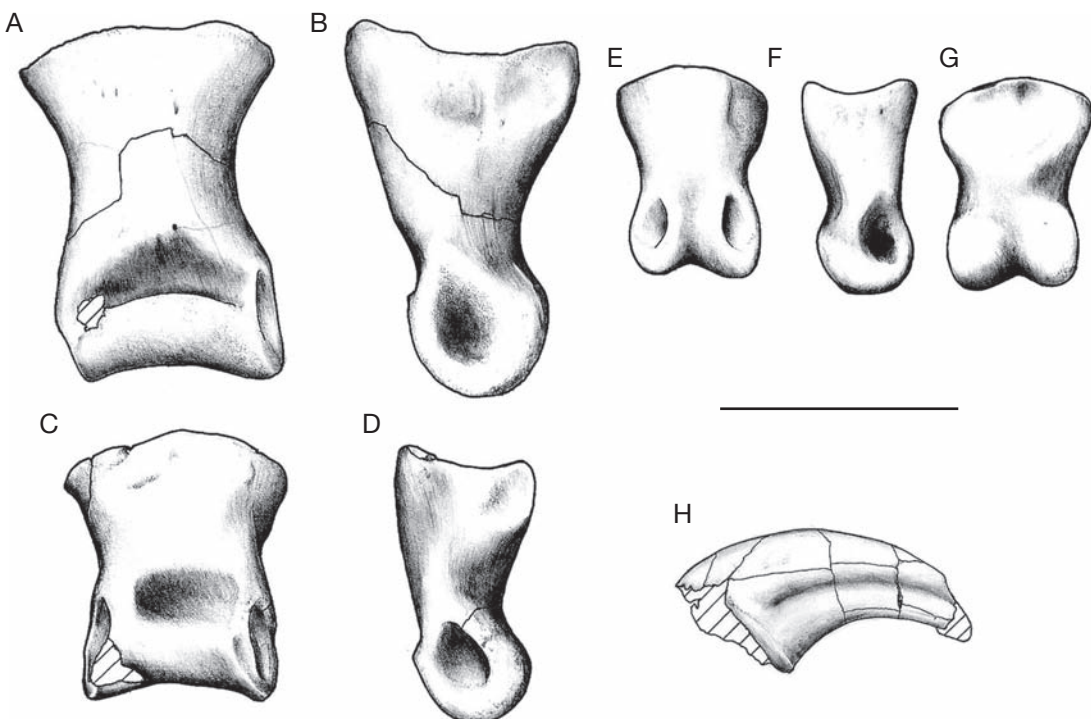


FIG. 34. — *Mapusaurus roseae* n. gen., n. sp.: A, B, left pedal phalanx III-1 (MCF-PVPH-108.23); A, dorsal view; B, medial view; C, D, pedal phalanx III-2 (MCF-PVPH-108.25); C, dorsal view; D, side view; E-G, pedal phalanx III-3 (MCF-PVPH-108.28); E, dorsal view; F, side view; G, ventral view; H, pedal ungual (MCF-PVPH-108.198), side view. Scale bar: 10 cm.

pit is shallow, whereas that of the lateral side is deep and large. The distal phalangeal articulation surface is deep but narrow (Fig. 32C).

In proximal view, the outlines of the second to fourth metatarsals (Fig. 33A-O) are fundamentally the same as in *Acrocanthosaurus*, *Allosaurus*, *Sinraptor* and other carnosaurs. In more primitive theropods like *Ceratosaurus*, the anterior margin of the third metatarsal is as wide as the posterior margin, and the contacts with the adjacent metatarsals are flat rather than sinuous (Gauthier 1986). The third metatarsal of *Mapusaurus* n. gen. (Fig. 33E) lacks the arctometatarsalian condition seen in tyrannosaurids and other coelurosaurs, and was presumably relatively shorter.

#### *Phalanges*

Eight of the pedal phalanges are represented in the quarry by more than 18 specimens. Only one of

these (MCF-PVPH-108.198) is an ungual (Fig. 34), which is asymmetrical and was probably from either the second or fourth digits.

MCF-PVPH-108.23 is a right pedal phalanx III-1 (Fig. 34A, B). The proximal articular surface has a roughly triangular outline, with a flat ventral border. The articular facet is dorsoventrally concave and transversely straight. In dorsal view, the proximal end is more transversely expanded than the distal. In the deeply grooved ginglymoid, the dorsal edges of the lateral pits are closer to the midline than the ventral ones. There are virtually no extensor or flexor fossae. MCF-PVPH-108.27 is another phalanx II-2, although from a slightly smaller individual.

MCF-PVPH-108.26 is another phalanx III-1 of the right side, although it corresponds to a smaller individual. The morphology is the same as in the other specimen, but the attachments are less well defined.

MCF-PVPH-108.25 is a left phalanx III-2 (Fig. 34C, D). Based on its dimensions, it could correspond to the same individual as MCF-PVPH-108.23. The bone is stout and slightly longer than wide. In lateral aspect, the proximal part is lower than phalanx III-1. The proximal articular surface is dorsoventrally concave but transversely flat. Both extensor and flexor fossae are shallow. MCF-PVPH-108.24 is another phalanx III-2, although it seems to correspond to the opposite foot of a slightly smaller individual.

MCF-PVPH-108.28 is identified as a right phalanx III-3 (Fig. 34E-G). In proximal view, the kidney-shaped articular surface is dorsoventrally concave and transversely slightly convex, with a shallow, vertical, median keel. In dorsal view, the proximal end is wider than the distal one. The ginglymoid is formed by two well defined condyles, separated by a deep central groove. In dorsal view, the lateral and medial margins of the condyles converge towards the midline (Fig. 34E). The collateral ligament pits open laterally, dorsally and slightly posteriorly. Ventrally, the flexor fossa is represented by a shallow depression with poorly defined borders (Fig. 34G).

MCF-PVPH-108.19 is phalanx IV-1 from the right foot. The proximal articular surface is roughly triangular in outline as in *Allosaurus* (Madsen 1976a). The bone is stout, and has a distal end slightly wider transversely than the proximal one. In lateral view, the proximal half of the phalanx is high. The condyle occupies almost 50% of the length of the phalanx and the distal articular surface is shallowly concave in dorsal view. The medial and lateral margins of the condyle are expanded slightly and are pierced by deep collateral ligament pits. In ventral view, there is a proximal depression for attachment of the flexor tendon.

Specimens MCF-PVPH-108.18 and -108.22 are identified as left and right phalanges IV-2, respectively. The sizes of these elements suggest they could belong to one individual that is about the same size as MCF-PVPH-108.19. These phalanges are antero-posteriorly and transversely subequal in length. The proximal ends are lower than wide, dorsoventrally concave and transversely straight. The ginglymoid is strongly asymmetrical, with the medial side higher

than the lateral. The degree of asymmetry is closer to the one present in *Sinraptor* (Currie & Zhao 1993) than that of *Allosaurus* (Madsen 1976a). The dorsal extensor fossa is well defined and anteroposteriorly narrow. The ventral flexor fossa is rather flat but transversely extensive. There is another right phalanx IV-2 (MCF-PVPH-108.21), which has been identified as belonging to a smaller individual.

## PHYLOGENETIC ANALYSIS AND DISCUSSION

New carcharodontosaurids (including *Carcharodontosaurus*, *Giganotosaurus*, and a new form from Chubut, Argentina) are in the process of being described and will be important for consideration of relationships within the family and in a broader context. For this and other reasons, a preliminary analysis of *Mapusaurus* n. gen. relationships was conducted within the framework of an existing phylogenetic hypothesis (Currie & Carpenter 2000). A matrix of 110 characters (Appendix I) was scored for *Mapusaurus* n. gen., of which 37 character states are unknown (Appendix II). Several features that were coded as unknown for *Giganotosaurus* in a previous analysis (Currie & Carpenter 2000) can now be established. Character 11 was changed to reflect the differences in composition of the supraorbital shelf (formed mostly by the palpebral in Carcharodontosauridae, prefrontal-postorbital in *Acrocanthosaurus*, and lacrimal-postorbital in tyrannosaurids). Characters coded as "9" in Currie & Carpenter (2000) are coded instead as question marks for use in TNT (Tree analysis using New Technology) Version 1 (Goloboff *et al.* 2003). Wherever there were multiple stages listed before for some taxa, only the more derived state was listed in the new analysis.

Using TNT, the implicit enumeration option was run and the new matrix produced three most parsimonious, 238-step trees. With the Nelsen option, the consensus tree shows an unsolved polytomy at the Node Carnosauria (Fig. 35), with a consistency index of 0.601 and a retention index of 0.583. This shows a monophyletic Carcharodontosauridae, which in the present analysis is diagnosed by having

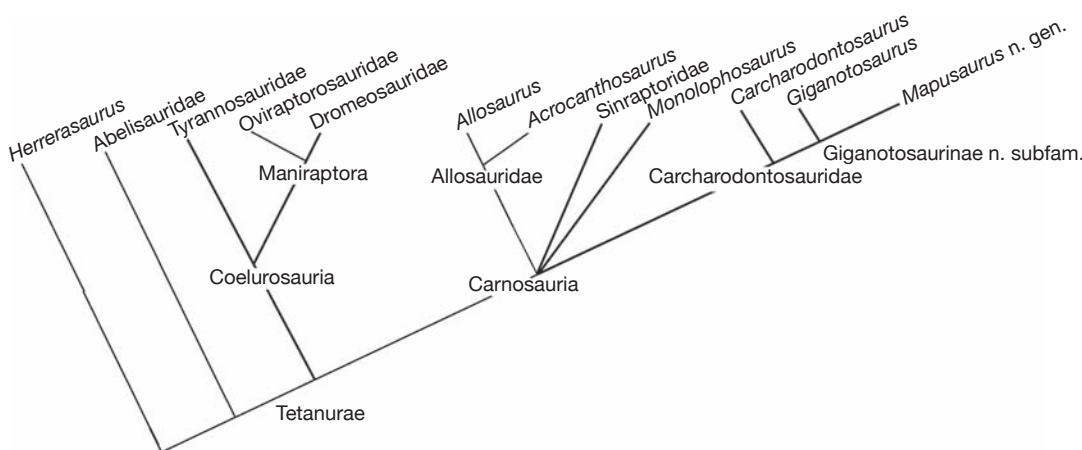


FIG. 35. — Cladogram depicting the strict consensus tree obtained from the phylogenetic analysis.

heavily sculptured facial bones (Character 6, which is convergent with abelisaurids), a supraorbital shelf formed mostly by the palpebral (Character 11), a small suborbital process on the postorbital (Character 12, convergent with *Monolophosaurus*), a lacrimal recess (Character 13, convergent with allosauroids and tyrannosaurids), a highly pneumatic braincase (Character 23), a posteroventrally sloping occiput (Character 25, convergent with *Sinraptor*), distally downturned paroccipital process (Character 26, convergent with *Sinraptor*), flat, bladelike maxillary and dentary teeth with wrinkles in the enamel next to the serrations (Character 42), cervical vertebrae with two pleurocoels in a single fossa (Character 52, shared with *Acrocanthosaurus* and tyrannosaurids) and a femoral head angled at more than 9° upward from the femoral shaft (Character 97).

*Mapusaurus* n. gen. is clearly nested within Carcharodontosauridae by sharing Characters 6, 12, 23, 25, 42 and 97. In the current analysis, two unequivocal features, femur with a weak fourth trochanter (Characters 102) and a shallow and broad extensor groove (Character 103) suggest a closer relationship between *Giganotosaurus* and *Mapusaurus* n. gen. than either has to *Carcharodontosaurus*. Plesiomorphically, in *Herrerasaurus*, tyrannosaurids, allosauroids and most theropods, the femur retains a fourth trochanter as a low but robust ridge. On the other hand, in

primitive theropods like *Herrerasaurus* the femur lacks a clear extensor groove on its distal end. In contrast, carcharodontosaurids bear shallow and broad grooves, converging in this condition with some maniraptorans.

Although geographic and temporal distributions agree with this hypothetical sibling relationship between the South American taxa, the phylogenetic evidence is presently weak and awaits the publication of additional anatomical information and the discovery of more specimens. With these caveats, a new monophyletic taxon – *Giganotosaurinae* n. subfam. – may be defined as all carcharodontosaurids closer to *Giganotosaurus* and *Mapusaurus* n. gen. than to *Carcharodontosaurus*.

Recently, Novas *et al.* (2005) briefly described a new carcharodontosaur from the Aptian of Chubut Province, Central Patagonia. *Tyrannotitan chubutensis* Novas, de Valais, Vickers-Rich & Rich, 2005 was proposed as the basal member of Carcharodontosauridae (Novas *et al.* 2005) by having dentary with a square rostral end, teeth with wrinkles in the enamel next to the serrations, pleurocoels present in dorsal vertebrae, absence of double ventral keel in caudal vertebrae, femoral head proximo-medially angled and fibula proportionally short with respect to femoral length (less than 70%). The two specimens known of *Tyrannotitan* await further and more detailed description. The

amount of missing data due in incompleteness of the specimens generates significant noise in the analysis. Therefore, they were not included in the present data matrix. Nevertheless, personal observations of the type material of *Tyrannotitan chubutensis* indicate the femora have the diagnostic synapomorphic conditions of the Giganotosaurinae n. subfam.

The two known specimens of *Giganotosaurus* are from the underlying Candeleros Formation at El Chocón, 50 km east of the Cañadón del Gato site (Coria & Salgado 1995), and from Cerro los Candeleros, located 50 km west of the *Mapusaurus* n. gen. site (Calvo & Coria 2000). The Candeleros and Huincul Formations of the basal part of the Neuquén Group are easily distinguishable on the basis of their lithologies (Garrido 2000) and faunas (Salgado *et al.* 1991).

Exposures of the Huincul Formation contain extremely rare dinosaur remains, which occur as isolated elements or partial skeletons. The Cañadón del Gato site is the only bonebed known in the formation. So far, 100% of the dinosaur bones removed from the quarry are theropod bones that can be assigned to *Mapusaurus* n. gen.

The depositional environment is interpreted as a channel deposit laid down by an ephemeral and/or seasonal stream in a region with a semiarid or arid climate (Eberth *et al.* 2000). The disarticulated bonebed elements are scattered throughout the base of a paleochannel, and experienced a complex history of decomposition, trampling by large animals, reworking, final burial and differential compaction.

Fifteen metatarsals had been recovered from the Cañadón del Gato bonebed. A right and a left second metatarsal (MCF-PVPH-108.34, -108.36), a right Metatarsal III (-108.32), and a right Metatarsal IV (-108.35) are the correct size and morphology to be from a single individual. The right metatarsals articulate well (Fig. 33), and came from the same part of the quarry (excavated in 1998). Metatarsals can be used to show that there was a minimum of seven individuals represented in the quarry (Table 3). Using equations of allometric size relationships for all theropods (Currie 2003a), the smallest metatarsal, when compared with those of other theropods,

probably came from an animal that was approximately 6 m long. The largest suggests an individual that was 7.3 m in length (Table 1).

Although the largest metatarsals are only about 25% longer than the smallest, there is a massive increase in robustness. For example, the shafts of MCF-PVPH-108.32 and -108.34 are 50 mm wide, whereas that of -108.33 is 77 mm (a 17% increase in length and a 54% increase in shaft width). It is well known that metatarsals undergo negative allometry during growth in theropod species (Currie 2003a), and that the overall effect is to produce more massive metatarsals in the adults (Madsen 1976a). In addition to the metatarsals, there is a dentary small enough to represent an eighth individual of about 5.5 m in total length. Several more bones show the presence of additional, even larger individuals than the minimum number of seven represented by the metatarsals. MCF-PVPH-108.68 is a 1040 mm long tibia, which is 7% smaller than the tibia of *Giganotosaurus*, and represents an animal 9.8 m in length (Table 1). MCF-PVPH-108.202 is an 860 mm long fibula that is actually 2 cm longer than the fibula of the 12.2 m long *Giganotosaurus* (MUCPv-CH-1; Coria & Salgado 1995). The shafts of a scapula (MCF-PVPH-108.185) and a pubis (-108.145) have similar dimensions to the same regions in the holotype of *Giganotosaurus*, whose estimated length reaches the 12.2 m. These bones suggest the presence of at least one individual that is larger than the animal represented by the largest metatarsals, and increase the minimum number of individuals to nine.

Monospecific assemblages of large theropods are scarce worldwide. Up to now, the site is only comparable with an *Albertosaurus* bonebed from Alberta, Canada (Currie 2000), and a new *Daspletosaurus* bonebed from Montana (Currie *et al.* 2005). Although it is conceivable that the theropod dominated bonebed of Cañadón del Gato represents a long term and/or coincidental accumulation of carcasses, the rarity of theropods and abundance of herbivores in all vertebrate ecosystems, and the presence of a single taxon with individuals of different ages suggest it is not a coincidental aggregate of *Mapusaurus roseae* n. gen., n. sp.

## Acknowledgements

The Wilburforce Foundation (Rose Letwin) made a dream come true by supporting the fieldwork of the Argentina-Canada Dinosaur Project between 1999 and 2001. Additional assistance was provided by the Museo Carmen Funes, the Royal Tyrrell Museum of Palaeontology, a Universal Studios/Amblyn Entertainment Dinosaur Research Grant (in 1998 to R. A. C.), Tilley International (Toronto) in 1999, and Troodon Resources Inc. (Calgary) in 1998 and 2004. The authors are very grateful for the logistic support of Dr. Eva B. Koppelhus, and to the many people who participated in the expeditions. Figures 2-11, 13-18, 22-25 and 31 were drawn by Fernando Cruz; Figures 1, 12 and 35 made by R. A. C.; credit for other figures goes to Alfredo Gerez. Drs. Paul Sereno (Chicago) and Hans Larsson (Montreal) kindly provided access to the beautifully preserved *Carcharodontosaurus* skull from Morocco, and Dr. Rubén Cúneo and Silvina de Valais (Museo "Egidio Feruglio", Trelew) made the Chubut carcharodontosaurid available for study. The manuscript was reviewed by Drs. Ronan Allain and Paul C. Sereno and their comments are greatly appreciated.

## REFERENCES

- ANDERSON J. F., HALL-MARTIN A. & RUSSELL D. A. 1985. — Long-bone circumference and weight in mammals, birds and dinosaurs. *Journal of Zoology* London (A), 207: 53-61.
- ARCUCCI A. B. & CORIA R. A. 2003. — A new Triassic carnivorous dinosaur from Argentina. *Ameghiniana* 40: 217-228.
- BAKKER R. T. 2000. — Brontosaur killers: Late Jurassic allosaurids as saber-tooth cat analogues. *Gaia* 15: 145-158 (dated 1998, published 2000).
- BAKKER R. T., KRALIS D., SIEGWARTH J. & FILLA J. 1992. — *Edmarka rex*, a new, gigantic theropod dinosaur from the middle Morrison Formation, Late Jurassic of the Como Bluff outcrop region. *Hunteria* 2: 1-24.
- BONAPARTE J. F. 1991. — The Gondwanian theropod families Abelisauroidea and Noasauridae. *Historical Biology* 5: 1-25.
- BONAPARTE J. F. & NOVAS F. E. 1985. — *Abelisaurus comahuensis*, n.g., n.sp., Carnosauria del Cretácico Tardío de Patagonia. *Ameghiniana* 21: 259-265.
- BONAPARTE J. F., NOVAS F. E. & CORIA R. A. 1990. — *Carnotaurus sastrei* Bonaparte, the horned, lightly built carnosaur from the Middle Cretaceous of Patagonia. *Contributions in Science, Natural History Museum of Los Angeles County* 416: 1-41.
- BRITT B. B. 1991. — The theropods of the Dry Mesa Quarry (Morrison Formation), Colorado: with emphasis on the osteology of *Torvosaurus tanneri*. *Brigham Young University, Geology Studies* 37: 1-72.
- CALVO J. & CORIA R. A. 2000. — A new specimen of *Giganotosaurus carolinii* Coria & Salgado 1995, supports it as the largest theropod ever found. *Gaia* 15: 117-122 (dated 1998, published 2000).
- CHARIG A. J. & MILNER A. C. 1997. — *Baryonyx walkeri*, a fish-eating dinosaur from the Wealden of Surrey. *Bulletin of the British Natural History Museum, Geological Series* 53: 11-70.
- CHATTERJEE S. 1978. — *Indosuchus* and *Indosaurus*, Cretaceous carnosaurs from India. *Journal of Paleontology* 52: 570-580.
- CHURE D. J. & MADSEN J. H. 1996. — On the presence of furculae in some non-maniraptoran theropods. *Journal of Vertebrate Paleontology* 16: 573-577.
- CHURE D. J., MANABE M., TANIMOTO M. & TOMIDA Y. 1999. — An unusual theropod tooth from the Mifune Group (Late Cenomanian to Early Turonian), Kumamoto, Japan. *National Science Museum Monographs* 15: 291-296.
- CORIA R. A. 2001. — New theropod from the Late Cretaceous of Patagonia, in TANKE D. H. & CARPENTER K. (eds), *Mesozoic Vertebrate Life*. Indiana University Press, Bloomington; Indianapolis: 3-9.
- CORIA R. A., CHIAPPE L. & DINGUS L. 2002. — A new close relative of *Carnotaurus sastrei* Bonaparte 1985 (Theropoda: Abelisauroidea) from the Late Cretaceous of Patagonia. *Journal of Vertebrate Paleontology* 22: 460-465.
- CORIA R. A. & CURRIE P. J. 1997. — A new theropod from the Río Limay Formation. *Journal of Vertebrate Paleontology* 17: 40A.
- CORIA R. A. & CURRIE P. J. 2002. — The braincase of *Giganotosaurus carolinii* (Dinosauria: Theropoda) from the Upper Cretaceous of Argentina. *Journal of Vertebrate Paleontology* 22: 802-811.
- CORIA R. A. & SALGADO L. 1995. — A new giant carnivorous dinosaur from the Cretaceous of Patagonia. *Nature* 377: 224-226.
- CORIA R. A. & SALGADO L. 2000. — A basal Abelisauroidea Novas, 1992 (Theropoda, Ceratosauria) from the Cretaceous of Patagonia, Argentina. *Gaia* 15: 89-102 (dated 1998, published 2000).
- CURRIE P. J. 1995. — New information on the anatomy and relationships of *Dromaeosaurus albertensis* (Dinosauria: Theropoda). *Journal of Vertebrate Paleontology* 15: 576-591.
- CURRIE P. J. 2000. — Possible evidence of gregarious

- behaviour in tyrannosaurids. *Gaia* 15: 271-277 (dated 1998, published 2000).
- CURRIE P. J. 2003a. — Allometric growth in tyrannosaurids (Dinosauria: Theropoda) from the Upper Cretaceous of North America and Asia. *Canadian Journal of Earth Sciences* 46: 651-665.
- CURRIE P. J. 2003b. — Cranial anatomy of tyrannosaurid dinosaurs from the Late Cretaceous of Alberta, Canada. *Acta Palaeontologica Polonica* 48: 191-226.
- CURRIE P. J. & CARPENTER K. 2000. — A new specimen of *Acrocanthosaurus atokensis* (Theropoda, Dinosauria) from the Lower Cretaceous Antlers Formation (Lower Cretaceous, Aptian) of Oklahoma, USA. *Geodiversitas* 22 (2): 207-246.
- CURRIE P. J. & CHEN P. J. 2001. — Anatomy of *Sinosauroptryx prima* from Liaoning, northeastern China. *Canadian Journal of Earth Sciences* 38: 1705-1727.
- CURRIE P. J., RIGBY K. JR. & SLOAN R. E. 1990. — Theropod teeth from the Judith River Formation of southern Alberta, Canada, in CARPENTER K. & CURRIE P. J. (eds), *Dinosaur Systematics: Approaches and Perspectives*. Cambridge University Press, New York: 107-125.
- CURRIE P. J., TREXLER D., KOPPELHUS E. B., WICKS K. & MURPHY N. 2005. — An unusual multi-individual, tyrannosaurid bonebed in the Two Medicine Formation (Late Cretaceous, Campanian) of Montana (USA), in CARPENTER K. (ed.), *The Carnivorous Dinosaurs*. Indiana University Press, Bloomington; Indianapolis: 313-324.
- CURRIE P. J. & ZHAO X. J. 1993. — A new carnosaur (Dinosauria, Theropoda) from the Jurassic of Xinjiang, People's Republic of China. *Canadian Journal of Earth Sciences* 30: 2037-2081.
- DEPÉRET C. & SAVORNIN J. 1927. — Sur la découverte d'une faune de vertébrés albiens à Timimoun (Sahara occidental). *Comptes rendus de l'Académie des Sciences*, Paris 181: 1108-1111.
- EBERTH D. A., CURRIE P. J., CORIA R. A., GARRIDO A. C. & ZONNEVELD J.-P. 2000. — Large-theropod bonebed, Neuquén, Argentina: Paleoecological importance. *Journal of Vertebrate Paleontology* 20: 39A.
- FARLOW J. O., BRINKMAN D. L., ABLER W. L. & CURRIE P. J. 1991. — Size, shape and serration density of theropod dinosaur lateral teeth. *Modern Geology* 16: 161-198.
- GARRIDO A. C. 2000. — *Estudio estratigráfico y reconstrucción paleoambiental de las secuencias fosilíferas continentales del Cretácico Superior en las inmediaciones de Plaza Huincul, provincial del Neuquén*. MSc. Thesis, Universidad Nacional de Córdoba, Facultad de Ciencias Exactas Físicas y naturales, Córdoba, Argentina, 78 p.
- GAUTHIER J. 1986. — Saurischian monophyly and the origin of birds. *California Academy of Sciences, Memoirs* 8: 1-55.
- GILMORE C. W. 1920. — Osteology of the carnivorous Dinosauria in the United States National Museum, with special reference to the genera *Antrodemus* (Allosaurus) and *Ceratosaurus*. *United States National Museum, Bulletin* 110: 1-159.
- GOLOBOFF P., FARRIS J. & NIXON K. 2003. — *T.N.T.: Tree Analysis Using New Technology*. Program and documentation, available from the authors, and at [www.zmuc.dk/public/phylogeny](http://www.zmuc.dk/public/phylogeny)
- HARRIS J. D. 1998. — A reanalysis of *Acrocanthosaurus atokensis*, its phylogenetic status, and paleobiogeographic implications, based on a new specimen from Texas. *New Mexico Museum of Natural History and Science Bulletin* 13: 1-75.
- HOLTZ T. R. 2000. — A new phylogeny of the carnivorous dinosaurs. *Gaia* 15: 5-61 (dated 1998, published 2000).
- HUTT S., MARTILL D. M. & BARKER M. J. 1996. — The first European allosaurid dinosaur (Lower Cretaceous, Wealden Group, England). *Neues Jahrbuch für Geologie und Paläontologie Monatshefte* 10: 635-644.
- LAMANNA M. C., MARTÍNEZ R. D. & SMITH J. B. 2002. — A definitive abelisaurid theropod dinosaur from the early Late Cretaceous of Patagonia. *Journal of Vertebrate Paleontology* 22: 58-69.
- LAPPARENT A. F. DE 1960. — Les dinosauriens du «Continental intercalaire» du Sahara central. *Mémoires de la Société géologique de France*, nelle sér. 88A: 1-57.
- LARSSON H. C. E. 2001. — Endocranial anatomy of *Carcharodontosaurus saharicus* (Theropod: Allosauroidea) and its implications for theropod brain evolution, in TANKE D. H. & CARPENTER K. (eds), *Mesozoic Vertebrate Life*. Indiana University Press, Bloomington; Indianapolis: 19-33.
- LEANZA H. A., APESTEGUÍA S., NOVAS F. E. & DE LA FUENTE M. 2004. — Cretaceous terrestrial beds from the Neuquén Basin (Argentina) and their tetrapods assemblages. *Cretaceous Research* 25: 61-87.
- LEGARRETA L. & GULISANO C. A. 1989. — Análisis estratigráfico secuencial de la Cuenca Neuquina (Triásico Superior-Terciario Inferior). X Congreso Geológico Argentino, in CHEBLI G. & SPALETTI R. (eds), *Cuencas Sedimentarias Argentinas, Serie Correlación Geológica 6*, Buenos Aires: 221-243.
- MADSEN J. H. 1976a. — *Allosaurus fragilis*: a revised osteology. *Utah Geological and Mineral Survey Bulletin* 109: 1-163.
- MADSEN J. H. 1976b. — A second new theropod dinosaur from the Late Jurassic of east central Utah. *Utah Geology* 3: 51-60.
- MAKOVICKY P. & CURRIE P. J. 1998. — The presence of a furcula in tyrannosaurid theropods, and its phylogenetic and functional implications. *Journal of Vertebrate Paleontology* 18: 143-149.
- MALEEV E. A. 1974. — [Gigantic carnosaurs of the family Tyrannosauridae]. *Joint Soviet-Mongolian*

- Paleontological Expedition, Transactions* 1: 132-191 (in Russian).
- NOVAS F. E. 1997. — Abelisauridae, in CURRIE P. J. & PADIAN K. (eds), *Encyclopedia of Dinosaurs*. Academic Press, San Diego: 1-2.
- NOVAS F. E., MARTÍNEZ R. D., DE VALAIS S. & AMBROSIO A. 1999. — Nuevos registros de carcharodontosauridae (Dinosauria, Theropoda) en el Cretácico de Patagonia. *Ameghiniana* 36: 17R.
- NOVAS F. E., DE VALAIS S., VICKERS-RICH P. & RICH T. 2005. — A large Cretaceous theropod from Patagonia, Argentina, and the evolution of carcharodontosaurids. *Naturwissenschaften* 92 (5): 226-230.
- RAMOS V. A. 1981. — Descripción Geológica de la Hoja 33c Los Chihuidos Norte, Provincia del Neuquén. *Servicio Geológico Nacional Boletín* 182: 1-103.
- RAUHUT O. W. M. 1995. — Zur systematischen Stellung der afrikanischen Theropoden *Carcharodontosaurus* Stromer, 1931 und *Bahariasaurus* Stromer, 1934. *Berliner geowissenschaftliche Abhandlungen* (E) 16: 357-375.
- RICH T. H., VICKERS-RICH P., NOVAS F. E., CUNEO R., PUERTA P. & VACCA R. 2000. — Theropods from the “Middle” Cretaceous Chubut Group of the San Jorge Sedimentary Basin, central Patagonia. A preliminary note. *Gaia* 15: 111-115 (dated 1998, published 2000).
- ROMER A. S. 1966. — *Vertebrate Paleontology*. University of Chicago Press, Chicago, Illinois, 468 p.
- RUSSELL D. A. 1970. — Tyrannosaurs from the Late Cretaceous of western Canada. *National Museum of Natural Sciences, Publications in Palaeontology* 1: 1-34.
- RUSSELL D. A. 1996. — Isolated dinosaur bones from the Middle Cretaceous of the Tafilalt, Morocco. *Bulletin du Muséum national d’Histoire Naturelle*, Paris, sér. 4, section C, 18 (2-3): 349-402.
- SALGADO L., CALVO J. & CORIA R. A. 1991. — Estudio preliminar de dinosaurios saurópodos de la Formación Río Limay (Cretácico Preseroniano, Provincia de Neuquén). *Ameghiniana* 28: 134.
- SAMPSON S. D., WITMER L. D., FORSTER C. A., KRAUSE D. W., O’CONNOR P. M., DODSON P. & RAVOAVY F. 1998. — Predatory dinosaur remains from Madagascar: implications for the Cretaceous biogeography of Gondwana. *Science* 280: 1048-1051.
- SERENO P. C. 1999. — The evolution of dinosaurs. *Science* 284: 2137-2147.
- SERENO P. C. & NOVAS F. E. 1993. — The skull and neck of the basal theropod *Herrerasaurus ischigualastensis*. *Journal of Vertebrate Paleontology* 13: 451-476.
- SERENO P. C., WILSON J. A., LARSSON H. C. E., DUTHEIL D. B. & SUES H.-D. 1994. — Early Cretaceous dinosaurs from the Sahara. *Science* 266: 267-271.
- SERENO P. C., DUTHEIL D. B., IAROCHENE S. M., LARSSON H. C. E., LYON G. H., MAGWENE P. M., SIDOR C. A., VARRICCHIO D. J. & WILSON J. A. 1996. — Late Cretaceous dinosaurs from the Sahara. *Science* 272: 986-991.
- STROMER E. 1931. — Wirbeltiere-Reste der Baharijestufe (unterstes Canoman). Ein Skelett-Rest von *Carcharodontosaurus* nov. gen. *Abhandlungen der Bayerischen Akademie der Wissenschaften, Mathematisch-naturwissenschaftliche Abteilung* 9, Neue Folge: 1-23.
- VICKERS-RICH P., RICH T. H., LANUS D. R., RICH L. S. V. & VACCA R. 1999. — “Big Tooth” from the early Cretaceous of Chubut Province, Patagonia: a possible carcharodontosaurid. *National Science Museum Monographs* 15: 85-88.
- WALKER A. D. 1964. — Triassic reptiles from the Elgin area: *Ornithosuchus* and the origin of carnosaurs. *Philosophical Transactions of the Royal Society of London* B 248: 53-134.
- WITMER L. M. 1997. — The evolution of the antorbital cavity of archosaurs: a study in soft-tissue reconstruction in the fossil record with an analysis of the function of pneumaticity. *Society of Vertebrate Paleontology Memoir* 3: 1-73.
- ZHAO X. J. & CURRIE P. J. 1993. — A large crested theropod from the Jurassic of Xinjiang, People’s Republic of China. *Canadian Journal of Earth Sciences* 30: 2027-2036.

Submitted on 12 July 2004;  
accepted on 25 July 2005.

## APPENDIX I

Data matrix used for phylogenetic analysis. **0**, primitive state; **1**, **2**, **3**, **4**, derived character states (multistates characters treated unordered); **?**, missing data. The matrix is the same as Currie & Carpenter (2000) except that it includes *Mapusaurus* n. gen., the revision of Character 11 required the recoding of characters for some taxa, and some previously unknown states could be coded because of new information.

1. Premaxillae and dentaries, shape of front of snout from above or below: 0, V-shaped; 1, U-shaped.
2. Premaxilla-nasal contact below external naris: 0, present; 1, absent; 2, extensive contact behind external naris.
3. Antorbital fossa, additional openings: 0, none; 1, promaxillary only; 2, promaxillary and maxillary; 3, promaxillary and maxillary, plus more.
4. Lateral temporal fenestra: 0, large and triangular; 1, reduced and keyhole-shaped; 2, constricted at midheight.
5. Maxilla, tooth row: 0, extends beneath orbit; 1, ends before orbit.
6. Facial bones (maxilla, nasal), sculpturing: 0, moderate; 1, heavily sculptured to edge of antorbital fenestra.
7. Nasal, participates in antorbital fossa: 0, no or slightly; 1, broadly.
8. Nasals, fused on midline: 0, no; 1, yes.
9. Prefrontal: 0, large; 1, reduced; 2, absent.
10. Postorbital, ventral end above ventral margin of orbit: 0, yes; 1, no.
11. Supraorbital shelf formed mostly by palpebral: 0, absent; 1, present.
12. Postorbital, suborbital flange: 0, absent; 1, small; 2, large.
13. Lacrimal pneumatic recess: 0, absent; 1, present.
14. Lacrimal horn: 0, non-existent; 1, low crest or ridge; 2, high-pointed cone.
15. Jugal pneumatic: 0, no; 1, yes.
16. Jugal, foramen on medial surface: 0, absent; 1, present.
17. Jugal, expressed on rim of antorbital fenestra: 0, no; 1, yes.
18. Jugal, qj process, length of upper prong to lower: 0, subequal; 1, upper shorter; 2, upper longer.
19. Preorbital bar, suborbital process: 0, not present; 1, present.
20. Quadrato short: 0, no; 1, yes.
21. Quadrato fenestra: 0, none; 1, between quadrato and quadratejugal; 2, surrounded by quadrato.
22. Orbit, expanded and circular: 0, no; 1, yes.
23. Braincase pneumatism: 0, apneumatic; 1, moderately; 2, highly pneumatic.
24. Basioccipital participates in basal tubers: 0, yes; 1, no.
25. Occiput: 0, nearly vertical; 1, slopes posterovertrally.
26. Paraoccipital process downturned distally: 0, no; 1, moderate; 2, distal ends below foramen magnum.
27. Exoccipital-opisthotic, posterovertral limit of contact with basisphenoid separated from basal tubera by notch: 0, no; 1, yes.
28. Trigeminal nerve, separation of ophthalmic branch: 0, no; 1, incipient; 2, complete.
29. Internal carotid artery, pneumatized opening: 0, no; 1, yes.
30. Basipterygoid processes: 0, long; 1, short.
31. Palatine: 0, subrectangular or trapezoidal; 1, tetra-
- radiate.
32. Palatine, subsidiary palatal fenestra: 0, absent; 1, present.
33. Palatine, meet medially: 0, no; 1, yes.
34. Palatine, jugal process expanded distally: 0, no; 1, yes.
35. Palatine, pneumatic recess: 0, none; 1, small fossa; 2, small foramen; 3, large fossa; 4, large fossa with at least one foramen.
36. Ectopterygoid, pneumatic recess: 0, elongate; 1, subcircular.
37. Surangular, dorsoventral height: 0, less than two times the maximum height of surangular; 1, more than two times.
38. External mandibular fenestra: 0, large; 1, reduced.
39. Splenial forms notched anterior margin of internal mandibular fenestra: 0, absent; 1, present.
40. Articular, retroarticular process broad and faces posteriorly: 0, no; 1, yes.
41. Teeth, premaxillary ones asymmetrical in cross-section: 0, no; 1, yes; 2, yes, D-shaped.
42. Teeth, flat and blade-like in maxilla and dentary with wrinkles in the enamel next to the serrations: 0, no; 1, yes; 2, no wrinkles, but teeth greatly thickened and enlarged.
43. Atlas, neurapophysis in lateral view: 0, not triangular; 1, triangular.
44. Axis, strong tilt of axial intercentrum to axial ventral margin: 0, subparallel; 1, tilted dorsally.
45. Axis, ventral keel: 0, absent; 1, present.
46. Axis, epiphysis: 0, none; 1, small; 2, large.
47. Axis, distal end of neural spine: 0, not expanded; 1, expanded (spine table).
48. Cervical vertebrae: 0, not opisthocoelous; 1, weakly opisthocoelous; 2, strongly opisthocoelous.
49. Cervical vertebrae, anterior facets reniform: 0, no; 1, yes.
50. Cervical vertebrae, posterior facets reniform and more than 20% broader than tall: 0, no; 1, yes.
51. Cervical vertebrae, prezygapophyses: 0, planar; 1, flexed.
52. Cervical vertebrae, postaxial pleurocoels: 0, absent; 1, fossa only; 2, fossa with one foramen; 3, more than one foramen.
53. Cervical vertebrae, interior: 0, apneumatic; 1, simple camerata; 2, complex camerata.
54. Cervical vertebrae, hypapophyses of posterior cervicals and anterior dorsals: 0, absent; 1, anterior dorsals only; 2, posterior cervicals and anterior dorsals.
55. Dorsal vertebrae, 10th presacral in dorsal series: 0, no; 1, yes.
56. Dorsal vertebrae, anterior dorsals opisthocoelous: 0, no; 1, yes.
57. Dorsal vertebrae, pleurocoels: 0, none; 1, on anterior dorsals; 2, on all dorsals.
58. Dorsal vertebrae, posterior neural spines incline

- anterodorsally: 0, no; 1, yes.
59. Sacral vertebrae, pleurocoelous: 0, no; 1, yes.
60. Sacral vertebrae, synsacrum: 0, absent; 1, present.
61. Caudal vertebrae, pleurocoels in proximal tail: 0, no; 1, yes.
62. Caudal vertebrae, double ventral keel: 0, absent; 1, present.
63. Caudal vertebrae, subsidiary foramina in proximal and distal excavations in neural spines: 0, absent; 1, present.
64. Haemal arches, paired anterior and posterior processes at base: 0, no; 1, yes.
65. Haemal arches, L-shaped in distal chevrons: 0, no; 1, yes.
66. Caudal vertebrae, transverse processes: 0, more than 15; 1, fewer than 15.
67. Cervical ribs, aliform process at base of anterior rib shafts: 0, no; 1, yes.
68. Scapulocoracoid, pronounced notch between acromial process and coracoid: 0, no; 1, yes.
69. Scapula, elongate blade set off from glenoid and acromial process: 0, grades smoothly; 1, abrupt.
70. Coracoid: 0, not rectangular; 1, subrectangular.
71. Sternum, sternal plates fused in adults: 0, no; 1, yes.
72. Humerus: 0, straight; 1, sigmoidal.
73. Ulna, bowed strongly posteriorly: 0, no; 1, yes.
74. Manus, manus length to length of humerus plus radius: 0, less than two thirds; 1, more than two thirds.
75. Carpals, semi-lunate carpal articular facets: 0, none (not truly semi-lunate); 1, proximal and distal facets.
76. Metacarpal I, at least half of proximal end closely applied to Mt II: 0, no; 1, yes.
77. Metacarpal I, ratio mcl/mcII: 0, more than one third; 1, less than one third.
78. Metacarpal III; long and slender: 0, no; 1, yes.
79. Metacarpal IV, retained: 0, yes; 1, no.
80. Forelimb length: presacral column; manus length; pes length: 0, < 75%, pes greater; 1, > 75%, manus and pes subequal.
81. Ilium, hook-like ventral process on anteroventral margin forming preacetabular notch: 0, absent; 1, present.
82. Ilium, pronounced ridge in lateral side divides ilium into pre- and postacetabular fossae: 0, absent; 1, present.
83. Ilium, posterodorsal margin in lateral view: 0, subvertical; 1, angled posteroventrally.
84. Ilium, pubic peduncle twice as long anteroposteriorly as mediolaterally: 0, no; 1, yes.
85. Pubis, obturator opening: 0, foramen; 1, incipient notch; 2, notch.
86. Pubis, in lateral view: 0, curves posteriorly; 1, straight; 2, curves anteriorly; 3, retroverted.
87. Pubis, distal opening: 0, none; 1, pubic notch; 2, pubic foramen.
88. Pubis, distal end: 0, not expanded; 1, 30% pubis length; 2, more than 30%.
89. Pubis, distal view of conjoined pubic boots: 0, not triangular; 1, triangular.
90. Pubis, anterior projection of pubic boot compared to posterior: 0, large; 1, small or absent.
91. Ischium, obturator opening: 0, none; 1, foramen; 2, notch.
92. Ischium, obturator process: 0, proximal; 1, distal.
93. Ischium, obturator process: 0, not triangular; 1, triangular.
94. Ischium less than two thirds of the length of pubis: 0, no; 1, yes.
95. Ischium, fusion of distal halves: 0, no; 1, yes.
96. Ischium, distal expansion: 0, absent; 1, present but not boot-shaped; 2, present, boot-shaped.
97. Femur, angle of caput to shaft in anterior or posterior view: 0, less than 90°; 1, perpendicular; 2, more than 90°.
98. Femur, mound-like greater trochanter: 0, no; 1, yes.
99. Femur, deep notch between greater and lesser trochanter: 0, no; 1, yes.
100. Femur, lesser trochanter: 0, distal in position, at or below level margin of head; 1, proximal in position.
101. Femur, lesser trochanter: 0, shelf; 1, non aliform; 2, aliform.
102. Femur, fourth trochanter: 0, robust; 1, weak; 2, absent.
103. Femur, extensor groove on distal end: 0, absent; 1, shallow and broad; 2, deep and narrow.
104. Femur, ridge for cruciate ligaments in flexor groove: 0, absent; 1, present.
105. Femur, distal end: 0, shallow, round depression bound laterally by low ridge; 1, sharp anteromedial ridge; 2, low, rounded anteromedial ridge.
106. Tibia, fibular fossa occupied all of medial aspect of proximal end: 0, no; 1, yes.
107. Astragalus and calcaneum fuse to each other and tibia: 0, no; 1, yes.
108. Fibula, distal end: 0, expanded more than twice shaft width; 1, less than twice width.
109. Astragalus, height of ascending process: 0, less than a sixth of tibial length; 1, one sixth to one quarter; 2, more than a quarter.
110. Astragalus, condyle orientation: 0, ventrally; 1, anteroventrally.

## APPENDIX II

Character matrix of 110 anatomical features scored among 12 taxa of theropod dinosaurs. *Herrerasaurus* was taken as the outgroup. No autapomorphies of any terminal taxa were run in the analysis.

	1	2	3	4	5	6	7	8	9	10	11	12	13	14	15	16	17	18	19	20	21	22	23	24
Abelisauridae	0	0	1	0	0	1	0	1	1	0	1	2	0	0	0	0	1	0	0	0	0	0	0	0
<i>Acrocanthosaurus</i>	0	0	2	0	1	0	1	0	1	0	1	0	1	1	1	1	1	1	0	1	0	1	1	1
<i>Allosaurus</i>	0	1	2	1	1	0	1	0	1	0	0	0	1	2	1	0	1	0	1	0	2	0	1	1
<i>Carcharodontosaurus</i>	0	?	1	0	1	1	1	0	1	0	1	1	1	1	1	?	1	1	0	0	1	0	2	0
Dromaeosauridae	0	0	2	2	1	0	0	0	2	0	0	0	0	0	1	?	1	1	0	1	1	1	1	0
<i>Giganotosaurus</i>	0	0	1	0	?	1	1	0	1	?	1	1	1	1	?	?	?	?	0	0	1	0	2	0
<i>Mapusaurus</i> n. gen.	0	0	1	?	1	1	1	0	0	0	1	?	1	1	1	0	1	1	1	0	1	0	?	?
<i>Herrerasaurus</i>	0	0	0	0	0	0	0	0	0	0	0	0	0	0	0	0	0	0	0	0	0	1	0	0
<i>Monolophosaurus</i>	0	1	1	1	0	1	1	1	1	0	1	0	2	?	1	1	1	1	0	1	0	1	0	0
Oviraptorosauria	1	2	2	2	1	0	0	?	2	1	0	0	0	0	0	0	0	0	?	0	1	?	1	1
Sinraptoridae	0	0	3	0	1	0	1	0	1	0	0	0	1	1	1	1	1	1	1	0	1	0	1	0
Tyrannosauridae	1	0	2	2	1	0	0	1	1	0	1	2	1	2	1	1	1	1	0	1	1	0	1	0
	25	26	27	28	29	30	31	32	33	34	35	36	37	38	39	40	41	42	43	44	45	46	47	48
Abelisauridae	0	0	0	1	0	1	?	?	?	?	?	?	1	0	0	?	1	0	0	0	1	2	0	1
<i>Acrocanthosaurus</i>	0	2	?	2	1	0	1	?	?	1	4	0	?	1	1	1	1	0	?	0	1	2	1	2
<i>Allosaurus</i>	0	2	1	2	1	0	1	0	1	1	2	0	0	1	1	1	1	0	1	0	0	1	1	2
<i>Carcharodontosaurus</i>	1	1	?	1	0	?	?	?	?	?	?	?	?	?	?	?	?	1	1	?	?	?	?	?
Dromaeosauridae	0	0	0	0	1	1	1	1	0	3	1	?	0	1	1	1	0	0	0	1	1	1	0	0
<i>Giganotosaurus</i>	1	1	?	?	0	?	?	?	?	?	?	?	?	?	?	?	1	1	?	1	1	2	?	2
<i>Mapusaurus</i> n. gen.	?	?	?	?	?	?	?	?	?	?	?	?	?	?	?	?	1	?	?	?	1	0	?	2
<i>Herrerasaurus</i>	0	0	0	0	0	1	0	0	0	0	0	0	0	0	0	0	0	0	0	0	0	1	1	0
<i>Monolophosaurus</i>	0	0	1	?	?	1	?	?	?	?	?	?	1	?	1	?	1	0	1	1	?	1	1	2
Oviraptorosauria	0	0	0	?	1	?	0	0	0	0	0	0	1	1	0	?	0	?	?	0	0	?	1	0
Sinraptoridae	1	1	1	1	0	1	1	0	1	4	0	0	0	1	1	1	1	0	1	1	0	2	1	2
Tyrannosauridae	0	0	0	2	1	0	1	1	?	?	4	1	1	1	1	2	2	?	0	1	?	1	0	0
	49	50	51	52	53	54	55	56	57	58	59	60	61	62	63	64	65	66	67	68	69	70	71	72
Abelisauridae	0	0	0	2	?	0	0	0	1	0	0	1	0	?	0	0	?	?	1	0	0	0	0	0
<i>Acrocanthosaurus</i>	0	0	0	3	2	?	1	1	2	1	1	0	0	1	1	1	1	0	1	1	1	0	?	1
<i>Allosaurus</i>	0	0	0	1	1	1	1	1	1	1	0	0	0	1	?	1	1	0	0	1	1	1	0	0
<i>Carcharodontosaurus</i>	1	1	0	3	?	?	?	2	1	?	?	?	?	0	?	0	?	?	?	?	?	?	?	?
Dromaeosauridae	1	1	1	2	1	2	0	0	2	0	1	1	0	1	0	0	0	1	0	0	0	1	0	1
<i>Giganotosaurus</i>	0	0	?	3	?	?	?	1	1	?	?	?	0	?	?	?	?	0	?	?	?	0	?	?
<i>Mapusaurus</i> n. gen.	0	0	0	3	2	1	?	1	2	0	1	?	0	0	0	0	0	1	0	0	0	0	0	0
<i>Herrerasaurus</i>	0	0	0	0	0	?	0	0	0	0	?	0	0	0	?	0	?	0	1	0	?	0	0	0
<i>Monolophosaurus</i>	?	0	?	1	20	1	1	1	?	?	?	0	1	?	?	?	?	?	?	?	?	?	?	?
Oviraptorosauria	1	1	1	2	2	1	0	0	2	0	1	1	1	1	1	0	0	0	0	0	1	1	1	1
Sinraptoridae	0	0	0	1	1	1	1	1	1	0	?	0	1	?	?	?	?	1	1	?	1	?	1	?
Tyrannosauridae	0	1	0	3	2	0	0	0	1	0	1	1	0	?	0	1	1	?	0	1	1	1	0	0
	73	74	75	76	77	78	79	80	81	82	83	84	85	86	87	88	89	90	91	92	93	94	95	96
Abelisauridae	0	0	0	0	0	0	0	0	1	0	0	?	0	1	1	1	?	1	0	?	?	0	1	2
<i>Acrocanthosaurus</i>	0	1	0	1	0	0	1	0	?	?	?	?	?	2	2	2	2	1	0	2	0	0	0	2
<i>Allosaurus</i>	0	1	0	1	0	0	1	0	1	0	0	1	2	2	2	2	1	0	2	0	0	0	0	1
<i>Carcharodontosaurus</i>	?	?	?	?	?	?	?	?	?	?	?	?	?	2	?	?	?	?	2	0	0	?	?	?
Dromaeosauridae	1	1	1	1	1	1	1	1	0	0	1	1	2	3	1	2	?	1	2	1	1	1	1	0
<i>Giganotosaurus</i>	?	?	?	?	?	?	?	?	1	0	0	0	0	2	1	1	2	1	0	2	0	0	0	1
<i>Mapusaurus</i> n. gen.	?	?	?	0	?	0	?	?	1	0	0	0	0	2	?	?	?	?	2	0	0	0	0	1
<i>Herrerasaurus</i>	0	0	0	0	0	0	0	0	0	0	0	0	0	0	1	2	?	0	0	?	?	0	1	0
<i>Monolophosaurus</i>	?	?	?	?	?	?	?	?	1	0	0	0	0	0	?	1	?	1	1	?	?	0	0	?
Oviraptorosauria	1	1	1	1	0	1	1	1	0	?	1	2	2	0	1	2	0	2	1	1	1	1	1	1
Sinraptoridae	?	?	?	1	0	0	0	?	1	2	0	1	1	1	2	1	1	2	1	1	2	0	0	1
Tyrannosauridae	0	1	0	1	0	1	1	0	1	2	0	1	2	2	0	2	1	0	2	1	1	1	0	0

	97	98	99	100	101	102	103	104	105	106	107	108	109	110
Abelisauridae	1	0	0	0	1	?	?	?	?	1	1	0	0	?
Acrocanthosaurus	1	0	1	1	2	0	2	1	1	?	0	1	1	1
Allosaurus	1	0	1	1	2	0	1	1	2	0	0	1	1	1
Carcharodontosaurus	2	0	1	0	2	0	2	?	1	?	?	?	?	?
Dromaeosauridae	1	1	0	1	1	2	1	0	2	1	0	1	2	0
Giganotosaurus	2	0	1	0	2	1	1	0	1	0	0	1	1	?
Mapusaurus n. gen.	2	0	1	0	2	1	1	0	1	0	0	1	1	0
Herrerasaurus	0	0	0	0	0	0	0	0	0	1	0	0	0	0
Monolophosaurus	?	?	?	?	?	?	?	?	?	?	?	?	?	?
Oviraptorosauria	1	1	1	1	1	1	0	?	?	0	1	2	0	
Sinraptoridae	1	0	1	1	2	0	2	1	1	0	0	1	0	1
Tyrannosauridae	1	1	1	1	2	0	2	0	2	0	0	1	2	0

### APPENDIX III

TABLE 1. — Estimated lengths (in mm) of animals represented in the *Mapusaurus* n. gen. bonebed. Calculations based on the relationship between femur length and body length for theropods in which both these values are known (equation is  $y = 1.0276x + 0.8437$ , where  $y$  is the logarithm of complete body length and  $x$  is the logarithm of femur length). Because of the diversity of theropod body forms, these calculations can only be considered as very rough estimates.

Specimen number	Element	Length	Side of body
MCF-PVPH-108.3	Dentary	5.5	Left
MCF-PVPH-108.44	Femur	9.9	Left
MCF-PVPH-108.203	Femur	10.2	Left
MCF-PVPH-108.233	Femur	9.5	Right
MCF-PVPH-108.58	Tibia	9.7	Left
MCF-PVPH-108.67	Tibia	8.1	Right
MCF-PVPH-108.68	Tibia	9.8	Left
MCF-PVPH-108.132	Fibula	8.4	Left
MCF-PVPH-108.189	Fibula	8.3	Left
MCF-PVPH-108.202	Fibula	8.8	Right
MCF-PVPH-108.33	Metatarsal II	7.2	Left
MCF-PVPH-108.34	Metatarsal II	6.1	Right
MCF-PVPH-108.38	Metatarsal II	6.6	Right
MCF-PVPH-108.31	Metatarsal III	6.4	Left
MCF-PVPH-108.32	Metatarsal III	6.0	Right
MCF-PVPH-108.188	Metatarsal III	6.5	Left
MCF-PVPH-108.201	Metatarsal III	6.3	Left
MCF-PVPH-108.37	Metatarsal IV	7.3	Right

TABLE 2. — Teeth of *Mapusaurus* n. gen. and other carcharodontosaurids. Abbreviations: **ANT**, lowest number of denticles per 5 mm along the anterior carina; **BW**, labial-lingual base width of crown (in mm); **Crown**, height of the crown, measured from the tip to the proximal end of the posterior carina or to the edge of the enamel layer (in mm); **dent**, dentary; **FABL**, fore-aft base length, which is anteroposterior length of tooth at the base of the crown (in mm); **Farlow**, tooth from the data base of Farlow *et al.* 1991; **max**, maxillary; **POST**, lowest number of denticles per 5 mm along the posterior carina; **TL**, total length of crown and root (in mm).

Genus	Catalogue number	Position	TL	Crown	FABL	BW	ANT	POST
<i>Mapusaurus</i> n. gen.	MCF-PVPH-108.8	isolated	174	65.0	33.0	20.0	9.0	10.0
	MCF-PVPH-108.9	isolated	164	71.0	32.0	17.0	8.5	8.5
	MCF-PVPH-108.10	isolated	92	41.0	25.0	13.0	10.0	10.0
	MCF-PVPH-108.16	isolated	-	50.0	28.0	15.0	10.0	-
	MCF-PVPH-108.41	isolated	-	-	23+	-	8.0	9.0
	MCF-PVPH-108.42	isolated	90	33.0	17.7	13.5	9.0	9.0
	MCF-PVPH-108.43	isolated	-	53.0	31.0	14.5	7.0	7.0
	MCF-PVPH-108.103	isolated	68	24.0	20.0	9.0	11.0	11.0
	MCF-PVPH-108.110	isolated	125	81.5	30.0	10.5	8.0	-
	MCF-PVPH-108.111	isolated	154	77.0	38.0	17.0	10.0	10.0
	MCF-PVPH-108.113	isolated	-	54.0	19.0	8.5	9.0	12.0
	MCF-PVPH-108.114	isolated	-	-	-	-	8.0	10.0
	MCF-PVPH-108.115	11th max	-	-	-	-	10.0	11.0
	MCF-PVPH-108.120	isolated	-	36.0	22.0	-	10.0	-
	MCF-PVPH-108.131	isolated	-	-	19.0	8.0	14.0	15.0
	MCF-PVPH-108.138	isolated	-	47.0	23.0	-	-	9.0
	MCF-PVPH-108.141	isolated	96	39.0	28.0	12.0	-	-
	MCF-PVPH-108.166	isolated	117	42.0	23.0	16.0	9.0	10.5
	MCF-PVPH-108.169	1st max	-	68.0	-	-	8.0	-
	MCF-PVPH-108.171	isolated	128	56.0	29.0	16.0	10.0	10.0
	MCF-PVPH-108.173	isolated	148+	73+	37.0	-	10.0	-
	MCF-PVPH-108.176	isolated	-	-	-	-	-	-
	MCF-PVPH-108.180	isolated	-	-	-	-	-	-
<i>Giganotosaurus</i>	MUCPv-CH-1	isolated	188+	82+	45.0	18.0	10.0	9.0
	MUCPv-CH-1	isolated	213	102.0	39.5	22.0	9.0	7.5
	MUCPv-CH-1	isolated	202	88.0	43.5	20.0	8.0	8.0
	MUCPv-CH-1	8th max	-	97.0	-	-	9.0	-
	MUCPv-CH-1	11th max	-	74.0	-	-	-	8.5
	MUCPv-CH-1	9th dent	-	-	-	-	-	9.0
	uncatalogued	isolated	-	56.0	31.5	17.0	8.0	8.0
<i>Carcharodontosaurus</i>	FPDM uncatalogued	isolated	-	87.0	44.2	19.5	8.0	8.0
	FPDM 15	isolated	113+	75.0	35.0	15.8	8.0	8.0
	FPDM 18	isolated	-	67.3	30.5	19.2	7.0	7.5
	Farlow 2b	isolated	-	-	27.0	15.0	10.0	12.0
	Farlow 2a	isolated	-	-	25.0	14.0	-	20.0

TABLE 3. — Minimum number of *Mapusaurus* n. gen. individuals as determined by metatarsals recovered from the Cañadón del Gato site. Abbreviation: **dw**, distal width (in mm).

<b>Individual</b>	<b>Side</b>	<b>Metatarsal</b>	<b>Length</b>	<b>Catalogue number</b>
1	Right	II	(dw = 72)	MCF-PVPH-108.124
2	Right	II	385 (dw = 78)	MCF-PVPH-108.34
2	Left	II	incomplete	MCF-PVPH-108.36
2	Right	III	434	MCF-PVPH-108.32
2	Right	IV	incomplete	MCF-PVPH-108.35
3	Right	III	410+	MCF-PVPH-108.200
3	Right	II	415	MCF-PVPH-108.38
4	Left	III	454	MCF-PVPH-108.31
5	Left	III	450	MCF-PVPH-108.201
6	Left	II	450	MCF-PVPH-108.33
6	Left	III	460	MCF-PVPH-108.188
7	Right	IV	475	MCF-PVPH-108.37